Diss. ETH No. 20114

Soil Moisture in Switzerland:
Analyses from the Swiss Soil Moisture Experiment

A dissertation submitted to the
ETH ZURICH

for the degree of
DOCTOR OF SCIENCES

presented by

Heidi Mittelbach

Dipl. Hydrol., University of Dresden
born 22 September 1980
citizen of Germany

accepted on the recommendation of

Prof. Dr. Sonia I. Seneviratne, examiner
Prof. Dr. Harry Vereecken, co-examiner
Prof. Dr. Adriaan J. Teuling, co-examiner
Dr. Irene Lehner, co-examiner

Zurich 2011

Abstract

Soil moisture is an essential climate variable as it affects the surface fluxes with consequent impacts on temperature, boundary layer stability, and precipitation. In recent years, the investigation of its influence for land surface-atmosphere interactions and its potential role in the climate system gained increasing attention. Soil moisture observations are crucial for these investigations. However, soil moisture is still not routinely measured and there is a lack of observation in many parts of the world.

The aim of this thesis is to fill a part of the gap in soil moisture observations for Europe through the setup of the large-scale and long-term SwissSMEX soil moisture network and through the analyses of this data set with respect to soil moisture dynamics in Switzerland. The emphasis is placed on the detailed evaluation of low-cost soil moisture sensors and on the investigation of the spatio-temporal variability of soil moisture dynamics within the established network. In addition, a first analysis of soil moisture patterns across grassland and forest sites is realized using the SwissSMEX data set.

A first part (Chapter 2 and Chapter 3) of this thesis focuses on the evaluation and comparison of low-cost soil moisture sensors. In a first study (Chapter 2), the performance of the applied low-cost soil moisture sensor 10HS (Decagon Devices, United States) is evaluated using laboratory and field measurements from two SwissSMEX sites. Measurements of absolute volumetric water content (VWC) at several installation depths, the integrated column soil moisture, as well as the loss of soil moisture for precipitation free days are compared with gravimetric samples and time domain reflectometry (TDR) measurements. The measurements of the 10HS sensors agree well for low VWC using both laboratory and field measurements. A considerable limitation of the 10HS sensor is found in the decreasing sensitivity of the sensor reading for VWC variations above 0.4 m^3/m^3. A dependency of the sensor on soil characteristics limits the applicability of a laboratory calibration function. However, with site-specific calibration functions derived from parallel 10HS and TDR measurements, the measurement error of the 10HS sensor can be decreased and the day-to-day variability of soil moisture is captured. Consequently, the 10HS sensor is found to be appropriate for many applications in climate research. The second study (Chapter 3) compares four parallel installed soil moisture sensor types under field conditions in Switzerland. This study does not intend to provide calibration functions for the sensors, but focuses on the sensors performance when using calibration functions provided by the manufacturer. Two years of measurements from parallel installed soil moisture sensors down to 110 cm are compared. The low-cost instruments 10HS (Decagon Devices, United States), CS616 (Campbell Scientific, United States), and SISOMOP (SMG University of Karlsruhe, Germany) are evaluated against the TDR-based TRIME-IT/-EZ

(IMKO GmbH, Germany) sensors. Under the given field conditions, the root mean square error (RMSE) of absolute VWC are up to 0.4 m³/m³ for the low-cost sensor compared to TDR measurements. The RMSE of the anomalies are lower with lowest values in summer, when lowest VWC occurs. For the CS616 sensor type, a strong temperature dependency is found, which is not minimized using the correction function provided by the manufacturer. The measurement errors are also reflected in poor estimations of the evapotranspiration, which is compared with measurements from a weighing lysimeter. We conclude that under the given conditions none of the evaluated low-cost sensors have a level of performance consistent with that indicated by the respective manufacturer. Thus, an evaluation of applied sensor types is essential to quantify measurement errors and to derive site-specific calibrations functions, which is also vital to improve soil moisture measurements.

In the second part of the thesis (Chapter 4 and 5) first analyses of soil moisture dynamics within the new SwissSMEX network are provided. A new persepective for the analyses of the spatio-temporal variability of soil moisture is tested (Chapter 4) using 15-month time series from 14 grassland sites of the SwissSMEX network. This study highlights the advantage of long-term soil moisture measurements, as they enable to distinguish between the temporal mean and the temporal anomalies of soil moisture and to assess their respective contributions to the overall spatial variability of soil moisture. For the given conditions, the time invariant temporal mean is found to be the most relevant contributor to the spatial variability of absolute soil moisture, while the time varying anomalies contribute less. Furthermore, we find that the temporal mean and the anomalies do not necessary present similar spatio-temporal characteristics. Largest differences with high negative correlations for the soil moisture mean and anomalies are found for the particularly dry 2011 spring. The application of the rank stability concept for the whole period shows that the rank stability of absolute soil moisture is mostly influenced by the time invariant temporal mean and does not reflect the rank stability of time varying anomalies. This study demonstrates that conclusions derived from spatio-temporal analyses of absolute soil moisture do generally not apply for the temporal anomalies of soil moisture, and thus do not reflect a behavior related to soil moisture dynamics. A second study (Chapter 5) compares soil moisture between grassland sites and nearby forest sites. Three of four paired SwissSMEX sites are considered in this study. The main focus is on the recession of soil moisture, which is related to evapotranspiration for dry-down periods. Grassland shows consistently a twice as fast decay of soil moisture compared to the forest sites, implying a twice as high evapotranspiration rate for the former. Thus, even under normal meteorological conditions, the vegetation cover is found to have a major impact on land surface-climate interactions.

In summary, this thesis considerably contributed to the development of the SwissSMEX network and the concluded analyses provided helpful insights on 1) the performance of soil moisture sensors, 2) spatio-temporal dynamics of soil moisture, and 3) distinction in soil moisture behavior between grassland and forest sites. We expect that the established SwissSMEX network and data set will be highly valuable for further analyses on the role of soil moisture for land surface-climate interactions in Central Europe.

Zusammenfassung

Bodenfeuchte ist eine bedeutende Klimavariable, die die bodennahen Flüsse der Energie und Wasserbilanz beeinflusst und damit verbunden Auswirkungen auf Temperatur, Grenzschichtstabilität und Niederschlag hat. In den vergangenen Jahren haben Untersuchungen auf Einflüsse auf Wechselwirkungen zwischen Landoberflächen und Atmosphären und deren potentielle Rolle für das Klimasystem immer mehr Aufmerksamkeit erlangt. Auch wenn Beobachtungen von Bodenfeuchte für solche Untersuchungen essentiell sind, wird diese Variable noch immer nicht routinemässig gemessen. Darüber hinaus existieren in vielen Teilen der Welt überhaupt keine Beobachtungen.

Das Ziel dieser Arbeit ist, Bodenfeuchtemessungen durch den Aufbau des grossflächig und langfristig angelegten SwissSMEX Bodenfeuchtenetzwerkes bereitzustellen und den erhaltenen Datensatz in Hinblick auf die Bodenfeuchtedynamik in der Schweiz zu analysieren. Der Schwerpunkt liegt in der Evaluation von kostengünstigen Bodenfeuchtesensoren sowie in der Unter-suchung der räumlich-zeitlichen Variabilität der Bodenfeuchtdynamik. Weiterhin wird das Verhalten der Bodenfeuchte für Wiese- und Waldflächen betrachtet.

Der erste Teil fokussiert auf die Evaluation und den Vergleich von kostengünstigen Bodenfeuchtesensoren (Kapitel 2 und 3). In der ersten Studie (Kapitel 2) werden die Eigenschaft des zur Anwendung kommenden 10HS Sensors (Decagon Devices, Vereinigte Staaten) unter Labor- und Feldbedingungen evaluiert. Dabei werden Messungen des absoluten Wassergehaltes in verschiedenen Tiefen, die Bodenfeuchte über eine definierte Bodensäule sowie die Bodenfeuchteänderung mit gravimetrischen Messungen und mit auf Time-Domain-Reflectometry (TDR) basierenden Messungen verglichen. Niedrige Wassergehalte werden vom Sensor gut erfasst. Eine wesentliche Limitierung des Sensors liegt jedoch in der Abnahme der Messgenauigkeit für Wassergehaltsänderungen über 0.4 m^3/m^3. Ausserdem schränkt eine Abhängigkeit von Bodeneigenschaften die Anwendung einer unter Laborbedingungen abgeleiteten Kalibrierungsfunktion ein. Werden standortspezifisch Kalibrierungsfunktionen verwendet, die für diese Studie mit Hilfe von parallel messenden TDR Sensoren erstellt werden, verringert sich der Messfehler des Sensors markant und die tägliche Variabilität der Bodenfeuchte wird gut erfasst. Schlussfolgernd ist der 10HS Sensor für Anwendungen in den Klimawissenschaften einsetzbar. In einer zweiten Studie (Kapitel 3) werden vier Bodenfeuchtesensoren für einen Standort in der Schweiz miteinander verglichen. Diese Studie beabsichtigt nicht Kalibrierungsfunktionen bereit zu stellen, vielmehr ist der Fokus im Vergleich der Messungen unter Anwendung der Herstellerfunktionen zu sehen. Es werden Messungen von den parallel installierten Sensoren über einen Zweijahreszeitraum verglichen. Die kostengünstigen Sensoren 10HS (Decagon Devices, Vereinigte Staaten), CS616 (Campbell Scientific, Vereinigte Staaten) und SISOMOP (SMG Universität Karlsruhe, Deutschland)

werden gegenüber dem TDR-basierten TRIME-IT/-EZ (IMKO GmbH, Deutschland) Sensor bewertet. Unter den Standortbedingungen ist die mittlere quadratische Abweichung (RMSE) des absoluten Wassergehaltes bis zu 0.4 m^3/m^3. Der RMSE der Bodenfeuchteanomalien ist im Sommer geringer, wenn die niedrigsten Wassergehalte auftreten. Der CS616 Sensor weisst eine zweifelhafte Temperaturabhängigkeit auf, welche sich durch Anwendung einer vom Hersteller gelieferten Korrektur nicht beheben lässt. Die aufgezeigten Messunsicherheiten spiegeln sich ebenfalls in einer mangelnden Bestimmung der Verdunstung wider, die mit Bodenfeuchtemessungen über den Bodenwasserhaushalt abgeschätzt werden kann. Für die gegebenen Standortbedingungen wird zusammengefasst, dass keiner der untersuchten kostengünstigen Sensoren die vom Hersteller angegebenen Messgenauigkeit aufweist. Die Evaluierung von Sensoren ist somit für die Quantifizierung von Messfehlern und zur Ermittlung einer standortspezifischen Kalibrierungsfunktion unerlässlich.

Der zweite Teil dieser Arbeit (Kapitel 4 und 5) beinhaltet erste Analysen des SwissSMEX Datensatzes. Ein neuer Ansatz für die Untersuchung der räumlich-zeitlichen Variabilität der Bodenfeuchte wird unter der Verwendung einer 15-monatigen Zeitreihe von 14 SwissSMEX Bodenfeuchtemessstandorten getestet (Kapitel 4). Diese Studie verdeutlicht den Vorteil von Langzeitmessreihen, welche eine Unterscheidung der absoluten Bodenfeuchte in eine zeitlich mittlere Bodenfeuchte und deren zeitliche Anomalie zulässt. Somit lässt sich deren jeweiliger Anteil zur gesamten Bodenfeuchtevariabilität beurteilen. Unter den gegebenen Bedingungen ist der Anteil der zeitlich invarianten Bodenfeuchte am bedeutendsten, während der Anteil der zeitlich variierenden Anomalie geringer ist. Weiterhin wird festgestellt, dass die räumlich-zeitlichen Eigenschaften der zeitlich invarianten und zeitlich variierenden Terme nicht zwingend ähnlich sind. Die grössten Unterschiede mit hohen negativen Korrelationen werden für den besonders trockenen Frühling 2011 beobachtet. Zudem verdeutlicht die Anwendung des "rank stability"- Konzeptes über den gesamten Zeitraum, dass die "rank stability" der absoluten Bodenfeuchte vorwiegend durch den zeitinvarianten Term beeinflusst wird und nicht die zeitlich variierende Bodenfeuchtedynamik widerspiegelt. Diese Studie zeigt auf, dass sich Schlussfolgerungen aus der Analyse der räumlich-zeitlichen Variabilität der Bodenfeuchte nicht generell auf die Variabilität ihrer Anomalie übertragen lassen. Eine zweite Studie (Kapitel 5) vergleicht die Bodenfeuchte zwischen Wiesen- und Waldstandorten dreier von insgesamt vier paarweisen SwissSMEX Standorten. Schwerpunkt dieser Studie liegt auf der Rückgangskurve der Bodenfeuchte, die für niederschlagsfreie Perioden mit der Verdunstung in Zusammenhang gebracht werden kann. Im Vergleich zu den Waldstandorten zeigen die Wiesenstandorte jeweils einen doppelt so schnellen Rückgang der Bodenfeuchte auf, was zu einer zweimal höheren Verdunstungsrate über Wiese führt. Dies verdeutlicht, dass selbst unter normalen meteorologischen Bedingungen die Vegetationsbedeckung für Landoberflächen-Klima-Wechselwirkungen einen wesentlicheren Einfluss hat als topographische Standorteigenschaften.

Diese Arbeit trägt erheblich zum Aufbau des SwissSMEX Bodenfeuchte Netzwerkes bei und liefert hilfreiche Erkenntnisse 1) zu Messeigenschaften von Bodenfeuchtesensoren, 2) zu der räumlichen und zeitlichen Dynamik der Bodenfeuchte in der Schweiz und 3) zum Verhalten der Bodenfeuchte für Wiesen- und Waldstandorte bei. Wir erwarten, dass das aufgebaute SwissSMEX Netzwerk und dessen Datensatz für weiter Analysen von Landoberflächen-Klima-Wechselwirkungen in Europa von hohem Nutzen ist.

Sommario

L'umidità del terreno è una delle principali variabili climatiche. L'umidità del terreno influenza direttamente i flussi superficiali, può determinare variazioni di temperatura, della stabilità dello strato limite planetario (o Planetary Boundary Layer, PBL) e delle precipitazioni. Negli ultimi anni l'umidità del terreno è stata riconosciuta come un fattore determinante dei sistemi climatici e dello scambio energetico tra terreno e atmosfera. Nonostante ciò, e nonostante quindi il fatto che sia stata riconosciuta l'importanza di effettuare misurazioni continue di umidità del terreno, le reti di misurazione permanente sono perlopiù inesistenti, o comunque parsimoniose ed inadeguate a fornire osservazioni sperimentali con la necessaria risoluzione spazio-temporale.

Con questo Dottorato di ricerca si è voluto migliorare la tecnica per la misurazione di umidità del terreno tramite la calibrazione e la messa in stazione di una nuova rete di misurazione permanente in Svizzera (SwissSMEX). In secondo luogo, tramite alcune delle misurazioni effettuate è stato poi possibile analizzare la variabilità spazio-temporale dell'umidità del terreno in Svizzera, facendo particolare attenzione alle differenze dovute alla copertura vegetativa dei siti (e.g., boschi o prati).

La prima parte di questa tesi (Capitolo 2 e Capitolo 3) presenta la valutazione dei sensori commerciali utilizzati per le misurazione dell'umidità del terreno: Decagon 10HS (Decagon Devices, Stati Uniti). La valutazione dell'affidabilità dei 10HS è effettuata sia tramite misure di laboratorio che con misure di campo SwissSMEX. In particolare, le analisi delle misure effettuate a diverse profondità hanno portato al confronto tra contenuto di acqua volumetrico assoluto (VWC), totale contenuto d'acqua integrato sull'intera sezione verticale, decadimento di umidità del terreno in seguito ad un periodo privo di precipitazioni e l'umidità del terreno misurata in campo con sensori di tipo TDR (Time Domain Reflectometry), i quali garantiscono un altissima precisione. Le misure effettuate con i sensori 10HS hanno mostrato piena affidabilità per misure di basso VWC, sia in laboratorio che in campo. Lo studio ha però anche mostrato che i sensori 10HS hanno una ridotta sensibilità per valori di VWC superiore a 0.4 m^3/m^3 e che le loro prestazioni dipendono dal tipo di terreno. L'ultimo aspetto limita l'applicabilità delle curve di calibrazione dedotte in laboratorio, che comunque si è visto non sia necessaria se una calibrazioni locale viene eseguita, ad esempio con misurazioni 10HS e TDR condotte in parallelo. In questa maniera, i sensori 10HS si sono rivelati capaci di misurare la variabilità giornaliera dell'umidità del terreno e sono quindi ritenuti affidabili per la maggioranza degli studi concernenti i cambiamenti climatici. Il secondo studio della prima parte della tesi (Capitolo 3) intende testare le curve di calibrazione normalmente fornite dalle case costruttrici dei sensori. In particolare, sono stati testati quattro tipologie di sensori, il 10HS, il CS616 (Campbell Scientific, Stati Uniti), il SISOMOP (SMG università di Karlsruhe,

Germania) e il TRIME-IT/-EZ (IMKO GmbH, Germania, il sensore di riferimento in quanto basato su tecnologia TDR) sulla base di due anni di osservazioni condotte in un unico sito Svizzero fino ad una profondità pari a 110 cm. Le misurazioni di umidità e i relativi tassi di evapotraspirazione sono poi stati confrontati con le misure di un lisimetro a bilancia installato nello stesso sito dell'esperimento. I risultati mostrarono un errore quadratico medio (RMSE) dei sensori commerciali pari a 0.4 m^3/m^3. L'RMSE delle anomalie erano inferiori, specialmente in estate in concomitanza dei bassi valori di VWC. Il sensore CS616 è risultato essere influenzato dalla temperatura. In conclusione, lo studio ha mostrato che tutti i sensori commerciali testati non presentano l'affidabilità invece indicate dalle case produttrici. Ciò indica anche il fatto che questo genere di studi è fondamentale per una corretta stima degli errori commessi e quindi dei veri valori di umidità del terreno.

La seconda parte di questa tesi di Dottorato (Capitolo 4 e Capitolo 5) focalizza sulla dinamica dell'umidità del terreno all'interno della rete di misurazione SwissSMEX. Lo sviluppo di una nuova metodologia, basata su 15 mesi di osservazioni in 14 siti coltivati a prato, ha portato a concludere che la variabilità spazio-temporale dell'umidità del terreno è principalmente attribuibile alla media temporale e solo secondariamente alle anomalie temporali. Inoltre, è stato dimostrato che la variabilità della media e delle anomalie temporali si comportano differentemente rispetto alle osservazioni condotte nella stazione più rappresentativa della rete di misurazione utilizzata. In particolare, è stato il caso della primavera del 2011. L'applicazione del concetto di Ranks Stability ha portato infine alla conclusione che gli studi basati solamente sulla misura di umidità del terreno assoluta non possono riprodurre la dinamicità della variabile di interesse, invece spiegata dalla media e dalle anomalie temporali. Il Capitolo 5 presenta invece i metodi e i risultati di uno studio riguardante le differenze di umidità del terreno osservate in zone coltivate a prato e boschive. I risultati hanno mostrato che il decadimento del VWC nelle zone a prato è doppio rispetto a quello delle zone boschive e che quindi la copertura vegetativa è un fattore chiave per la regolazione degli scambi energetici tra suolo e atmosfera.

In conclusione, questa tesi di Dottorato ha dato un contribuito fondamentale allo sviluppo della rete di osservazioni SwissSMEX. Queste misurazioni sono poi state utilizzate per analizzare e valutare: 1) l'attendibilità dei sensori di umidità del terreno utilizzati, 2) la variabilità spazio-temporale dell'umidità del terreno e 3) le differenze tra l'umidità del terreno nei siti boschivi e quelli coltivati a prato. Le misurazioni della rete SwissSMEX si sono dimostrate molto importanti e verranno certamente impiegate per espandere le analisi devote ad approfondire l'importanza dell'umidità del terreno per lo studio della relazione superficie terrestre – clima in Europa centrale.

Contents

Chapter 1

Introduction

Water has always had,
and will continue to have,
a controlling influence on the Earth's evolution.
(Moustafa T. Chahine, 1992)

Water is said to be the basis for life. Our planet is covered to approximately 75% by water in liquid and solid forms. Its transport through the Earth-atmosphere system constitutes the water cycle, which does not only transport and redistribute water itself, but also salt, energy, nutrients, and minerals (Trenberth et al., 2007). In addition, the water cycle affects the dynamics and thermodynamics of the climate system through the exchange of moisture and heat between land surface and atmosphere and through condensation of water vapour in the atmosphere. Over land approximately 60% of precipitation is returned back to the atmosphere through evapotranspiration (Oki and Kanae, 2006). This process requires up to more than 50% of the net radiation on land (Dirmeyer et al., 2006).

Interest in the influence of the water cycle on climate dates back to the 1980s and 1990s (Shukla and Mintz, 1982; Chahine, 1992). Already in these first studies the availability of moisture in the soil was indicated as having a major influence on the climate system. In recent years, investigations of possible effects of soil moisture on the climate system received an increasing attention (e.g. Seneviratne et al., 2010). Climate models help to understand the interactions of highly complex and non-linear processes of the climate system, as well as the role of terrestrial, atmospheric and oceanic variables in future climate. Under a changing climate, which implies changes in extreme events, climate models are essential to assess the impact of climate change on natural, human, and managed systems. Climate, land surface and hydrological models are sophisticated approximations of reality, which can be used to assess the past, present, or future state of a given system. Observations are crucial to initialize and to evaluate these models.

Several programs and institutions, such as the Global Terrestrial Observation System (GTOS) and the Global Climate Observation System (GCOS), have agreed to monitor and to improve the quality and coverage of climate variables. Despite the evident importance of climate variables, relevant observations, both in-situ or remotely sensed, are still scarce. Regarding terrestrial climate variables, the Food and Agriculture Organization of the United Nations (FAO, 2008) emphasized the need for soil moisture observations, as it is linking the atmospheric and terrestrial branches of the hydrological cycle through its interaction with evapotranspiration.

1

As part of this thesis a long-term soil moisture measurement network was set up for Switzerland, thus filling a part of the gap in soil moisture measurements over the European continent. In the following, the water and energy balances are introduced in Section 1.1. Then, in Section 1.2 the importance of soil moisture for the climate system is described. An overview about soil moisture measurement methods is given in Section 1.3. In Section 1.4, the Swiss Soil Moisture Experiment (SwissSMEX) is introduced. Finally, the overall aims and the different chapters of this thesis are outlined in Section 1.5.

1.1   Energy and water balances

A schematic illustration of both energy and water balances is shown in Figure 1.1. The energy balance can be expressed as:

$$\frac{dQ}{dt} = R_{net} - SH - \lambda \cdot ET - G, \tag{1.1}$$

where dQ/dt is the change of energy content in a given layer, SH is the sensible heat flux, $\lambda \cdot$ET is the latent heat (where λ is the latent heat of vaporization and ET is the evapotranspiration) and G the ground heat flux (Figure 1.1a). The energy input at the land surface is the net radiation R_{net}. It is defined as the sum of net shortwave radiation SW_{net} and net longwave radiation LW_{net}. SW_{net} is the difference between the incoming and the reflected solar radiation, and LW_{net} is the difference between the incoming LW_{in} and outgoing terrestrial radiation LW_{out}. The available energy at the surface is partitioned into the sensible, latent and ground heat fluxes, as well as storage. This partitioning is strongly dependent on the soil moisture in transitional climate regions (e.g. Koster et al., 2004; Seneviratne et al., 2006a).

The water balance of the land surface can be expressed as:

$$\frac{dS}{dt} = P - ET - R_s - R_g, \tag{1.2}$$

where dS/dt is the change of water content in a given soil layer, P is precipitation, ET the evapotranspiration, R_s the surface runoff, and R_g the runoff through drainage. Precipitation is the input in the system and is partitioned into evapotranspiration, runoff, and storage (Figure 1.1b). Evapotranspiration includes direct evaporation from bare soil and open water, and transpiration, water loss regulated physiologically by plants. Runoff is generally subdivided into surface and groundwater runoff, the latter being affected by groundwater storage. Both evapotranspiration and runoff are strongly influenced by the soil moisture content.

The energy and water balances are coupled through evapotranspiration. Hence, soil moisture is a major variable influencing the fluxes in both energy and water balance.
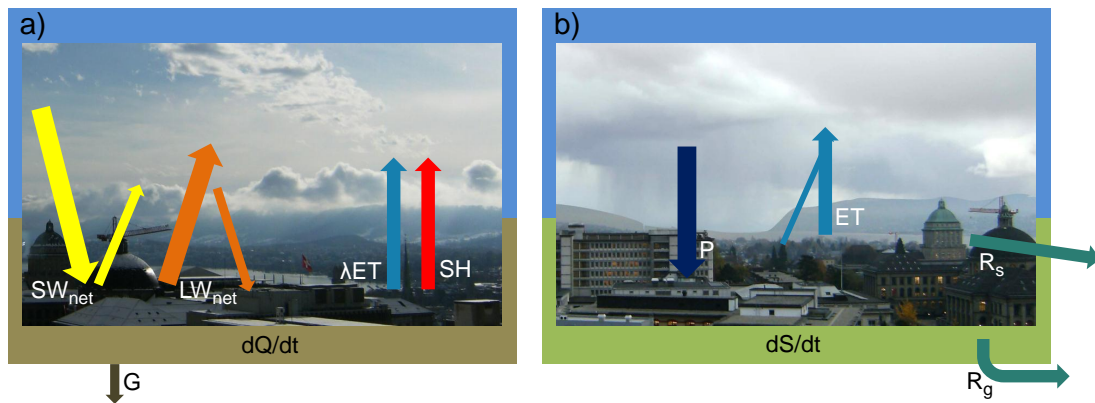
Figure 1.1: *Schematic of the (a) energy balance and the (b) water balance. Details are given in the text.*

1.2   Soil moisture as an essential climate variable

1.2.1   Importance of soil moisture in the climate system

The essential role of soil moisture in different environmental disciplines is well known. Its contribution to processes e.g. for runoff generation and drought development as well as for irrigation purposes is evident. As highlighted above, soil moisture also affects the partitioning of the incoming shortwave radiation into the sensible and the latent heat fluxes. This has consequent impacts on evapotranspiration, temperature, precipitation, and boundary-layer stability.

The major effect of soil moisture on the climate is given through its role on evapotranspiration in regions (transitional climate regions) and time periods (warm season) where and when soil moisture is the limiting factor for evapotranspiration. Figure 1.2 illustrates the dependency of the evaporative fraction (λET/R_{net}) on soil moisture. In wet climate regions, where soil moisture is sufficiently available, evapotranspiration is limited by the available energy. In dry climate regions, the amount of soil moisture is too limited to strongly impact evapotranspiration. In contrast, in transitional regions between wet and dry climates, soil moisture varies strongly on both intra- and interannual time scales within a range when it is limiting for evapotranspiration. Therefore, soil moisture may significantly impact the partitioning of incoming radiation in those regions (Koster et al., 2004; Seneviratne et al., 2006a), with possible impact on temperature extremes (Jaeger and Seneviratne, 2011).

The sensitivity of atmospheric fields to soil moisture has been established by a number of numerical studies (Koster et al., 2004; Seneviratne et al., 2006a; Diffenbaugh et al., 2007; Fischer et al., 2007a; Jaeger and Seneviratne, 2011). The impacts induced by its coupling to evapotranspiration has been shown to be of high relevance in mid-latitude regions, in particular for the occurrence of heat waves (e.g. Seneviratne et al., 2006a; Fischer et al., 2007b). In addition, Lorenz et al. (2010) illustrate the dependency of the occurrence, intensity and length of heat waves on soil moisture persistence. In the context of climate change, regions with transitional climate regimes are expected to be shifted polewards, with a possible increase in climate variability induced by soil moisture feedbacks in regions with currently wet climate regimes (Seneviratne et al., 2006a). Supporting numerical studies, analyses using observational data

Figure 1.2: *Soil moisture SM and evapotranspiration regimes (evaluated from evaporative fracction EF=λR_{net}. Soil moisture plays the most crucial role in transitional regimes ($SM_{WILT} < SM < SM_{CRIT}$). Details are given in the text. After Seneviratne et al. (2010).*
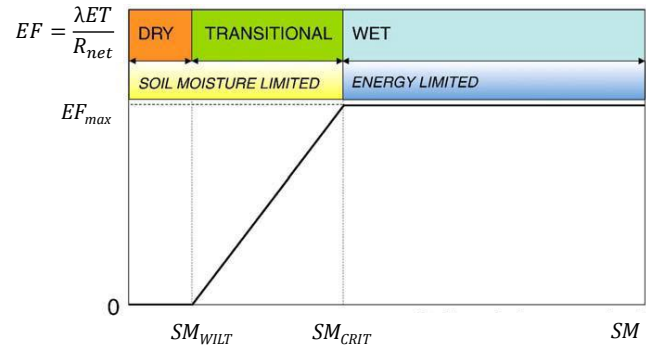
recently confirmed the evidence for the soil moisture impact on trends in evapotranspiration (Teuling et al., 2009; Jung et al., 2010) and on hot extremes (Hirschi et al., 2011). A relationship between the depletion of early summer soil moisture and the development of heat lows over the Mediterranean region in late summer has been identified in Haarsma et al. (2009). Beside heat waves and droughts, also extreme flood events are affected by soil moisture anomalies. Pal and Eltahir (2003) have shown that the initial soil moisture state was important for the intensity and persistence of the 1993 summer flood event over the midwest of the United States. In addition, soil moisture anomalies over relatively small regions are found to induce flood and drought not only locally, but also over distant areas. Over short time scales, relevant for numerical weather prediction, soil moisture variations seem to have a stronger influence on the surface energy budget and on the planetary boundary layer structure (Mahfouf, 1991). In a recent work by Koster et al. (2010a) improved skill for sub-seasonal and seasonal forecasting is found over time periods of two to six weeks with realistic soil moisture initializations. Soil moisture memory plays an important role for such improvements (Vinnikov et al., 1996; Entin et al., 2000; Seneviratne et al., 2006b).

Another important issue when assessing soil moisture and validating model results with observations is its integration over a defined soil column, which is necessary to relate it to the water and energy fluxes (Teuling et al., 2006b; Ventura et al., 2006; Vereecken et al., 2008). Evapotranspiration for example can be estimated by the soil water balance approach, assuming that evapotranspiration is isolated from other fluxes (e.g. infiltration) after several days after a precipitation event. Thus, the recession of soil moisture over a precipitation free period can approximately be assumed to be controlled by evapotranspiration, although percolation still occurs.

1.2.2   Impact of vegetation

Vegetation is influencing soil moisture-climate interactions. Transpiration, which is the largest contributor to overall evapotranspiration (Dirmeyer et al., 2006), is regulated by the opening of the stomata, which is influenced by several factors including vegetation type and soil moisture. Therefore, land cover and its variation in time are expected to play a crucial role for soil moisture-climate interactions.

Recent studies compare the mean annual evapotranspiration as well as the interannual variation of evapotranspiration at grassland and forest sites for similar climatic conditions, but also for different climate regimes (e.g. Peel et al., 2010; Zha et al., 2010). Zha et al. (2010) compare

the interannual variation of evapotranspiration between grassland, deciduous and coniferous forest. They show that evapotranspiration is highest and more variable for grassland and deciduous forest and conclude that the potential for drought impacts in the northern ecosystems is greatest for grassland, moderate for deciduous and smallest for coniferous forest. Furthermore, soil moisture is found to be a dominant climate control for grassland and deciduous trees during summer in western Canada under the present climate. A possible impact of vegetation cover on temperature extremes has been shown in Zaitchik et al. (2006). Their comparison of temperature anomalies during the 2003 European heat wave over pasture and forest for a region in France show higher temperature anomalies over pasture for the peak temperature during this event. They argue that the clear difference in local temperature anomalies over the different land uses reflects differences in adaptation to drought and heat stress resulting from different rooting depth. The study by Teuling et al. (2010b), based on observational data from the FLUXNET network, also illustrate the difference in the energy fluxes over grassland and forest sites during heat wave days. For typical heat waves in temperate Central European regions, forest is found to lead to a higher warming of the atmosphere, as it uses less energy for evapotranspiration than grassland. However, the soil moisture depletion over grassland is faster than over forest. In the long term, this would consequently lead to a higher warming of the atmosphere over grassland, a result consistent with the hypothesis of Zaitchik et al. (2006). The striking result of this study is the time-scale dependency of feedbacks between land surface and the atmosphere, which is strongly related to soil moisture dynamics.

1.2.3   Spatial and temporal scales of soil moisture dynamics

Soil moisture is variable on both spatial and temporal scales. Vinnikov et al. (1996) separated soil moisture variations into two scales: the land surface scale and the meteorological scale. The land surface scale (less than 20 km) is characterized by small-scale variability, such as topography, soil properties, and vegetation, as well as short-term processes, such as surface runoff, infiltration, and percolation. On the other hand the meteorological scale (50 to 400 km) is characterized by large-scale and long-term processes caused by atmospheric forcing, such as precipitation and radiation. The spatial and temporal scales are often assessed from autocorrelation analyses, which indicate the similarity between soil moisture as a function of distance and time differences, respectively. Figure 1.3 illustrates the autocorrelation function for both scales of soil moisture variability as suggested by Robock et al. (1998). The land surface scale is about tens of meters or days, reflecting land surface characteristics (soil type, land cover). In contrast, the meteorological scale is about hundreds of kilometers and 1 week to 3 months, reflecting the scales of the atmospheric forcing linked with weather and climate anomalies. Several studies, based on in-situ soil moisture observations and soil moisture estimates from remote sensing as well as land surface models, confirm the existence of both small-scale and large-scale variability. Furthermore, the strength of correlation was found to depend on the season, latitude, as well as depth of the soil layer, as a consequence of the relation to their drivers (e.g. Vinnikov et al., 1999; Entin et al., 2000; Western et al., 2002; Albertson and Montaldo, 2003; Wu and Dickinson, 2004; Teuling and Troch, 2005; Famiglietti et al., 2008; Joshi and Mohanty, 2010; Wang et al., 2010).

The characterization of the spatial and temporal scales of soil moisture dynamics is an essential

issue for many environmental applications. Its investigation are mostly based on observations, which are still scarce and limited to several regions (see Dorigo et al., 2011, for an overview of existing in-situ networks and remote sensing observations). Moreover, soil moisture observations have restricted spatial and temporal resolutions, they differ from the scale required for environmental applications. Understanding the soil moisture dynamics on those different scales results in its aggregation in both space and time and gives the possibility to link the soil moisture observations to relevant applications. This can lead to improved climate and hydrological model parameterizations, to improved remote sensing-based estimates, and to the optimization of soil moisture monitoring networks (e.g. Entekhabi and Rodriguez-Iturbe, 1994; Vinnikov et al., 1996; Koster et al., 2004; Jackson et al., 2010; Brocca et al., 2010).

Figure 1.3: Schematic diagram of typical temporal and spatial scales of soil moisture variations. r is the autocorrelation function. The scales are determined by the slope of the lines. Note that the exact values may differ in the field. After Entin et al. (2000). Figure reprinted from Robock et al. (1998), copyright Elsevier Science.
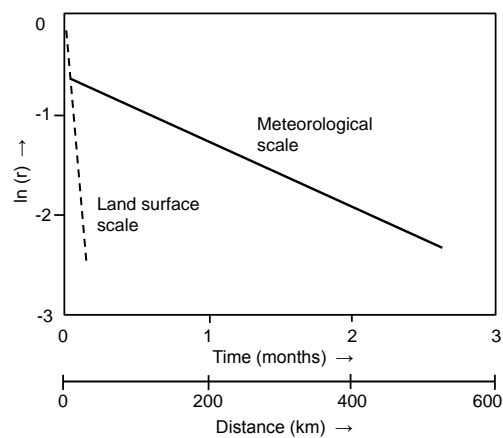
1.3   Measurement of soil moisture

Soil moisture can be measured on different scales ranging from point to continental scale. In-situ measurements, also referred to as ground or contact-based measurements (Robinson et al., 2008), measure on the point scale and are reliable only at the point of measurement. They have a high resolution in the vertical direction and, if continuously measured, a high temporal resolution. Ground measurements make use of different physical properties, such as permittivity and soil thermal properties, as well as change in mass and cosmic-ray neutrons to relate these characteristics to the soil water content. In contrast, remote-sensing techniques, also referred to as contact-free measurements (Robinson et al., 2008), have a low temporal resolution and provide measurements with a footprint up to continental scale, but with only small penetration depth in the case of microwave remote sensing estimates (de Jeu et al., 2008) or with no distinction between soil moistures and other forms of water storage as in the case of Gravity Recovery And Climate Experiment (GRACE) (Tapley et al., 2004). Microwave instruments operate either on the ground or from air- or spaceborne platforms.

For completeness, the possibility to apply land surface models using observation-based forcing to determine soil moisture is mentioned here. Realistic simulation of soil moisture requires a large amount of information about meteorological, vegetation, and soil characteristics. Land

surface models are not of further interest in this study. However, it should be mentioned that a combination of all three methods to derive soil moisture is supposed to be a promising tool for soil moisture estimations (Seneviratne et al., 2010). While accurate point measurements are used for calibration and validation of remote-sensing estimates and land surface models, the latter have the potential to extent soil moisture information on a wider range of both spatial and temporal scales and to provide estimates in isolated regions (e.g. Schmugge et al., 1980; Robinson et al., 2008).

Measurement techniques and sensors for in-situ as well as for remote sensing applications are described and evaluated by a considerable amount of literature (e.g. Jackson, 2002; Schmugge et al., 2002; Walker et al., 2004; Blonquist et al., 2005; Evett et al., 2006; Bogena et al., 2007; Wagner et al., 2007a; Robinson et al., 2008; Vereecken et al., 2008; Rüdiger et al., 2010; Mittelbach et al., 2011). In this chapter, a summary of frequently used ground based-measurements techniques as well as spaceborne microwave remote sensing techniques is presented.

1.3.1 Ground measurements

Gravimetric Measurements
The thermogravimetric method is known to be the standard method and is often used as reference (Schmugge et al., 1980; Dean et al., 1987). An undisturbed soil sample of a defined volume is taken in the field and its mass is weighted at the time of sampling and after drying at 105 °C until the mass is at equilibrium (usually after 24 hours). The gravimetric soil water content θ_g (mass/mass) is defined as:

$$\theta_g = \frac{M_{wet} - M_{dry}}{M_{dry}}, \tag{1.3}$$

where M_{wet} is the mass of the wet soil sample and M_{dry} is the mass of the oven-dried soil. As soil moisture is frequently related to surface fluxes, the expression as volumetric water content (volume/volume) is more common:

$$\theta_v = \theta_g \frac{\rho_{bulk}}{\rho_{water}}, \tag{1.4}$$

where ρ_{bulk} is the bulk density of the sample and ρ_{water} is the density of water. Although this method is qualified as harmless and as the most accurate method for soil moisture measurements, it is destructive, which makes multiple and continuous measurements impossible and, furthermore, it requires substantial manpower.

Electromagnetic Techniques
Electromagnetic techniques are indirect measurement techniques, which measure the permittivity ϵ of a soil sample. The permittivity of a material is a physical quantity of the extent to which the electric charge distribution in the material can be polarized by the application of an electrical field (Hasted, 1973). The relative permittivity (-) is defined as

$$\epsilon_r = \frac{\epsilon}{\epsilon_0}, \tag{1.5}$$

where ϵ is the permittivity of the material (F/m) and ϵ_0 is the permittivity of vacuum (8.854 F/m). The relative permittivity of water is about 80 and of clear contrast to the one

of air and solid material, which is about 1 and 3 to 5, respectively. Consequently, it provides a good characteristic to determine the water content in the soil. For brevity, the term relative is dropped in the following text and the term permittivity is used.

The complex permittivity ϵ_r^* (-) consists of a real part and an imaginary part and is expressed as (e.g. Kelleners et al., 2005):

$$\epsilon_r^* = \underbrace{\epsilon_r'}_{real\ part} - j(\underbrace{\epsilon_{relax}'' + \frac{\sigma_{dc}}{2\pi f \epsilon_0}}_{imaginary\ part}), \tag{1.6}$$

where ϵ_r' is the real part, ϵ_{relax}'' the dielectric relaxation, σ_{dc} is the electrical conductivity, f is the frequency, and j is the imaginary number $\sqrt{-1}$. The real part describes energy storage and is caused by the polarization of the water molecules. On the other hand the imaginary part describes energy loss which is associated with electrical conductivity and with molecular relaxation, occurring if molecules can no longer keep up with the speed of field alternation (Robinson et al., 2003).

Sensing systems measure electromagnetic properties, such as travel time or charge time, which can directly be related to the permittivity of the surrounding material and subsequently related to the volumetric water content. Several studies (e.g. Seyfried and Murdock, 2004; Blonquist et al., 2005; Kelleners et al., 2005; Bogena et al., 2007; Escorihuela et al., 2007) showed that the measurement accuracy of a soil moisture sensor depends on the dielectric relaxation, temperature, soil texture and electrical conductivity, and that the effects of these contributors are to a large extent frequency dependent. Furthermore, the polarization of dipoles shows a temperature dependency. With increasing temperature, the polarization of dipoles disappears first. Thus, the challenge of soil moisture measurements using electromagnetic sensors is to measure the permittivity at a frequency with optimal alignment of dipoles and minimal contribution of the imaginary components.

Figure 1.4 illustrates the main contributors to the imaginary part of the permittivity for a wet porous material. Commonly used soil moisture sensors operate at a frequency ranging between 50 MHz and 1 GHz. For low frequencies the main contributor are the ionic conductivity, which is related to the electrical conductivity and the bound water relaxation, whereas for high frequency the major contributor is the relaxation of free water. Blonquist et al. (2005) found that low-frequency systems are generally more sensitive to electric conductivity and molecule relaxation. Or and Jones (2002) summarized a difference in the temperature dependency for free and bound water: For soils, where the main part of soil water is in free state (e.g. sands) a decrease in permittivity corresponds to an increase of temperature. In contrast, the permittivity for soils with main part of bound water (e.g. clay) increases with increasing temperature. In addition, Escorihuela et al. (2007) illustrated a different temperature effect for bound and free water due to their relaxation frequency. A major impact was thereby found for sensors operating below 500 MHz. Moreover, the study by Kelleners et al. (2005) showed a frequency dependency of the real part of the permittivity for sensors operating at frequencies lower than 500 MHz, which cannot be ignored. For low-frequency electromagnetic sensors laboratory and site specific calibration of the soil moisture sensors are strongly recommended (e.g. Seyfried and Murdock, 2004; Logsdon, 2009; Rüdiger et al., 2010; Mittelbach et al., 2011).
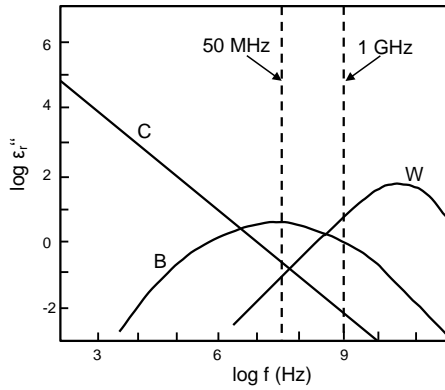
Figure 1.4: *Major contributors to the permittivity loss on wet porous media. C: ionic conductivity; B: bound-water relaxation; W: principal relaxation of free water. After Escorihuela et al. (2007).*

The advantages of electromagnetic sensors are to provide non-destructive, continuous and harmless soil moisture measurements. Two commonly used electromagnetic sensor types are based on time domain reflectometry TDR (e.g. Topp et al., 1980; Ledieu et al., 1986; Robinson et al., 2003) and capacitance (e.g. Dean et al., 1987; Blonquist et al., 2005; Robinson et al., 2008) techniques.

Time-domain reflectometry (TDR) sensors operate at a frequency above 500 MHz (Robinson et al., 2008). Because of the operation frequency and the above mentioned factors, they are known to be of high accuracy. TDR based sensors measure the travel time of an electromagnetic pulse along waveguides, which are in contact with the soil. The travel time t_{tdr} depends on the permittivity of the soil and is described as (e.g. Robinson et al., 2003):

$$t_{tdr} = \frac{2L\sqrt{\epsilon_r}}{c}, \tag{1.7}$$

where L is the length of the probe and c is the speed of light in vacuum. The factor 2 accounts for the two-way travel of the pulse. Topp et al. (1980) found a polynomial function to describe the relation between the permittivity and volumetric water content (θ_v) for different mineral soils:

$$\theta_v = -5.3 \cdot 10^{-2} + 2.92 \cdot 10^{-2}\epsilon_r - 5.5 \cdot 10^{-4}\epsilon_r^2 + 4.3 \cdot 10^{-6}\epsilon_r^3. \tag{1.8}$$

Capacitance sensors operate in a frequency range between 5 and 150 MHz (Robinson et al., 2008). Because of their lower operation frequency and the above-mentioned factors, they are known to have a lower accuracy than the TDR sensors. However, they are a good alternative for soil moisture measurements (Robinson et al., 2003). Moreover, they are of lower cost. Capacitance sensors measure the charge time of a capacitance. The soil is part of the capacitor in which the permanent dipoles of the soil water become polarized and respond to the frequency of the electric field. The charge time t_{cap} of the applied sensor is defined as (Decagon Devices, 2009):

$$t_{cap} = RC \cdot ln\left[\frac{(V - V_f)}{(V_i - V_f)}\right], \tag{1.9}$$

where R is the series resistance, V the voltage at time t_{cap}, V_i is the starting voltage, and V_f the supplied voltage. The relation between the capacitance C and the ϵ_r is defined as (e.g. Dean et al., 1987):

$$C = g\epsilon_r \qquad (1.10)$$

where g is a geometric constant, depending on the electrode configuration, such as size, shape, and distance between the electrodes. The relation between the permittivity and the volumetric water content is expected to be dependent on the frequency. Thus, an individual calibration function is provided by the manufacturer and site-specific calibration functions are recommended to increase the measurement accuracy.

1.3.2   Microwave remote sensing

Remote sensing instruments for soil moisture estimates use the reflected and emitted electromagnetic radiation from the land surface. Similar to electromagnetic ground based soil moisture sensors (Section 1.3.1), microwave remote sensing methods use the large difference of the permittivity of water compared to solid material. The permittivity of water and dry soils results in a emissivity of 0.4 for water and 0.95 for dry land, respectively, which lead to a determination of the water content of the land surface for the uppermost soil layer (down to 5 cm, Schmugge et al., 2002). Remote sensing for soil moisture estimation operates at microwave frequencies, particular in the frequency range of 1-10 GHz (corresponding to a wavelength λ of 30 to 2.5 cm). At this frequency measurements depend strongly on the permittivity, the atmosphere is transparent, and measurements are independent of the solar illumination (Jackson, 2002). For soil moisture estimation the most important frequency bands are the L-Band (λ = 30-15 cm), C-Band (λ = 7.5-3.8 cm), and X-Band (λ = 3.8-2.5 cm), whereas low frequencies provide the best information for soil water content estimations (Wagner et al., 2007a). Vegetation cover has a major impact on the accuracy of the measurements, as it attenuates the signal and adds emissivity, as well as surface roughness. Figure 1.5 shows the dependency of penetration depth and permittivity on frequency and leads to the conclusion that the L-Band has the optimal measurement frequency. Microwave remote sensing can be applied both with passive and active sensors.

The *passive sensors* are based on radiometric techniques. They measure the radiation naturally emitted by the soil, which is expressed as brightness temperature T_b. The emissivity e is related to the measured T_b of a surface using the temperature T (e.g. Schmugge et al., 2002):

$$e = \frac{T_b}{T}. \qquad (1.11)$$

A major issue for microwave radiometry is the Radio Frequency Interference (RFI). The perturbation takes place mainly over dense populated areas. It degrades the brightness observations and thus impairs the retrieval of soil moisture.

One of the latest spaceborne radiometer is the Advanced Microwave Scanning Radiometer for National Aeronautics and Space Administration's (NASA) Earth Observing System (AMSR-E), which was launched in 2002. The most recently launched radiometer is that from the Soil

a)

Penetration into Vegetation

low   high

λ (cm)

1   5   10   15   20   25

b)

Dielectric Constant of Wet Soil

λ (cm) wavelength

1   5   10   15   20   25
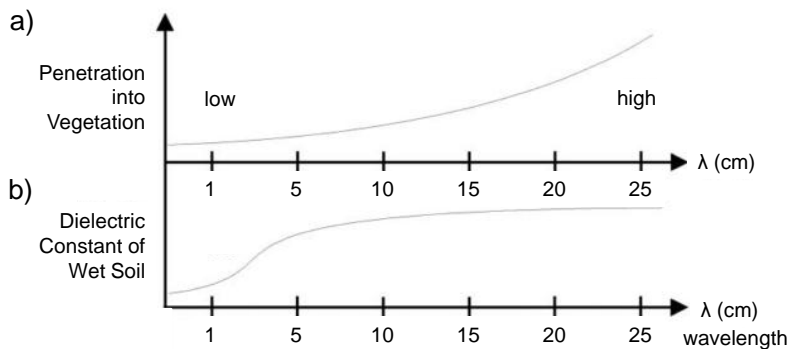
Figure 1.5: *Dependency of (a) penetration into vegetation and (b) permittivity on wavelength. After Wagner et al. (2007a).*

Moisture and Ocean Salinity (SMOS) mission of the European Space Agency (ESA), which was launched in 2009. It operates in the optimal L-Band and provides soil moisture with a spatial resolution of 30-50 km. Beside soil moisture it estimates salinity.

The *active sensors* are based on radar and scatterometer techniques. They emit and receive electromagnetic radiation to yield the backscatter coefficient. The backscatter coefficient is related to the surface reflectivity and depends on their permittivity but is also sensitive to surface roughness, hence, its definition is a challenging problem for soil moisture retrieval (Robinson et al., 2008). Similar to radiometers, the accuracy of the instruments depends on the measurement frequency. The lower the frequency, the higher is the accuracy and the deeper the penetration depth. One example for an active sensor is the Advanced Scatterometer (ASCAT), which provides soil moisture estimates since 2008.

In the near future the Soil Moisture Active Passive (SMAP) satellite will be launched by NASA. The satellite carries a L-band radiometer and a L-band radar on board. The goal of this mission is to combine the positive attributes of radiometer and radar techniques and thus to provide accurate soil moisture estimates with a high spatial resolution.

1.4 SwissSMEX - The Swiss Soil Moisture Experiment

"Data! Data! Data!"
he cried impatiently.
"I can't make bricks without clay."
(Sherlock Holmes in "The Adventure of the Copper Beeches" by Sir A.C. Doyle, 1892)

1.4.1 Objectives

As highlighted in Section 1.2 soil moisture observations are important for many climate applications. However, soil moisture is still not routinely measured and there is a lack of observations in most parts of the world. For this reason the Swiss National Science Foundation (SNSF) project SwissSMEX (http://www.iac.ethz.ch/url/SwissSMEX) was initiated in June 2008 by ETH Zurich, MeteoSwiss, and Agroscope Reckenholz-Tänikon (ART). The first goal of this

project was to establish a long-term soil moisture measurement network in Switzerland that allows a comprehensive assessment of soil moisture in this region. In 2010 the network was expanded and upgraded thanks to the equipment project SwissSMEX-*Veg* to enhance the coverage over different land use types. This extension was conducted in collaboration with the Swiss Federal Institute for Forest, Snow and Landscape Research (WSL) at sites of the Swiss Long-term Forest Ecosystem Research (LWF).

The specific objectives of the SwissSMEX project, within which this PhD thesis was conducted:

- the setup of a soil moisture network for Switzerland.

- the evaluation of low-cost (e.g. capacitance) vs. highly accurate but expensive (e.g. TDR) soil moisture sensors.

- the assessment of the spatial variability of soil moisture in Switzerland.

- the investigation of the role of land cover (grassland vs. forest) for soil moisture-vegetation-climate interactions in Switzerland.

In parallel and future projects, the soil moisture measurements of the SwissSMEX network will be used to assess the temporal variability of soil moisture and its link to main climate drivers, to determine the impact of soil moisture for the local and regional climate, to validate land surface and climate models with regard to soil moisture representation in Central Europe, and to investigate regionalization approaches as well as to evaluate indirect soil moisture measurement techniques and approaches.

In Europe, several small-scale and/or short-term networks, such as the RHEMEDUS in Spain (Martinez-Fernandez and Ceballos, 2005) and the SMOSMANIA in France (Albergel et al., 2008), were established in the recent years. Furthermore, the TERENO project, a network of various observations was recently established in Germany (http://teodoor.icg.kfa-juelich.de/overview-de). The SwissSMEX soil moisture network is the first of its type in Switzerland. Moreover, it is one of the first networks in Europe that intends to measure soil moisture on long-term and large scale. Its specification includes climatic gradients spanned by its spatial extent as well as it includes four "paired" forest/grassland sites, which allow comparisons across different land cover types. Furthermore, with measurements down to 120 cm, the root water uptake and surface-subsurface interaction can be determined, which gives an additional possibility to optimize the parametrization of regional climate models (van den Hurk et al., 2005). In addition, this project provides an exhaustive evaluation of low-cost versus high-cost sensors for climate science (Chapter 2 and 3).

1.4.2   Soil moisture network

At present the SwissSMEX network consists of 19 sites at 17 different locations over a spatial extent of about 150x210 km. The main land use is grassland (14 sites), followed by 4 forest sites and 1 arable site. The concept of the project was to establish a possible dense soil moisture network over a large spatial extent, including locations with relatively deep soils and similar conditions regarding meteorology, land use, elevation, slope, and aspect. Furthermore, a major

requirement of the chosen sites was the availability of measurements of meteorological variables very close to the soil moisture measurements, to allow the assessment of different climate variables. Consequently, most sites of the SwissSMEX network cover the region of the Swiss Plateau. However, as Switzerland has different climatic regions (see Appendix A), sites were additionally installed in Ticino and Valais to have an indication of soil moisture dynamics under different climatological conditions. All sites are at elevations below about 1000 m a.s.l. The sites were first concentrated on grassland sites, whereas within SwissSMEX-*Veg* also forest land use was included. Measurements of meteorological variables, such as 2-m air temperature, precipitation, wind speed, relative humidity, and global radiation are available at each site as they are set up at selected SwissMetNet sites (http://www.meteoswiss.admin.ch), Swiss FluxNet sites (http://www.swissfluxnet.ch), LWF sites (http://www.wsl.ch/lwf/), as well as at the Rietholzbach research catchment site (http://www.iac.ethz.ch/url/rietholzbach). Furthermore, eddy-covariance measurements are available at the Swiss FluxNet sites Rietholzbach, Oensingen, Laegern, and Chamau. Lysimeter data are available at Rietholzbach and Basel. Each SwissSMEX/-*Veg* site consists of soil moisture and soil temperature measurements at 5, 10, 30, 50, 80, and 120 cm depth. The measurements are logged at a 10 minute interval to ensure analogy to the meteorological variables. The installation is described in detail in Section 1.4.3. Moreover, soil characteristics, such as bulk density, particle size, organic fraction and pH value, were analyzed in the laboratory in collaboration with the group of Soil Protection and the group of Soil and Terrestrial Environmental Physics of the Institute of Terrestrial Ecosystems, ETH Zurich. The location of the sites and their basic characteristics are illustrated in Figure 1.6 and Table 1.1. Detailed information on the site characteristics can be found in Appendix B.
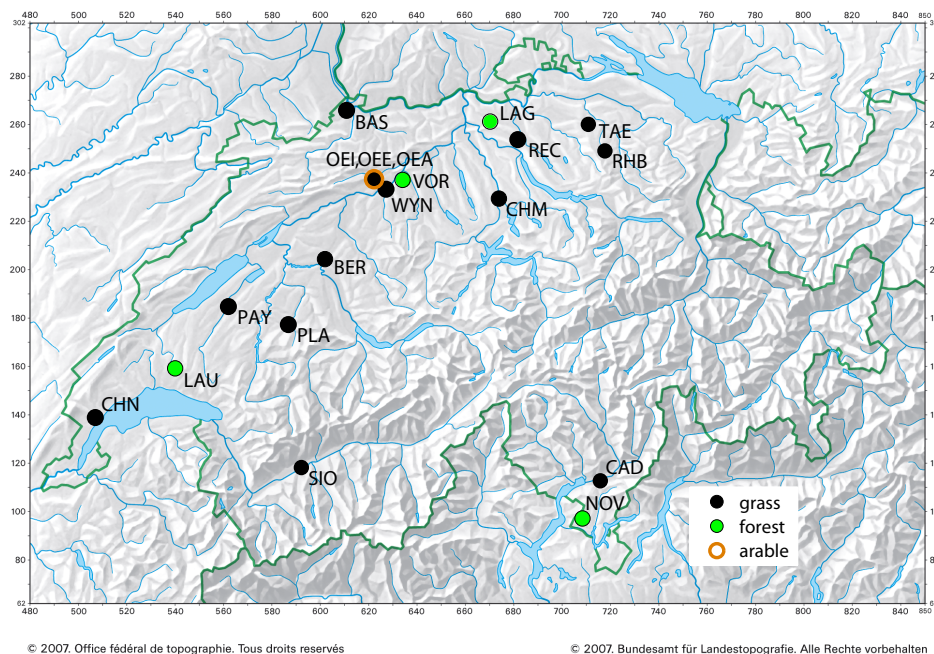
Figure 1.6: Map of Switzerland showing the location and land use of the SwissSMEX/-Veg soil moisture monitoring sites.

Table 1.1: *Basic characteristics of the SwissSMEX/-Veg.*

Site		Site code	Swiss grid		Elevation	Land use	Texture[a,b]
			y coord	x coord	(m a.s.l.)		
Changins	1	CHN	507280	139170	430	grass	loam
Payerne	2	PAY	562150	184855	490	grass	loam
Plaffeien	3	PLA	586850	177400	1042	grass	sandy loam
Bern	4	BER	601935	204410	553	grass	loam
Oensingen intensiv	5	OEI	622200	237220	450	grass	silty clay loam
Oensingen extensiv	6	OEE	622210	237220	450	grass	silty clay loam
Wynau	7	WYN	626400	233860	422	grass	silt loam
Chamau	8	CHM	673635	229265	400	grass	sandy loam
Basel	9	BAS	610850	265620	316	grass	silt loam
Reckenholz	10	REC	681425	253555	443	grass	loam
Taenikon	11	TAE	710500	259820	536	grass	loam
Rietholzbach	12	RHB	717400	248900	754	grass	loam
Sion	13	SIO	592200	118625	482	grass	sandy loam
Cadenazzo	14	CAD	715475	113162	197	grass	silt loam
Lausanne	15	LAU	540175	159445	800	deciduous forest	sandy loam
Vordemwald	16	VOR	633925	236995	480	mixed forest	loam
Laegern	17	LAG	670000	261000	868	mixed forest	clay
Novaggio	18	NOV	708090	97695	950	deciduous forest	loamy sand
Oensingen arable	19	OEA	622590	237450	450	arable	silty clay loam

[a] Averaged over the whole soil column.

[b] According to USDA taxonomy.

1.4.3 Setup and instrumentation

The setup of a SwissSMEX soil moisture site is realized in four steps. Their sequence is shown in Figure 1.7. For the installation holes were dug by hand and by taking care to preserve the original sequence of the soil horizons. The grass layer as well as the different horizons were each laid on different tarps and covered to prevent evapotranspiration (Figure 1.7a,b). A first soil analysis was carried out in the field. For detailed laboratory analyses, undisturbed and disturbed soil samples were taken from each soil horizon (Figure 1.7c-e). Afterwards, the soil moisture and soil temperature sensors were installed horizontally into the undisturbed soil (Figure 1.7f,g). After the installation of the sensors, the hole was refilled by taking care that the soil horizons were arranged in the original order and with as close as possible original density (Figure 1.7h).
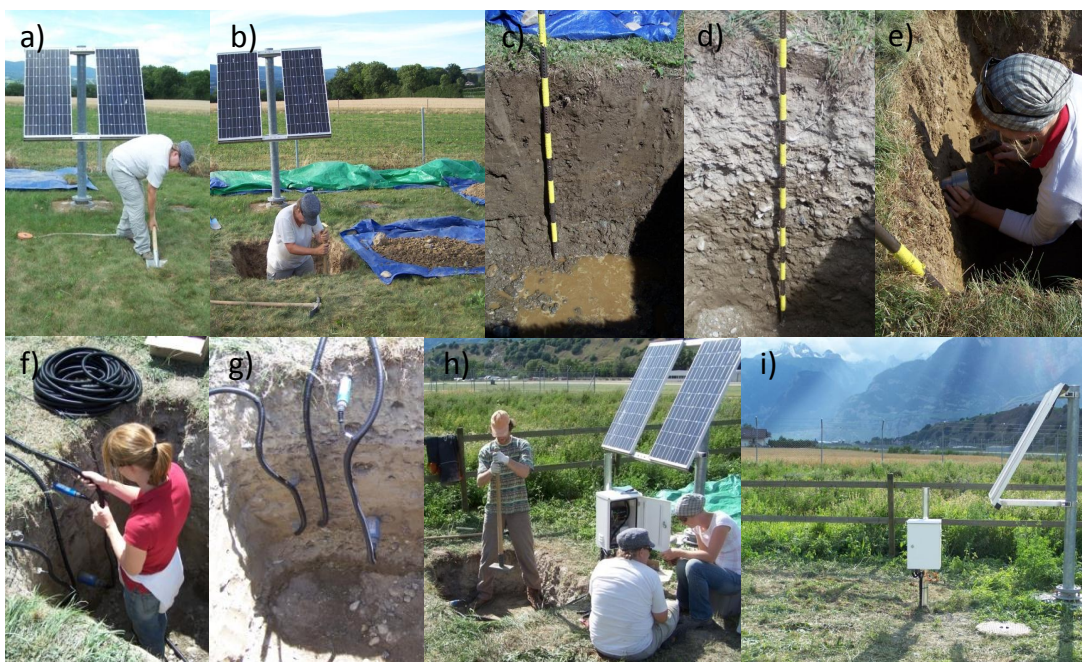
Figure 1.7: *Different steps of the setup of a SwissSMEX/-Veg site. (a,b) digging hole; (c-e) taking soil samples; (f,g) sensor installation; (h) refilling hole; (i) finalized site.*

Each SwissSMEX site consists of soil moisture and soil temperature measurements at 5, 10, 30, 50, 80, and 120 cm depth, whereas the installation was adapted to the local conditions. The standard instrumentation consists of capacitance soil moisture sensors at all measurement depths, TDR based soil moisture sensors at 10 and 80 cm depth, and soil temperature sensors at all depths. Within the complementary project SwissSMEX-*Veg*, the TDR based soil moisture sensors were installed at 10, 30, and 80 cm depth. Furthermore, the forest sites include each two profiles of capacitance and TDR measurements. The basic instrumentation is shown in Figure 1.8 and detailed information on the installation at each site is provided in Appendix B.

The applied soil moisture sensor types are the capacitance soil moisture sensor 10HS (Decagon Devices, United States) and the TDR-based soil moisture sensor TRIME-IT,-EZ and TRIME-PICO32/-PICO64, respectively (IMKO GmbH, Germany) (Figure 1.9). The 10HS sensor is

the successor of the commonly used EC-5 soil moisture sensor, but integrates over a larger soil volume (rod length is 10 cm compared to 5 cm for the EC-5). It operates at a frequency of 70 MHz with operating temperature ranging from 0 to +50 °C. It measures in a range between 0 and 0.57 m^3/m^3 with a reported accuracy using the standard calibration of ±0.03 m^3/m^3 in mineral soils that have a solution electrical conductivity < 10 dS/m. Using a soil specific calibration the accuracy is reported to be ±0.02 m^3/m^3 (Decagon Devices, 2009). The 10HS sensor consists of two parallel-pronged plastic rods of 100 mm length and 9.8 mm width, and a spacing of 12.1 mm. The TDR based soil moisture sensor type TRIME-IT,-EZ and TRIME-PICO32/-PICO64, respectively operate at a frequency of 1 GHz with operating temperature ranging from -15 to +50 °C. They measure in a range of 0 to 1 m^3/m^3 with a reported accuracy of ±0.01 m^3/m^3 for 0 to 0.40 m^3/m^3 and ±0.02 m^3/m^3 for 0.40 to 0.70 m^3/m^3 in soils with bulk electrical conductivity of up to 2 dS/m (IMKO, 2006). TRIME-PICO32/-PICO64 are the successor of the TRIME-IT,-EZ. TRIME-PICO32 and TRIME-IT consists of two parallel round rods of 110 mm length with 3.5 mm diameter and a spacing of 20 mm. They have a smaller measurement volume than the TRIME-PICO64 and TRIME-EZ, which consists of two round metal rods but of 160 mm length with 6 mm diameter and a spacing of 40 mm. Due to its smaller measurement volume, the TRIME-IT was installed at 5 and 15 cm depth, whereas the TRIME-EZ was installed at deeper depths down to 110 cm. The applied soil temperature sensor is the 107-L (Campbell Scientific, United States). The measurements are logged at a 10 minute interval with a Campbell Scientific CR1000 data logger. Most of the sites have commercial power supply, except at the forest sites, which are operated with stand-alone power supply. The data transfer is at most sites realized via Modem and GSM or FTP, respectively.

The accuracy of both soil moisture sensor types has been investigated within this PhD work using laboratory and field measurements. The setup and results of the measurements used for the evaluation can be found in Chapter 2. Regarding the laboratory measurements, sensor calibration is often based on the following two steps: First, the signal response of the sensors to permittivity is estimated and in the second step, the permittivity is related to the volumetric water content (e.g. Seyfried and Murdock, 2004; Jones et al., 2005). Here, however, we directly related the sensor reading to the volumetric water content. Personal communication with C. Campbell and M. Galloway from Decagon Devices on 16 March 2009 confirmed that the calibration procedure described in Chapter 2 is an appropriate alternative. As a result of the first study of this PhD the 10HS sensors were specifically calibrated at each site using field measurements of parallel installed TDR-based sensors. To establish the calibration function, the sensor reading of the 10HS was related to the TDR measurements (m^3/m^3) by a least square exponential fit. If possible, a single calibration function for each depth was established. For sites without TDR measurements at all depths, the 10HS measurements closest to the TDR measurement in either 10 or 80 cm (or 10, 30 and 80 cm for the SwissSMEX-*Veg* sites) were merged and related to the corresponding depth.
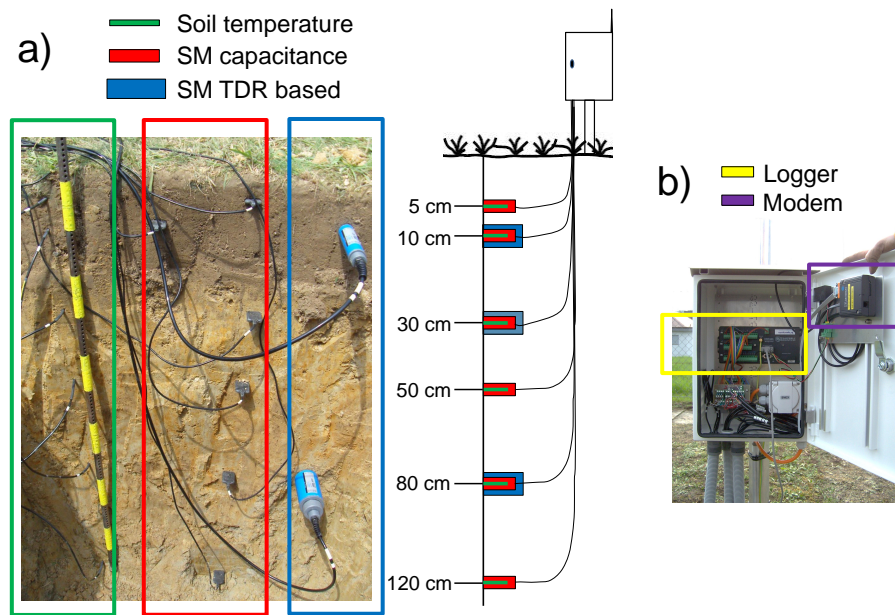
Figure 1.8: *Schematic of the general instrumentation of a SwissSMEX/-Veg site. (a) Soil moisture (SM) and soil temperature sensors. Note that the TDR based sensors at 30 cm depth is additionally installed at SwissSMEX-Veg sites. For detailed information about the site-specific instrumentation see Appendix B. (b) Logger and communication module.*
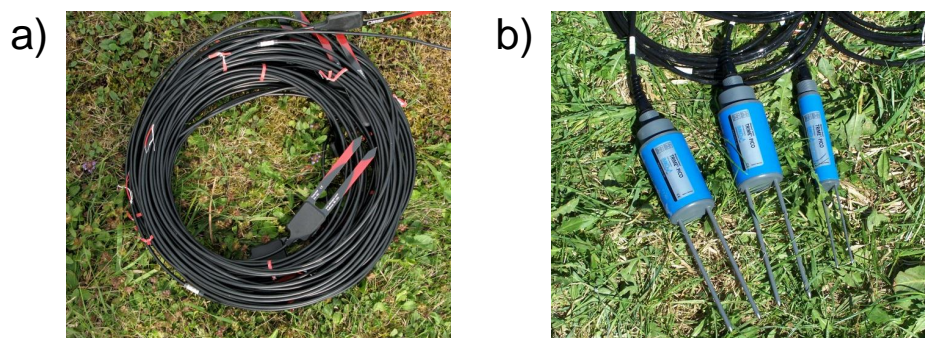
Figure 1.9: *Soil moisture sensors used in the SwissSMEX/-Veg project: (a) The capacitance sensor 10HS (Decagon Devices, United States) and (b) the TDR based sensors TRIME-PICO32 and TRIME-PICO64 (IMKO GmbH, Germany).*

1.5   Aims and outline

The previous sections have shown that soil moisture can significantly impact the climate system through feedbacks with evapotranspiration, temperature, and precipitation and that it is an important memory component for the regional climate. For climate science, observations and estimates of soil moisture are versatile: They can be used to estimate surface fluxes, to investigate and better understand the processes underlying land-climate interactions, and to evaluate climate models and their parameterizations. Nevertheless, long-term soil moisture measurement networks have traditionally been scarce (Robock et al., 2000). The main objective of this thesis was to establish the SwissSMEX network (Section 1.4.2) for long-term soil moisture measurements, and to analyze the resulting measurements with respect to soil moisture dynamics in Switzerland. The planing, sensor calibration using laboratory and field measurements, as well as the set up of the 19 sites took a major part of this thesis. As a result, time series of soil moisture with high temporal resolution (10 minutes) on a large spatial extent (about 150x210 km) are the data basis for the presented analyses. The thesis is organized in five Chapters and an Appendix. As a low-cost soil moisture sensor type is used for the set up of the sites, the need of a quantification of its accuracy and its evaluation for climate research is the topic of the first two studies (Chapters 2 and 3). Both studies include the assessment of the sensors for applications in climatology and/or hydrology. Chapter 4 presents a new perspective on the analysis of spatio-temporal variability of soil moisture and its temporal anomalies. The impact of different vegetation cover on soil moisture is investigated in a preliminary study (Chapter 5). Two of the chapters are already published (Chapter 2), one is accepted for puplication (Chapter 3) and one is submitted (Chapter 4) and are therefore presented in the form of self-contained scientific papers. Chapter 5 is based on a supervised Bachelor Thesis and will serve as basis for a fourth publications. The detailed outline is as follows:

- **Chapter 2:** Soil moisture monitoring for climate research: Evaluation of a low-cost sensor in the framework of the Swiss Soil Moisture Experiment (SwissSMEX) campaign *(Mittelbach et al., 2011)*

- **Chapter 3:** Comparison of four soil moisture sensors under field conditions in Switzerland *(Mittelbach et al., 2012a, accepted)*

- **Chapter 4:** A new perspective on the spatio-temporal variability of soil moisture: Temporal dynamics versus time invariant contributions *(Mittelbach and Seneviratne, 2012b, submitted)*

- **Chapter 5:** Soil moisture and soil temperature development across different land cover types

- **Chapter 6:** Conclusion and Outlook

- **Appendix A:** Climatic Regions of Switzerland according to (Müller 1980)

- **Appendix B:** Site-specific characteristics of the SwissSMEX network

Chapter 2

Soil moisture monitoring for climate research: Evaluation of a low-cost sensor in the framework of the Swiss Soil Moisture Experiment (SwissSMEX) campaign

Soil moisture monitoring for climate research: Evaluation of a low-cost sensor in the framework of the Swiss Soil Moisture Experiment (SwissSMEX)

Heidi Mittelbach[1], F. Casini[2], I. Lehner[1], A.J. Teuling[1,3], and S.I. Seneviratne[1]

Abstract

Soil moisture measurements are essential to understand land surface-atmosphere interactions. In this paper we evaluate the performance of the low-cost 10HS capacitance sensor (Decagon Devices, United States) using laboratory and field measurements. Measurements with 10HS sensors of volumetric water content (VWC, Vol.%), integrated absolute soil moisture (millimeters) over the measured soil column, and the loss of soil moisture (millimeters) for rainless days are compared with corresponding measurements from gravimetric samples and time domain reflectometry (TDR) sensors. The field measurements were performed at two sites with different soil texture in Switzerland, and they cover more than a year of parallel measurements in several depths down to 120 cm. For low VWC, both sensor types present good agreement for laboratory and field measurements. Nevertheless, the measurement accuracy of the 10HS sensor reading (millivolts) considerably decreases with increasing VWC: the 10HS sensors tend to become insensitive to variations of VWC above 40 Vol.%. The field measurements reveal a soil type dependency of the 10HS sensor performance, and thus limited applicability of laboratory calibrations. However, with site-specific exponential calibration functions derived from parallel 10HS and TDR measurements, the error of the 10HS compared to the TDR measurements can be decreased for soil moisture contents up to 30 Vol.%, and the day-to-day variability of soil moisture is captured. We conclude that the 10HS sensor is appropriate for setting up dense soil moisture networks when focusing on medium to low VWC and using an established site-specific calibration function. This measurement range is appropriate for several applications in climate research, but the identified performance limitations should be considered in investigations focusing on humid conditions and absolute soil moisture.

2.1 Introduction

Soil moisture is a key variable of the climate system. It affects surface fluxes and can subsequently impact air temperature, boundary layer stability, and precipitation (see e.g. Seneviratne et al., 2010, for a review). Long-term measurement networks of soil moisture have traditionally been scarce (e.g. Robock et al., 2000), due to the associated high costs and delayed recognition of the importance of soil moisture for climate modeling and regional weather prediction. However, the investigation of soil moisture-climate relationships has gained increasing attention in

---

[1]Institute for Atmospheric and Climate Science, ETH Zurich, Zurich, Switzerland

[2]Institute for Geotechnical Engineering, ETH Zurich, Zurich, Switzerland

[3]Hydrology and Quantitative Water Management Group, Wageningen University, Wageningen, Netherlands

recent years (e.g. Betts, 2004; Koster et al., 2004; Seneviratne et al., 2006a; Dirmeyer et al., 2006; Vautard et al., 2007; Teuling et al., 2010b; Hirschi et al., 2011), and new measurement techniques, such as ground penetrating radar GPS (Larson et al., 2008), the measurement of cosmic ray neutrons (Zreda et al., 2008) distributed temperature sensors (Steele-Dunne et al., 2010) and remote sensing (e.g. Schmugge et al., 2002; Tapley et al., 2004; Jackson, 2005; Wagner et al., 2007b; de Jeu et al., 2008) have been developed. Remote sensing, in particular, has several limitations: Microwave-based measurements only capture soil moisture from top soil layers (few centimeters), and estimates from the Gravity Recovery and Climate Experiment (GRACE) only provide large-scale estimates (400-500 km resolution, Ramillien et al. (2008) and do not distinguish between soil moisture, groundwater, snow, and other forms of land water storage.

Hence, ground-truth data remain crucial for the calibration and validation of remote sensing-derived estimates and for the evaluation of land surface and climate models. Historically, long-term networks were only available in a few regions, for example in Illinois (Hollinger and Isard, 1994), the former Soviet Union (Vinnikov and Yeserkepova, 1991), as well as in China and Mongolia (see Robock et al., 2000; Seneviratne et al., 2010, for an overview). These networks used labor-intensive, non-continuous and/or destructive measurement techniques, e.g. gravimetric sampling or neutron probe measurements. Continuous measurements of soil moisture, however, may be of key relevance when investigating e.g. soil moisture persistence patterns or soil moisture-atmosphere interactions and feedbacks. This latter aspect is also relevant for the validation of remote sensing products. Through the increasing interest of soil moisture in different disciplines, in 2010 the International Soil Moisture Network (ISMN) was established (http://www.ipf.tuwien.ac.at/insitu). It is operated in cooperation with the Global Soil Moisture Databank (Robock et al., 2000) and involves several non-continuous and continuous networks in America, Australia, Asia and Europe.

Two of the most common techniques allowing continuous soil moisture measurements make use of the dependency of the permittivity of the soil on volumetric water content (Robinson et al., 2008). These are either based on time domain reflectometry (TDR) (see e.g. Topp and Reynolds, 1998; Robinson et al., 2003; Topp, 2003; Robinson et al., 2008) or soil capacitance techniques (e.g. Dean et al., 1987; Topp, 2003; Bogena et al., 2007; Robinson et al., 2008). TDR sensors operate at higher frequencies and have been shown to be of higher accuracy than the capacitance-based sensors (e.g. Walker et al., 2004; Robinson et al., 2008). The capacitance sensors, on the other hand, are less accurate but are also of significantly lower cost. This allows the use of a higher number of instruments and thus much denser networks. Given the strong spatial and temporal variability of soil moisture at relatively small scales (e.g. Teuling and Troch, 2005), it has been suggested that it would be an advantage for some applications to choose less accurate but cheaper sensors in order to decrease the sampling error due to spatial variability (see e.g. Teuling et al., 2006b; Bogena et al., 2007; Robinson et al., 2008). Accordingly, several networks have been established recently using capacitance probes. One example is the Soil Climate Analysis Network (SCAN) in the United States (http://www.wcc.nrcs.usda.gov/scan/), where soil moisture is measured since 1991.

Several previous studies have evaluated the performance of low cost sensors (e.g. Roth et al., 1990; Veldkamp and O'Brien, 2000; Czarnomski et al., 2005; Bogena et al., 2007). The con-

clusions for the calibration differ and depend on the sensor type. In general, laboratory tests are needed to verify whether the volumetric water content (VWC) can be estimated accurately with a universal calibration equation, often supplied by the manufacturer (Baumhardt et al., 2000; Veldkamp and O'Brien, 2000). Baumhardt et al. (2000) stress the need of a soil-specific calibration for a multisensor capacitance probe especially under conditions of near-saturation. Bogena et al. (2007) evaluated a low cost soil moisture sensor by including laboratory and field experiments with a TDR as reference sensor. They found significant differences between the TDR and the low-cost sensor measurements when a calibration function derived from laboratory experiments was used. Veldkamp and O'Brien (2000) solved the limited applicability of the manufacturer's empirical calibration function using a three phase mixing model to generate a more robust calibration for a sensor based on frequency domain reflectometry.

In the present article, we evaluate the performance of a low cost soil moisture sensor for climate monitoring under controlled and field conditions, using laboratory measurements and measurements from two different Swiss Soil Moisture EXperiment (SwissSMEX, Section 2.3) sites. The main objectives of this study are to derive error estimates associated with these instruments, the possibility to transfer laboratory findings of the performance of the low cost sensor to field conditions and to evaluate the possibility to represent VWC and absolute soil moisture using the capacitance sensor. These aspects are of key relevance for the validation of land surface and climate models and the possible assimilation of soil moisture observations in these models.

The article is structured as follows. First, data and methods, including instruments, laboratory and field measurements as well as data processing used in this study are presented in Section 2.2. Results from the laboratory and field measurements are presented and evaluated in Section 2.3. A discussion of the results and their significance for the climate community, as well as the main conclusions are provided in Section 2.4.

2.2 Data and method

2.2.1 Instruments

The instruments used in this study are the TRIME-EZ and TRIME-IT sensors (IMKO GmbH, Germany) based on the TDR technique, and the 10HS sensor (Decagon Devices, USA) based on the capacitance technique. The used TRIME-IT and TRIME-EZ sensors have rod lengths of 11 and 16 cm, respectively. They measure at a frequency of 1 GHz and are independent of the excitation voltage. The applied 10HS sensor has a rod length of 10 cm and measures with a frequency of 70 MHz. The 10HS is superior to the forerunner and widely used EC-5 sensor (Decagon Devices, USA) because of its independency from the excitation voltage and the larger sampling volume, which results in more robust estimates of average spatial soil moisture conditions. Data are logged with a Campbell Scientific CR1000 data logger. Characteristics of both sensor types as provided by the manufacturers are listed in Table 2.1.

Table 2.1: *Characteristics of the two investigated sensor types provided by the manufacturers[a]*

Sensor Measurement Technique	Range of VWC[b]	Operating Temperature	Accuracy	Relation mV-VWC
10HS (Decagon Devices, USA) capacitance technique	0 to 57 Vol.%	0 °C to 50 °C	± 3 Vol.% using the standard calibration ± 2 Vol.% using soil specific calibration	polynomial third order
TRIME-IT, TRIME-EZ (IMKO GmbH, Germany) time domain reflectometry	0 to 100 Vol.%	-15 °C to 50 °C	± 1 Vol.% for 0 to 40 Vol.% ± 2 Vol.% for 40 to 70 Vol.%	linear

[a] See Decagon Devices [2009] and IMKO [2006].
[b] Volumetric water content.

2.2.2 Laboratory measurements

The aim of the laboratory measurements is to estimate the difference in VWC between the 10HS and the TRIME-IT/-EZ sensors, to estimate the sensitivity as well as the variability within the 10HS sensors. Gravimetric samples are taken as reference measurements.

The experiment included five calibration runs (hereafter referred to as CAL1 to CAL5). For each calibration run three plastic containers (26.6 cm x 36.6 cm x 23 cm) with different levels of water content were prepared. These water contents were chosen such that the 'first-guess' values cover the range of interest: The necessary mass of soil and water was calculated using the known volume of the plastic containers, the density of solid material (quartz was assumed for both soils) and a mean target porosity. The target porosity was chosen by taken the mean porosity from the Swiss field site of Rietholzbach (http://www.iac.ethz.ch/url/rietholzbach, Weiler (2001)). When the measurements with the sensors were completed, three gravimetric samples were taken out of each container in the depth of the sensor measurements. These gravimetric samples were then used to correct the 'first-guess' values to a reference VWC for the laboratory experiment.

Two different materials with known soil properties were used for the measurements: 1) Australian sand (AUS-S), which was chosen because of its homogeneous grain size distribution, with a VWC ranging from 5.2 to 30.2 Vol.%; and 2) fine material with grain size < 2 mm from the soil of the SwissSMEX field site Oensingen (OEN-S) with three VWCs ranging from 3.2 to 55.4 Vol.%. The measurements with the sensors were conducted one day after preparing the AUS-S/OEN-S soils with the assumed water content in order to obtain equilibrium water content conditions. Each of the three containers entailed four 10HS sensors; one of them was left in the container as reference to ensure that the VWC during one calibration run was steady. In total 107 10HS sensors were tested. Seven TRIME sensors were included in CAL3 and CAL5. These measurements were conducted parallel to the measurements with the 10HS. During the whole experiment the boxes were covered to minimize evaporation. A summary of the single VWC for each calibration run is provided in Table 2.2. The listed mean VWC and the corresponding standard deviation refer to the three VWC of the gravimetric samples.

Table 2.2: *Material, Mean and Standard Deviation (std) of Volumetric Water Content (VWC), and Bulk Density (ρ_B) of the Gravimetric Samples for the Different Calibration Runs*

Calibration Run	Material	Mean VWC (Vol.%)	std VWC (Vol.%)	Mean ρ_B (g/cm^3)	std ρ_B (g/cm^3)
CAL1	AUS-S	5.9	1.0	1.51	0.04
		16.3	1.5	1.53	0.01
		28.9	1.1	1.55	0.01
CAL2	AUS-S	5.2	1.0	1.51	0.01
		18.4[a]	-	1.49	-
		30.3	1.7	1.54	0.00
CAL3	AUS-S	6.8	0.47	1.49	0.03
		13.3	0.42	1.51	0.00
		30.1	1.4	1.5	-
CAL4	AUS-S	6.9	0.4	1.46	0.03
		11.4	0.09	1.42	0.03
		29.3	2.9	1.37	0.12
CAL5	OEN-S	3.2[a]	-	1.27	-
		39.0	2.22	1.12	0.05
		55.4	2.47	1.02	0.04

[a] Only one gravimetric sample.

2.2.3 Field measurements

The SwissSMEX project (Swiss Soil Moisture EXperiment, http://www.iac.ethz.ch/url/research/SwissSMEX) has been initiated by ETH Zurich, Agroscope ART, and MeteoSwiss in June 2008 with the aim to establish a long-term soil moisture measurement network in Switzerland. In 2010 the complementary project SwissSMEX-Veg was established to enhance the coverage of different land covers. At present, the network consists of 19 sites (Figure 2.1), including the Rietholzbach research catchment site (http://www.iac.ethz.ch/url/research/rietholzbach), several Swiss FluxNet sites (http://www.swissfluxnet.ch), and selected SwissMetNet stations (http://www.meteoswiss.admin.ch). The sites were set up at grassland (14 sites), forest (4 sites) and arable land (1 site) sites. When the holes were dug for installation of the sensors, care was taken to preserve the original sequence of soil horizons. Soil moisture sensors were installed horizontally into the undisturbed soil. After the installation of the sensors, the soil was compacted upon refilling taking care that the soil horizons were arranged in the original order and with the original density.

For the present field evaluation of the 10HS sensors, data from the SwissSMEX sites Oensingen (OEN) and Payerne (PAY) were used. Land use at both sites is managed grassland. For the grain size analysis, the pipette method (Scott, 2000) was used after the organic matter was removed by oxidation with hydrogen peroxide. The organic fraction was determined using the dichromate oxidation method (Margesin, R. and Schinner, 2005). Details about the soils properties are listed in Table 2.3. At both sites soil moisture is measured with parallel profiles of 10HS and TRIME-IT/-EZ at a temporal resolution of 10 minutes. At OEN the sensors were installed at depths of 5, 10, 30, 50, 73, and 120 cm. A gravel layer exists between 75 and 95 cm

depth. At PAY the sensors were installed at 5, 10, 30, 50, and 80 cm depth (the deepest sensor could not be installed due to the presence of molasse). This study is based on observations over a 13-month period (1 September 2008 to 1 October 2009).
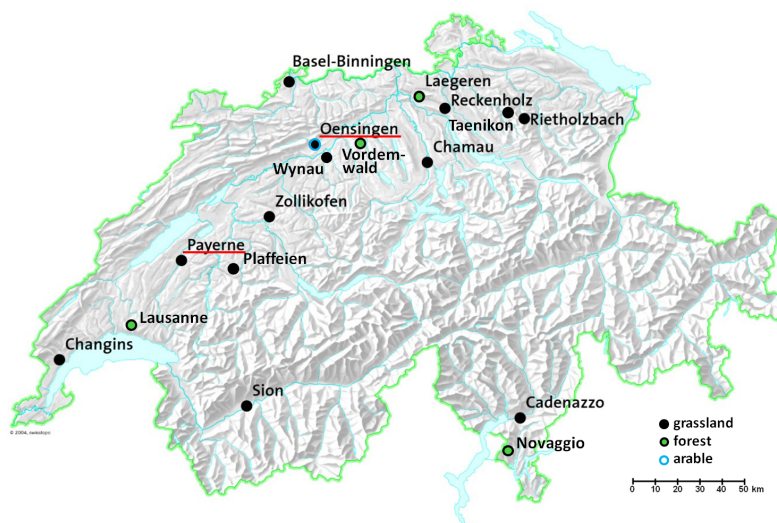
Figure 2.1: *Map of Switzerland showing the location and land use of the SwissSMEX/-Veg soil moisture monitoring sites; highlighted are the sites OEN and PAY involved in this evaluation.*

Table 2.3: *Basic soil properties for OEN and PAY, with texture according to USDA soil taxonomy*

Site	Depth (cm)	Clay (<2 μm)	Silt (2-63 μm)	Sand (>63 μm)	Texture	Bulk Density (g/cm^3)	Organic Fraction (%)
OEN	0-25	28.2	57.9	13.9	Silty clay loam	1.39	3.4
	25-75	25.8	56.3	17.9	Silt loam	1.49	2.2
	75-95				Gravel layer		
	95-120	30.2	62.5	7.3	Silty clay loam	1.45	1.4
PAY	0-30	5.9	41.8	52.3	Sandy loam	1.49	1.5
	30-100	19.0	41.7	39.3	Loam	1.49	0.4

2.2.4 Data processing

For the evaluation of the 10HS sensor four evaluation criteria were taken into account: 1) the accuracy of sensor reading [mV]; 2) the absolute VWC [Vol.%] for the laboratory and field measurements; 3) the absolute soil moisture [mm], and 4) the daily soil moisture loss [mm]. The accuracy of the 10HS sensor reading was performed with the laboratory measurements and included the standard deviation between the used 10HS sensor for each VWC and the sensitivity of the sensor reading with increasing VWC. The sensitivity was performed by including the difference in sensor reading (dv_n) per unit of VWC ($dVWC_n$) as used in Bogena et al. (2007):

$$\frac{dv_n}{dVWC_n} \approx \frac{v_{n+1} - v_{n-1}}{VWC_{n+1} - VWC_{n-1}}, \tag{2.1}$$

The second criteria for the evaluation considered the transformation of the 10HS sensor reading [mV] to VWC [Vol.%]. This was realized using three different approaches. First, the 3rd order polynomial function provided by the manufacturer (Decagon Devices, 2009) was used. In the second approach, a calibration function was established by relating the sensor reading [mV] to the reference VWC [Vol.%] by a least square exponential fit. For the laboratory measurements the gravimetric samples were used as reference. The resulted function is hereinafter called the "Best lab fit". The more reliable TDR sensors (Robinson et al., 2008) that were installed paralleled with the 10HS were used as reference in the field. The resulted function is hereinafter called "Best field fit". For the computation of the Best field fit, only measurements in 10 cm and 80 cm depths were used, since most other SwissSMEX sites entail TDR measurements in these two depths only. By considering the 10 cm and 80 cm measurements, information about the variability of soil moisture of the 10 cm near-surface layer was implemented directly and information of soil properties of two different depths was implemented indirectly. The TDR and capacitance measurements at the two depths were merged and binned with the accuracy of the 10HS (3 Vol.%) mentioned by the manufacturer (Decagon Devices, 2009). The validation of the established function hereafter was performed for the measurements in all depths. In a third approach to transform the sensor reading into VWC was based on the concept of the three-phase mixing model (Veldkamp and O'Brien, 2000) using:

$$\theta = \frac{[x^\alpha - (1 - \varphi)Per_s^\alpha - \varphi Per_a^\alpha]}{Per_w^\alpha - Per_a^\alpha}, \tag{2.2}$$

where θ volumetric water content, x Sensor output [mV], α geometric parameter, φ porosity, Per_s specific sensor output for soil matrix [mV], Per_a specific sensor output for air [mV], and Per_w specific sensor output for water [mV]. The porosity was estimated using the specific weight of quartz of 2.65 g/cm^3 and the mean bulk density for each calibration run for the laboratory measurements (Table 2.2) and for each soil horizon for the field measurements (Table 2.3), respectively. The sensor output for air and water included measurements of the sensor in air and water. For the sensor output of the soil matrix, measurements made in oven-dried AUS-S were used. The parameter α, which defines the shape of the calibration function, was fitted.

For the field measurements, the difference in absolute soil moisture S [mm] for the hydrological year 01.10.2008 to 30.09.2009, spring 2009 (MAM) and summer 2009 (JJA) was involved as the third criteria for the evaluation. S was calculated by integrating the measurements of the TRIME and 10HS capacitance sensors, respectively, over the whole soil column. Each measurement is representative for one soil layer. The soil layer thickness is given by the mean distance to the closest upper and lower sensor (Figure 2.2). As last evaluation criteria the daily soil moisture loss [mm] and its translation in evapotranspiration [mm] and latent heat flux [W m^{-2}] was quantified and involved due to its interest in the context of land surface-atmosphere interactions and related climate investigations (e.g. Seneviratne et al., 2010). To isolate evapotranspiration from other fluxes (i.e. drainage), only recession periods starting at the fourth day after a precipitation event, for the period June to September 2009 were considered. As goodness of fit the adjusted R^2 and RMSE regarding to the gravimetric (RMSE$_G$) and TDR measurements (RMSE$_T$), respectively, were used. Furthermore, density and frequency plots were considered to highlight the performance of points with higher probability.
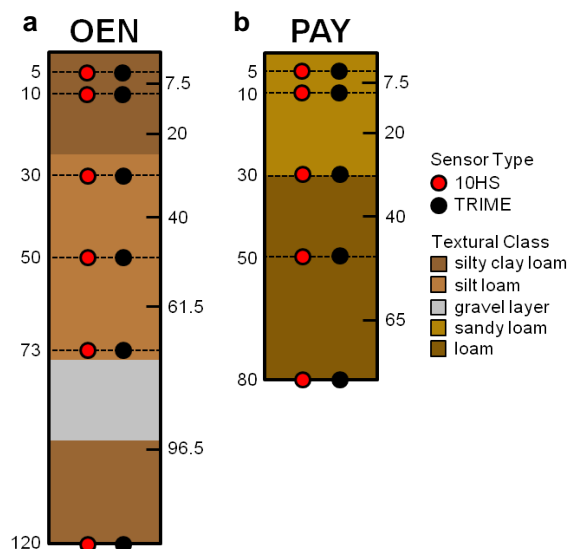
Figure 2.2: *Measurement profile at sites (a) OEN and (b) PAY. The numbers on the left side of the profiles indicate measurement depths of the sensors. The numbers on the right side indicate the integration depth for each sensor used to calculate the absolute soil moisture (millimeters).*

2.3   Results

2.3.1   Laboratory measurements

The results of the laboratory measurements for both soils (AUS-S and OEN-S) with VWCs ranging from 3.9 to 55.4 Vol.% are shown in Figure 2.3a. The TRIME sensor captured the reference VWC with an overall $RMSE_G$ of 1.5 Vol.%, which corresponds to the specification from the manufacturer (Table 2.1). By contrast, the 10HS sensor showed considerable biases in the measured VWC, independently of the fitting curve (Decagon Version 2.0 function or Best lab fit). The Decagon Version 2.0 calibration function displayed an erroneous relationship, with approximately correct VWC for 10 Vol% and 30 Vol%, but an overestimation in between, and underestimation (plateauing values) above 30-40 %. The overall $RMSE_G$ amounted to 7.1 Vol.%. The plateauing behavior means that the calibration function is not suitable above 30-40 Vol%, a performance considerably lower than the 57 Vol.% suggested by the manufacturer (Decagon Devices, 2009). The Best lab fit improved the overall $RMSE_G$ to 3.5 Vol.%. Furthermore, it allowed for a reliable conversion of the sensor reading up to 50 Vol.%. However, application of the Best lab fit increased the variability around 30% VWC.

The variation within the 10HS sensor type is shown in Figure 2.3b and is nearly steady over the whole measurement range. The sensor sensitivity as derivation dv/dVWC [mV/Vol.%] in respect to the VWC showed a strong decrease with increasing VWC. For a mean VWC of about 5 Vol.% the derivation is about 21 mV/Vol.%. In contrast for a VWC of 50 Vol.% the derivation is about 4 mV/Vol.%. The decreasing sensitivity is caused by the measurement principle of capacitance sensors, by which the capacitor charges slower at high VWC.
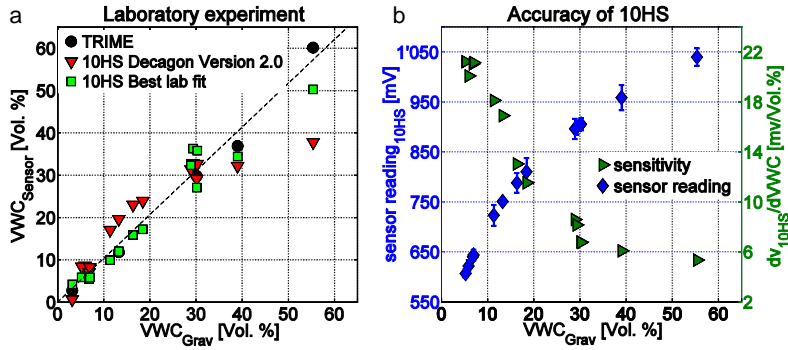
Figure 2.3: *Results of the laboratory measurements with TRIME (TDR) and 10HS (capacitance) sensors as a function of the volumetric water content of the gravimetric samples. (a) VWC from TDR and 10HS. For the 10HS sensor, two calibration functions are displayed (Decagon Version 2.0 function and best lab fit). (b) Measurement accuracy of sensor reading, showing the variability within the 10HS sensor type (blue) and the derivation dv/dVWC of the 10HS sensor (green). Error bars represent the standard deviation within the tested 10HS sensors.*

2.3.2   Field measurements

As mentioned in the Section 2.2.4 and verified by the laboratory results (Section 2.3.1), the TDR sensors can be used as a reliable reference to evaluate the performance of the 10HS capacitance sensors in the field. The validation of the 10HS measurements using the three calibration functions (Decagon Version 2.0, Best lab fit, Best field fit) for measurements at all depths (6 in OEN and 5 in PAY) is shown as density plots in Figure 2.4. Similarly to the laboratory experiment, the VWC resulting from the Decagon Version 2.0 calibration leveled off at 30-40 Vol.% (Figure 2.4a, e). This effect had the most impact at the OEN site, which is characterized by high clay content (Table 2.3) and thus results in a generally higher VWC. Nevertheless, the absolute value of the derived VWC for low water contents ($< 30\text{-}35$ Vol%) agreed well for both field sites. Application of the Best lab fit (Figure 2.4b, f) resulted in an expansion of VWC estimates to higher values, but also in an enhanced spread of the data over the whole range of measured VWC. The VWCs with highest relative occurrence is overestimated and the lower VWCs are not represented well anymore. Consequently, the $RMSE_T$ increased for the Best lab fit compared to the Decagon Version 2.0 function from 4.4 to 6.5 Vol.%, and 4.0 to 5.5 Vol.%, for OEN and PAY, respectively. By contrast, the Best field fit (Figure 2.4c, g) led to a marked improvement in the estimation of the VWC values that occur most frequently. The data were expanded to higher VWC, while lower VWC were still well represented. This results in a decrease of the $RMSE_T$ compared to the Decagon Version 2.0: from 4.4 to 3.2 Vol.% for OEN and from 4.0 to 3.0 Vol.% for PAY. The parameters and statistics of the Best field fit at the two sites are listed in Table 2.4. The application of the three-phase mixing model (Figure 2.4d, h) with $RMSE_T$ of 6.7 Vol.% and 7.7 Vol.% for OEN and PAY, respectively, did not lead to improved estimates within this study. Because of the low performance of the Best lab fit and the three-phase model within this study, the Best field fit was used in subsequent analyses.

The mean absolute error of the VWC of the 10HS sensor at the OEN and PAY sites using the Decagon Version 2.0 and Best field fit is shown in Figure 2.5. Additionally, the frequency histogram for each 3 Vol.%-class is displayed in the bottom panels of Figure 2.5. Consistent
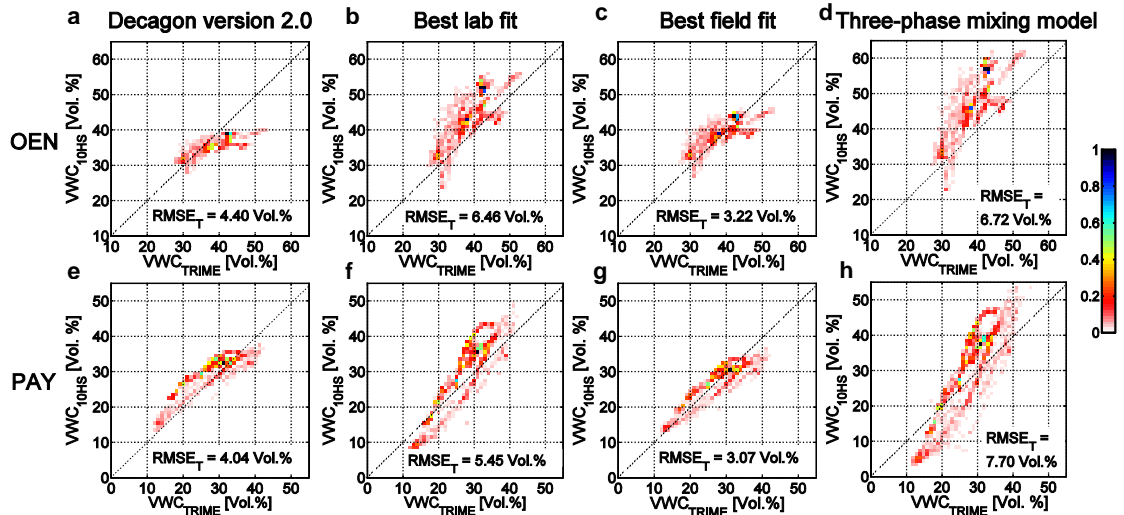
Figure 2.4: *Relations between TRIME (TDR) and 10HS (capacitance) measurements of volumetric water content in the field: (a, b, c, d) OEN and (e, f, g, h) PAY. Applied functions provided by the manufacturer Decagon version 2.0 (Figures 2.4a, e), the best lab fit (Figures 2.4b, f), the best field fit (Figures 2.4c, g), and three phase mixing model (Figures 2.4d, h). Panels show the occurrence (relative to maximum) of volumetric water content (Vol.%) for the whole time period 1 September 2008 to 1 October 2009. The $RMSE_T$ is calculated with respect to TRIME (TDR) measurements.*

with Figure 2.4, this analysis revealed that the 10HS sensor slightly overestimates the VWC at lower soil moisture contents ($< 30\text{-}35$ Vol%) and underestimates it at higher VWC. The Best field fit resulted in an absolute error of less than 2 Vol.% for VWC ranges including most measurements (34 to 43 Vol.% for OEN and 24 to 36 Vol.% for PAY). However, the behavior of the sensor was different for the two sites, due to their difference in measured VWC. For the clayey OEN site (Figure 2.5a), the Decagon Version 2.0 function led to smaller absolute errors than the Best field fit at low VWC. On the other hand, for high VWC values the absolute errors were much larger than using the Best field fit (13 Vol.% compared to a maximum error of 8 Vol.% using the Best field fit). By contrast, at the loamy site PAY (Figure 2.5b), the Best field fit limited the absolute error to around 2 Vol.% starting from low VWC up to 36 Vol.%, while for VWC larger than 36 Vol.% the absolute error increased up to 8 Vol.% and was smaller using the Decagon Version 2.0 function (with a maximal error of 6 Vol.%). This analysis thus reveals the important role of the soil type for the performance of the site-specific calibration.

The temporal evolution of precipitation and 2-m air temperature, together with the absolute soil moisture S [mm] are displayed for both sites in Figure 2.6a-d. Both the TRIME and 10HS sensor agreed well regarding the timing of soil moistening and drying, which also matched the meteorological data. Using the Best field fit for the 10HS sensor generally improved the derived absolute soil moisture, with the exception of the summer 2009 time period at the OEN site. The corresponding $RMSE_T$ for four time periods (hydrological year 1 October 2008 to 30 September 2009, spring 2009, summer 2009, and spring-summer 2009) are shown in Figure 2.7.
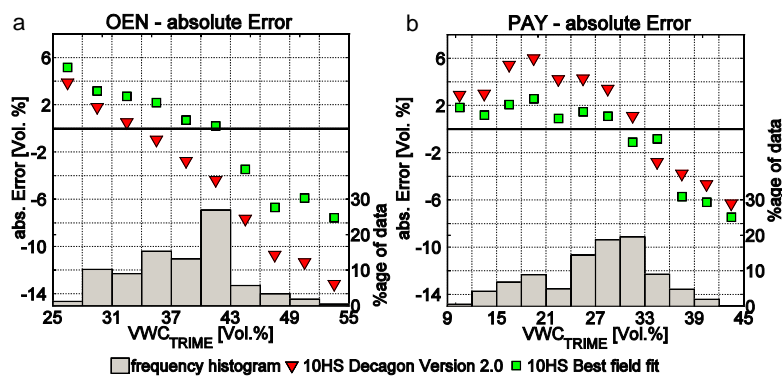
Figure 2.5: *Absolute errors of the 10HS measurements using the manufacturer (Decagon Version 2.0) and best field fit functions with frequency distribution of volumetric water content at the (a) OEN and (b) PAY sites. The error is calculated as the difference between 10HS and TRIME.*
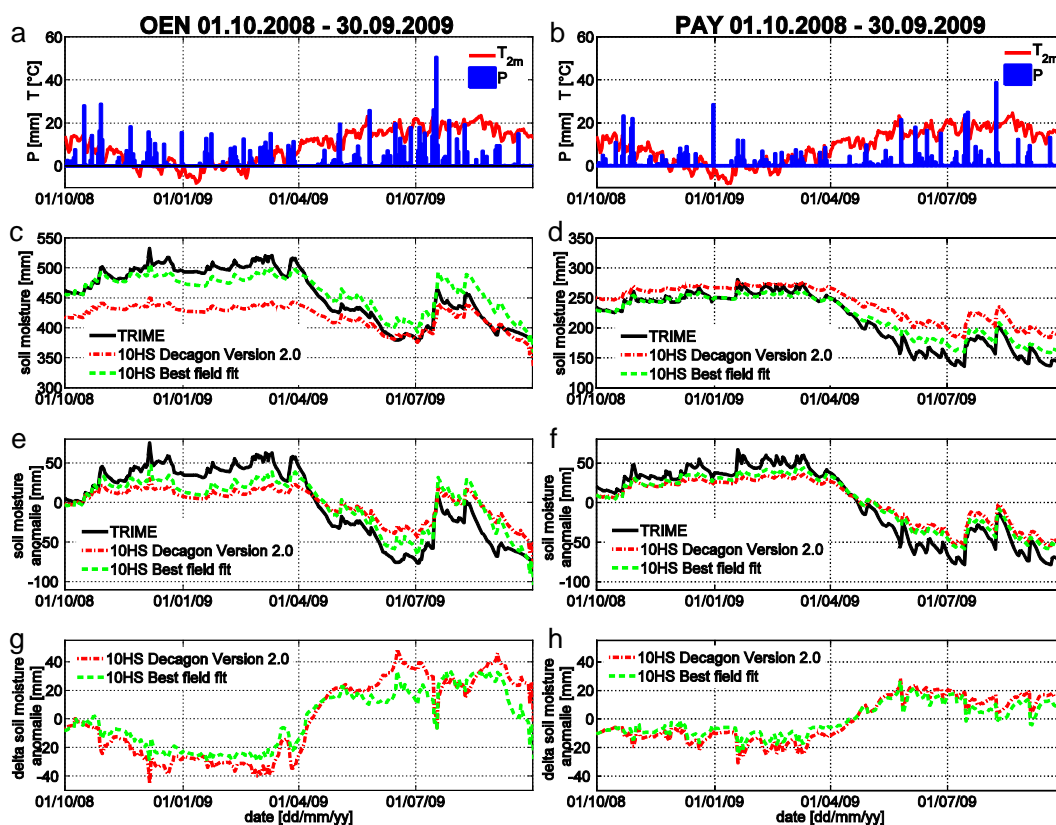
Figure 2.6: *Temporal evolution of the main climate drivers and soil moisture during the field experiment at the site (a, c, e, g) OEN and (b, d, f, h) PAY. Figures 2.6a, b show daily precipitation (P) and temperature (T), Figures 2.6c and 2.6d show soil moisture, Figures 2.6e and 2.6f show the soil moisture anomalies (soil moisture relative to the average of available time period), and Figures 2.6g and 2.6h show the difference in soil moisture anomalies (10HS-TDR) (mm) over the soil column with different calibration functions during the hydrological year 1 October 2008 to 30 September 2009.*
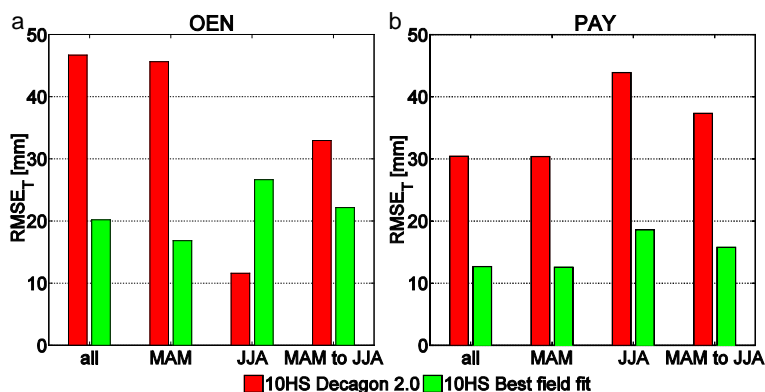
Figure 2.7: *Difference between absolute 10HS measurements derived using two calibration functions and TRIME measurements expressed as $RMSE_T$ (millimeters) for the hydrological year 1 October 2008 to 30 September 2009 (all), spring 2009 (MAM), and summer 2009 (JJA), and over the period spring to summer 2009 (MAM to JJA) at the sites (a) OEN and (b) PAY.*
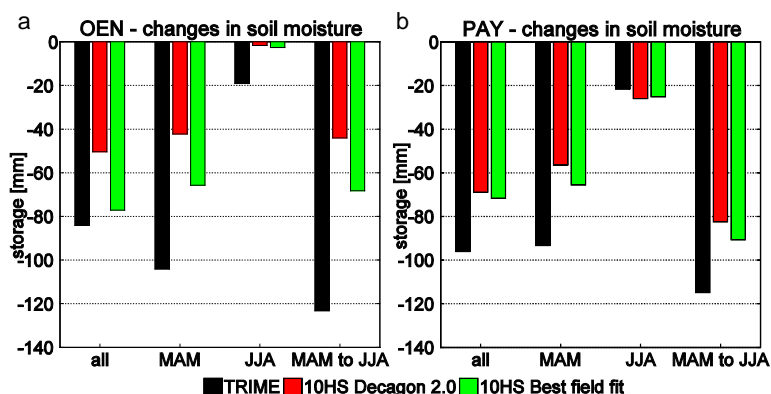
Figure 2.8: *Changes in soil moisture (millimeters) during the hydrological year 1 October 2008 to 30 September 2009 (all), spring 2009 (MAM), and summer 2009 (JJA), and over the period spring to summer 2009 (MAM to JJA) at the sites (a) OEN and (b) PAY.*

Over the whole hydrological year, the $RMSE_T$ decreased from 47 mm to 20 mm at the OEN site, and from 30 mm to 13 mm for the PAY site. At the PAY site, similar decreases (ca. 60%) in $RMSE_T$ were found for all analyzed time periods. The only case when the Best field fit did not reduce the $RMSE_T$ (as also identified in Figure 2.6 is at the OEN site for the 2009 summer. For this time period and site, one should note that with either estimates (Decagon Version 2.0 function and Best field fit), the 10HS sensor measurements erroneously suggest that the summer 2009 absolute soil moisture values are close to winter values (and thus close to saturation), while the TRIME measurements revealed a depleted absolute soil moisture. The reason is the small sensitivity of the 10HS due to the non linearity between the sensor reading and the VWC (see Figure 2.3b) with increasing VWC. Focusing on soil moisture anomalies (absolute soil moisture relative to the long term mean, Figure 2.6e, f) and the difference of the soil moisture anomalies (Figure 2.6g, h) between the 10HS and TDR, only a slight improvement using the Best field fit compared to the Decagon Version 2.0 was identified. Nevertheless, using the Best

field fit, the standard error was decreased from 27 mm to 20 mm for the OEN site and from 15 to 11 mm for the PAY site (not shown). Taking into account the changes in absolute soil moisture [mm] for the considered time periods, the largest errors for the 10HS sensor measurements were found during the spring dry-downs (Figure 2.8), with smaller errors when applying the Best field fit. For the OEN site the difference in spring compared to TRIME was decreased by 22% using the Best field fit. For the site PAY this difference was reduced by 10%.

The daily soil moisture loss, used to estimate the evapotranspiration [mm] or the latent heat flux [Wm^{-2}], is shown in Figure 2.9. For PAY, the TRIME and the 10HS sensors displayed decreasing soil moisture loss with decreasing mean absolute soil moisture (Figure 2.9b). The limitation of the 10HS sensor readings for high VWC led to a maximum daily soil moisture loss in the order of 4 mm. The 10HS got more comparable to the TRIME with decreasing daily soil moisture. As a consequence, the latent heat flux on a daily time scale under dry conditions was represented satisfactorily using the low cost sensor. The maximal difference in absolute soil moisture was 1.5 mm (corresponds to a latent heat flux of 42 Wm^{-2}) and 1.7 mm (corresponds to a latent heat flux of 48 Wm^{-2}) between the Decagon Version 2.0 and Best field fit, respectively. For the OEN site, this effect was neither detectable for the TRIME nor the 10HS sensor Figure 2.9a). The response of both sensors scattered and a clear dependency of evapotranspiration on soil moisture was not seen. A possible explanation for the difference between the OEN and PAY site is the impact of groundwater. At the OEN site, a shallow groundwater system combined with clayey soils may result in considerable capillary rise effectively decreasing the estimated evapotranspiration for periods with high groundwater tables. At the PAY site, which is located on a Molasse plateau, this effect is absent.
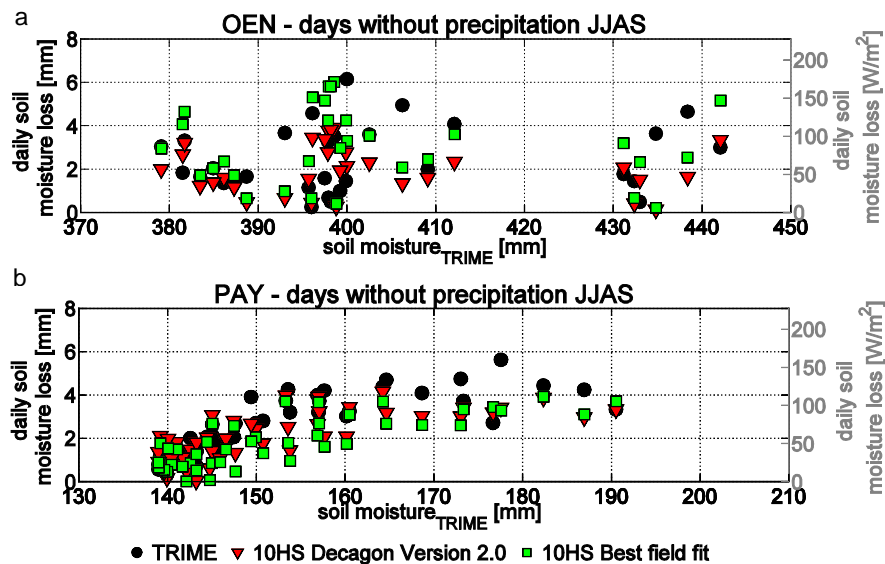
Figure 2.9: *Absolute daily soil moisture loss in millimeters and Wm^{-2} for the TRIME and 10HS sensors at the sites (a) OEN and (b) PAY for precipitation free periods June to September 2009.*

2.4   Discussion and conclusion

In the current study the capacitance-based soil moisture sensor 10HS was evaluated regarding its accuracy for climate research applications, based both on laboratory and field measurements at two sites with different soil types in Switzerland. We find that the variations between the different 10HS sensors are small. On the other hand, the sensitivity of the 10HS sensor output to VWC decreases with increasing VWC. This effect is caused by the capacitance principle, however, stronger than expected, since the forerunner sensor EC-5 from Decagon Devices was found to react slightly more sensitively at similar higher VWCs (Bogena et al., 2007). Nevertheless the 10HS is more advantageous due to its independence of the power supply and the larger measurement volume (Decagon Devices, 2009). The standard calibration provided by the manufacturer does not accurately predict the absolute VWC over the whole measurement range, neither under laboratory conditions nor under field conditions. The performance of the 10HS sensor is found to vary as a function of the soil conditions (Figure 2.2 and Figure 2.3). Due to this dependency, it was not possible to transfer findings of calibration functions established under laboratory conditions to field conditions. These two aspects conform to different studies, which evaluated other capacitance based soil moisture sensors (Veldkamp and O'Brien, 2000; Polyakov et al., 2005). The manufacturer's function was found not to be appropriate above 30-40 Vol.%. This result is unexpected since it implies a considerably lower performance than that of about 57 Vol.% indicated by the manufacturer (Decagon Devices, 2009). Good agreement was nonetheless shown for low VWCs (< 30-40 Vol.%). In addition, the daily variability for precipitation-free periods was also represented reasonably well, compared to the behavior of the TDR sensor.

Regarding climate applications, extreme soil moisture values are more relevant than medium soil moisture content. Indeed, higher predictability is found for extreme soil moisture contents (Koster et al., 2010b), which may in particular apply to extreme events such as heat waves (Jaeger and Seneviratne, 2011; Hirschi et al., 2011). Thus, it may be exactly those VWC conditions that are least well captured (either at the dry or wet end) that are most relevant for climate investigations and applications. With the site-specific calibration function it is possible to reduce the absolute error to about 2 Vol.% for the majority of the measurements including low and moist soil moisture conditions. Nevertheless, larger errors may occur under conditions more extreme than those encountered during the field experiment (despite its length of more than one year), such as those that prevailed in the 2003 summer drought and heat wave in Europe characterized by high soil moisture depletion (e.g. Andersen, 2005; Granier et al., 2007; Loew et al., 2009; Teuling et al., 2010b).

In climate research, dry soil moisture conditions are of particular relevance to investigate land-atmosphere interactions. It can be expected that evapotranspiration will decrease at low soil moisture when a soil moisture-limited evapotranspiration regime is reached (e.g. Seneviratne et al., 2010), which is also the regime at which the strongest feedbacks between land and the atmosphere are expected (e.g. Koster et al., 2004; Hirschi et al., 2011). These medium to low soil moisture conditions appeared to be relatively well captured by the 10HS sensor, and represented well for the PAY site. In contrast the peculiar behavior of the sensor measurements for the OEN site in spring and summer 2009 which might be impacted by the groundwater and

thus the approach to isolate evapotranspiration from other fluxes (i.e. drainage) is not valid for this site and time period. This illustrates that soil moisture-evapotranspiration relationship can strongly vary on relatively small spatial scales (see Figure 2.1 for location of the two sites). Beside the representation of dry soil moisture conditions, also accurate measurements during moist conditions are relevant, because it is important to estimate the change in absolute soil moisture [mm] over e.g. a seasonal period in an accurate way. Moreover, moist conditions are also highly relevant for runoff generation (e.g. Koster and Milly, 1997; Teuling et al., 2010a). The measurement range of the 10HS sensor can be increased to up to 50 Vol.% with applying a site-specific calibration. The site-specific calibration involved measurements of two TDR sensors (at 10 cm and 80 cm depth), which recorded the VWC parallel to the 10HS sensors. Therewith the calibration is conducted not only using the local soil texture, but also taking into account the actual climate conditions, rise and recession of soil moisture.

The results of our study highlight that the 10HS sensor requires site-specific calibration functions and is mostly appropriate for research investigations related to dry soil moisture conditions. Care has to be taken when measuring at high VWC levels. Our laboratory measurements also confirm the very high accuracy of TDR sensors compared to that of low-cost capacitance sensors. Given the high variability of soil moisture and cost of TDR sensors, we conclude that the most appropriate set-up for efficient and accurate soil moisture networks consists of parallel capacitance and TDR measurements, using the latter as reference for the calibration of the low-cost sensors.

Acknowledgement

Supplementary Material
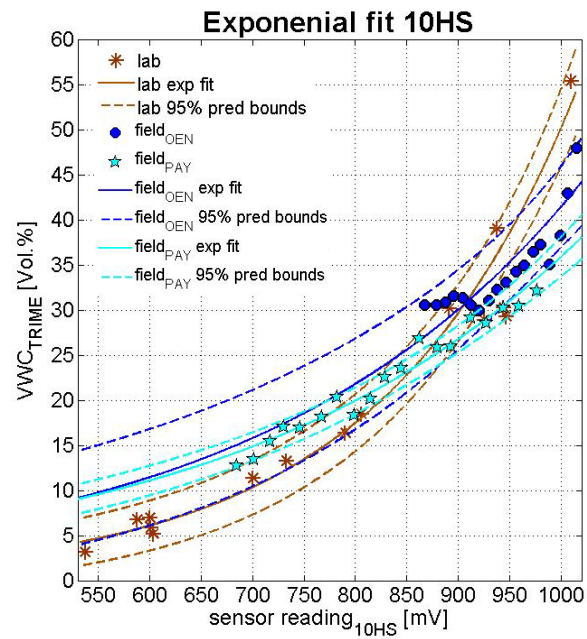
Figure 2.10: *Calibration function for the laboratory and field measurements.*

Chapter 3

Comparison of four soil moisture sensor types under field conditions in Switzerland

Comparison of four soil moisture sensor types under field conditions in Switzerland

Heidi Mittelbach[1], I. Lehner[1], and S.I. Seneviratne[1]

Abstract

Many environmental and hydrological applications require knowledge about soil moisture. Its measurement accuracy is known to depend on the sensor technique, which is sensitive to soil characteristics such as texture, temperature, bulk density and salinity. However, the calibration functions provided by instrument manufacturers are generally developed under laboratory conditions, and their accuracy for field applications is rarely investigated, in particular over long time periods and in comparison with other sensors types. In this paper, four side-by-side profile soil moisture measurements down to 110 cm using three low-cost sensors and one high-accuracy and high-cost time domain reflectometry (TDR) sensor are compared over a 2-year period at a clay loam site in Switzerland. The low-cost instruments include the (1) 10HS (Decagon Devices, United States), (2) CS616 (Campbell Scientific, United States), and (3) SISOMOP (SMG University of Karlsruhe, Germany) sensors, which are evaluated against the (4) TDR-based TRIME-IT/-EZ (IMKO GmbH, Germany) sensors. For the comparison, the calibration functions provided by the manufacturers are applied for each sensor type. The sensors are evaluated based on daily data regarding their representation of the volumetric water content (VWC) and its anomalies, as well as the respective temperature dependency of the measurements. Furthermore, for each sensor type the actual evapotranspiration is estimated using the soil water balance approach and compared with measurements from a weighing lysimeter. It is shown that the root mean square difference (RMSD) of VWC for the low-cost sensors compared to the TDR measurements are up to 0.3 m^3/m^3, with highest values in near-surface layers. However, the RMSD for the VWC anomalies are lower compared to those for absolute values. We conclude that under the studied conditions none of the evaluated low-cost sensors has a level of performance consistent with the respective manufacturer specifications. Hence the derivation of site-specific calibration functions is vital for the interpretation of measurements with low-cost soil moisture sensors. Furthermore, some weaknesses of the tested low-cost sensors such as the lack of sensitivity in certain soil moisture regimes or spurious dependency on soil temperature, imply intrinsic issues with the measurements derived with this type of instruments. This is particularly critical for a number of environmental and hydrological applications, including the assessment of remote sensing measurements.

3.1 Introduction

Soil moisture is an essential environmental, hydrological and climate variable. In particular, it strongly affects the land surface fluxes of the water and energy balances with consequent

[1]Institute for Atmospheric and Climate Science, ETH Zurich, Switzerland

impacts on temperature, evapotranspiration, planetary boundary layer stability or runoff generation (see Seneviratne et al., 2010, for an overview). In recent years, soil moisture-atmosphere interactions received increasing attention in climate research. In particular, both numerical and observational studies highlighted their potential role for climate variability and extremes, including heat waves (Seneviratne et al., 2006a; Diffenbaugh et al., 2007; Fischer et al., 2007b; Vautard et al., 2007; Lorenz et al., 2010; Teuling et al., 2010b; Jaeger and Seneviratne, 2011; Hirschi et al., 2011). Moreover, potential (positive or negative) feedbacks with precipitation have also been suggested in various regions (Koster et al., 2004; Hohenegger et al., 2009; Seneviratne et al., 2010; van den Hurk and van Meijgaard, 2010; Findell et al., 2011; Taylor et al., 2011). Global effects of soil moisture variability on climate have been proposed as well (Jung et al., 2010), and recent studies have further highlighted the potential role of soil moisture for sub-seasonal to seasonal forecasting (e.g. Koster et al., 2010b,a; Weisheimer et al., 2011).

Ground truth data for soil moisture are essential to analyze the processes underlying land-atmosphere interactions and to evaluate their role in land surface and climate models (e.g. Vinnikov et al., 1996; Dirmeyer et al., 2006). Thereby, information about root-zone soil moisture is particularly critical, given that feedbacks of soil moisture on climate are mostly mediated by vegetation (e.g. Seneviratne et al., 2010). Comprehensive ground-based soil moisture observational networks are nonetheless still very scarce, although some networks have been recently established, such as the Oklahoma Mesonet in United States (Bassara and Crawford, 2000), OzNet in Australia (C et al., 2007) and in Europe the networks RHEMEDUS in Spain (Martinez-Fernandez and Ceballos, 2005), SMOSMANIA in France (Albergel et al., 2008), SwissSMEX in Switzerland (http://www.iac.ethz.ch/url/SwissSMEX; (e.g. Mittelbach et al., 2011), and the TERENO observatoins in Germany (http://teodoor.icg.kfa-juelich.de/). These measurements are also essential for the development and evaluation of new remote sensing-based soil moisture estimates (Wagner et al., 2007b; de Jeu et al., 2008). For instance, (Jackson et al., 2010) recently emphasized the need for more ground-truth observations networks over wide spatial scales and with increased temporal frequency to improve respective satellite algorithms. Many of the newly available but also already existing long-term networks, as well as remote sensing observations have been recently collected and harmonized as part of the International Soil Moisture Network (ISMN; (Dorigo et al., 2011).

Different techniques for soil moisture measurements have been developed over the last decades (see e.g. (Robinson et al., 2008) for a review). Most commonly, electromagnetic sensors are used to establish continuous in-situ soil moisture networks. These sensors make use of the high permittivity of water to estimate the volumetric water content (VWC) in the soil (Topp, 2003), and are generally based either on time domain reflectometry (TDR), frequency domain reflectometry (FDR), or capacitance techniques. The TDR-based sensors are known to be of higher accuracy, but are also of significantly higher cost than the FDR and capacitance probes. Due to the accuracy of TDR measurements, these sensors are used as reference sensors in previous studies (e.g. Plauborg et al., 2005; Bogena et al., 2007; Mittelbach et al., 2011). Nevertheless, because of the spatial and temporal variability of soil moisture (e.g. Western et al., 1999; Famiglietti et al., 1999; Albertson and Montaldo, 2003; Western et al., 2004; Teuling and Troch, 2005; Vereecken et al., 2010), it has been suggested to use less accurate but cheaper sensors in order to increase the density of measurements within soil moisture networks (e.g.

Bogena et al., 2007; Robinson et al., 2008), (Vereecken et al., 2010). In addition to their cost, the high power consumption of TDR instruments (Veldkamp and O'Brien, 2000) may be another dissuasive argument for their use if a site has to be e.g. operated with stand-alone power supply.

As for any types of measurements, the sensors' performance and accuracy are important. Many sensor types for soil moisture measurements have been evaluated in previous studies (e.g. Roth et al., 1990; Walker et al., 2004; Czarnomski et al., 2005; Robinson et al., 2008; Blonquist et al., 2005). These studies generally concluded that the accuracy of the measured VWC when using universal calibration functions provided by the manufacturers, needs to be carefully evaluated using laboratory and field measurements. Further studies (e.g. Seyfried and Murdock, 2004; Evett et al., 2006; Logsdon, 2009; Rüdiger et al., 2010; Mittelbach et al., 2011) also recommended more specifically to establish soil- or site-specific calibration functions in such applications. It should be noted that the accuracy of the respective sensors may also depend on the site characteristics for various reasons (e.g. soil moisture regime, soil type, soil homogeneity, presence of stones and roots). Some of these site-specific effects may not only be related to the measurement technique, but also to the sensor design. For instance, soil moisture sensors with long rods provide a more representative soil moisture measurement due to the integration over a larger volume. But their installation in stony and also clayey soils with low water content can be more difficult compared to that with smaller and more compact sensors.

The present study is designed to compare the performance of two FDR- and one capacitance-based sensor types, when applying the calibration function supplied by the manufacturers. For their evaluation TDR measurements are used as reference. The analysis is based on two years of field measurements at a site of the SwissSMEX network using parallel measurements down to 110 cm. The focus of the investigation is on the uncertainties in measured VWC and its anomalies, as well as on the temperature dependency of the measurements. Furthermore, the ability of the four sensor types to represent changes in absolute soil moisture storage is evaluated using the soil water balance approach and a direct comparison with evapotranspiration measurements from a weighing lysimeter. This study does not provide new calibration functions for the investigated sensors. Our emphasis is rather on assessing issues with the quality of soil moisture measurements when the manufacturers' calibration function is applied without correction. In addition, we provide an extensive cross-evaluation of several commonly used sensors under field conditions, which is useful when assessing measurements of distinct soil moisture networks, as they often rely on the use of a single sensor type.

The article is structured as follows. First, data and methods, including instruments, field measurements and applied methods for the sensor comparison are described in Section 3.2. The results are presented in Section 3.3. The discussion of the results and conclusions with respect to climate, hydrology and remote sensing applications are provided in Section 3.4 and Section 3.5, respectively.

3.2   Data and method

3.2.1   Field site measurements

Field measurements from the research catchment Rietholzbach (http://www.iac.ethz.ch/url/ rietholzbach are used in this study. This pre-alpine catchment is located in northeastern Switzerland (47.37°N, 8.99°E) and has been in operation since 1975. For the period 1976 to 2006 the catchment is characterized by a mean annual precipitation of 1459 mm, an actual yearly evapotranspiration, estimated using a weighing lysimeter, of 560 mm and a mean annual 2 m air temperature of 7.1 °C. The weighing lysimeter of the Rietholzbach site is a backfilled lysimeter with a surface of 3.14 m2 and a depth of 2.5 m. The container is positioned on a scale which has a resolution of 100 g. For further information about the catchment and respective observations see Seneviratne et al. (2011). A comparison of evapotranspiration measurements and estimates for the catchment are also provided in (Lehner et al., 2010).

Within the SwissSMEX project (http://www.iac.ethz.ch/url/SwissSMEX, the grassland site Rietholzbach was enhanced in 2009 with additional soil moisture measurement profiles. The setup of a SwissSMEX site is carried out in several steps: First, a hole is dug taking into account the original sequence of the soil horizons, and separating the respectively extracted soil amounts. Second, disturbed and undisturbed soil samples are taken from each soil horizon for subsequent soil analysis. In a third step, all sensor types are installed horizontally in the undisturbed soil to provide similar conditions. Finally, the hole is systematically refilled, ensuring that the soil horizons are arranged in the original order and close to the original density using compaction. For the Rietholzbach site, the TRIME-IT/EZ, 10HS, and CS616 sensors as well as the soil temperature sensors were installed side-by-side at seven depths: 5, 15, 25, 35, 55, 80, and 110 cm. The SISOMOP sensors were installed at five depths: 5, 15, 35, 55, and 80 cm.

In this study, measurements of soil moisture and soil temperature down to 110 cm, precipitation and 2 m air temperature as well as data from the weighing lysimeter of the time period 1 June 2009 to 31 May 2011 were considered. The temporal evolution of these variables is shown in Figure 3.1. Basic soil characteristics for the site and each soil horizon are listed in Table 3.1.

Table 3.1: *Basic soil characteristics of the Rietholzbach site with texture according to USDA soil taxonomy.*

Depth (cm)	Clay ($<2\ \mu$m)	Silt (2-63 μm)	Sand ($>63\ \mu$m)	Texture	Bulk Density (g/cm^3)	Organic Fraction (%)	pH
0-15	30.6	35.9	33.5	Clay loam	1.08	4.7	6.9
15-23	30.8	31.0	38.2	Clay loam	1.37	2.5	7.0
23-70	25.6	32.7	41.7	Loam	1.37	1.3	7.1
70-120	26.9	34.4	38.7	Loam	1.50	1.7	7.1
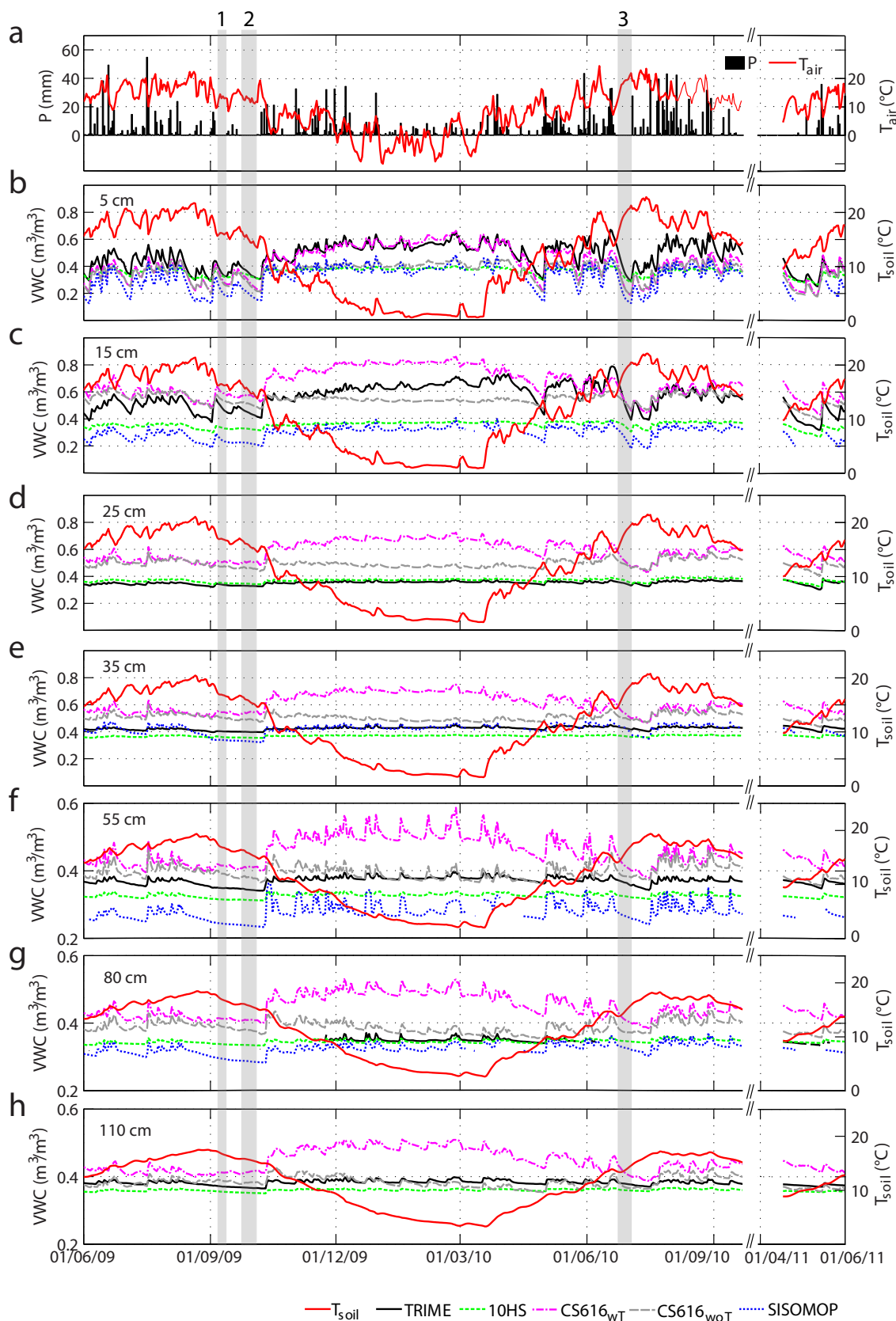
Figure 3.1: *Temporal evolution of (a) precipitation and 2-m air temperature and of (b to h) soil moisture measurements of the different sensors and soil temperature measurements at the different depths at daily resolution. Dry down periods are indicated in grey and correspond to the following time frames: 8-13 September 2009 (1), 24 September - 05 October 2009 (2), and 25 June - 04 July 2010 (3). Note the different scale for the y-axis in plots f to h.*

3.2.2 Instruments

The considered soil moisture instruments are the TRIME-IT/-EZ (IMKO GmbH, Germany), the 10HS (Decagon Devices, United States), the CS616 (Campbell Scientific, United States), and the SISOMOP (SMG University of Karlsruhe, Germany). All four sensor types make use of electromagnetic characteristics to estimate the permittivity of a medium and relate this information to VWC. Details of the instruments are provided in the next subsections.

Parallel to the soil moisture measurements, soil temperature (Tsoil) was measured in all depths using the temperature sensor 107-L (Campbell Scientific, United States). All measurements, except those from the SISOMOP sensor, are logged with a Campbell Scientific CR1000 data logger. The data from the SISOMOP sensor are logged with the SISOMOP logging unit (Schlaeger, 2007a). All data are measured and recorded at a 10-minute interval. For the present analysis they are averaged and analyzed on a daily time scale.

TRIME-IT/-EZ sensor (TDR)

The TRIME-IT and TRIME-EZ sensors are based on the TDR technique. This technique makes use of the travel time of an electromagnetic impulse propagating along the rods of a sensor. The signal is reflected at the end of the rods and the returned signal is sampled. The travel time of the electromagnetic impulse is related to the permittivity of the medium, which can itself be related to the VWC (Blonquist et al., 2005). The TRIME-IT/-EZ operate at a frequency of 1 GHz. They measure in a range of 0 to 1 m^3/m^3 and operate at temperatures ranging from -15 to +50 °C. The accuracy is reported to be of ±0.01 m^3/m^3 for 0 to 0.40 m^3/m^3 and ±0.02 m^3/m^3 for 0.40 to 0.70 m^3/m^3 in soils with bulk electrical conductivity of up to 2 dS/m (IMKO, 2006). The TRIME-IT and TRIME-EZ sensors are similar sensors that have only different dimensions. The TRIME-IT instrument consists of two parallel round rods of 110 mm length with 3.5 mm diameter, and a spacing of 20 mm. It has a smaller measurement volume than the TRIME-EZ, which also has two round metal rods but of 160 mm length with 6 mm diameter, and a spacing of 40 mm. Due to its smaller measurement volume, the TRIME-IT was installed at 5 and 15 cm depth, whereas the TRIME-EZ was installed at deeper depths down to 110 cm. The sensor output rawTRIME (mV) range between 0 and 1000 mV and is linearly related to the VWC_{TRIME} (m^3/m^3):

$$VWC_{TRIME} = raw_{TRIME}/1000. \tag{3.1}$$

10HS sensor (capacitance)

The 10HS sensor is based on the capacitance technique. The charging time of an electromagnetic field is related to the capacitance of the soil, which is related to the permittivity of the medium. The permittivity can then be related to the VWC of the soil. The 10HS is the successor of the commonly used EC-5 soil moisture sensor, but integrates over a larger soil volume (rod length is 10 cm instead of 5 cm). It operates at a frequency of 70 MHz with a measurement range indicated by the manufacturer between 0 and 0.57 m^3/m^3. The instrument operates between 0 and +50 °C. The accuracy using the standard calibration is reported to be ±0.03 m^3/m^3 in mineral soils that have a solution electrical conductivity <10 dS/m. Using a soil specific calibration the accuracy is reported to be ±0.02 m^3/m^3 (Decagon Devices, 2009). The sensor consists of two parallel-pronged plastic rods of 100 mm length and 9.8 mm width, and a spac-

ing of 12.1 mm. The sensor reading raw10HS (mV) was transformed to VWC10HS (m^3/m^3) using the standard calibration function provided by the manufacturer (Decagon, 2009):

$$VWC_{10HS} = 2.97 \cdot 10^{-9} raw_{10HS}^3 - 7.37 \cdot 10^{-6} raw_{10HS}^2 + 6.69 \cdot 10^{-3} raw_{10HS} - 1.92. \quad (3.2)$$

CS616 and SISOMOP sensors (FDR)

Both the CS616 and SISOMOP sensors are based on the FDR technique. The CS616 sensor directly relates the period, which is inversely related to the number of reflected pulses, to the VWC (Blonquist et al., 2005). The frequency of pulsing in free air is about 70 MHz. The CS616 measures in a range of 0 to 1 m^3/m^3 and operates between -25 and +50 °C. The accuracy between 0 and 0.50 m^3/m^3 is reported to be ± 0.025 m^3/m^3 using standard calibration with a bulk electrical conductivity ≤ 0.5 dS/m and a bulk density of 1.55 g/cm^3 (Campbell Scientific, 2006). The sensor consists of two parallel round rods of 300 mm length, 3.2 mm diameter, and a spacing of 32 mm. The sensor output raw_{CS616} (μsec) was transformed to VWC$_{CS616}$ (m^3/m^3) using the standard calibration provided by the manufacturer (Campbell Scientific, 2006):

$$VWC_{CS616} = -0.0663 - 0.0063 raw_{CS616} + 0.0007 raw_{CS616}^2. \quad (3.3)$$

The manufacturer reports an error in measured VWC caused by the temperature dependency of the CS616 sensor, and provides the following correction equation to be applied to the uncorrected sensor output $raw_{CS616woT}$ (μsec) using the soil temperature T$_{soil}$ (°C) in the specific installation depth (Campbell Scientific, 2006):

$$raw_{CS616wT} = raw_{CS616woT} + (20 - T_{soil}(0.526 - 0.052 raw_{CS616woT} + 0.00136 raw_{CS616woT}^2. \quad (3.4)$$

In this study both the $raw_{CS616wT}$ and the $raw_{CS616woT}$ sensor output were transformed to VWC (m^3/m^3). The respective CS616 estimates are distinguished as CS616$_{wT}$ (with temperature correction) and CS616$_{woT}$ (without temperature correction).

The SISOMOP sensor is made up of a ring oscillator based on a digital inverter, driving a transmission line, whose end is fed into its input (Schlaeger, 2007b). The resulting oscillation frequency is expressed as moisture counts (MC) and has a relative accuracy of the permittivity of $\pm 4\%$. The sensor measures in a permittivity range of 5 to 25 and operates at -5 to 60 °C (Schlaeger, 2007b). The measurement range of VWC (m^3/m^3) is not explicitly provided by the manufacturer. The sensor consists of one flat pronged plastic rod with 100 mm length and 30 mm width. The exponential relationship between the measurement unit and the VWC requires a material dependent calibration (Krauss et al., 2010):

$$VWC_{SISOMOP} = a \cdot exp(bMC)/100. \quad (3.5)$$

The manufacturer provides a sensor and soil specific calibration based on Krauss et al. (2010).

3.2.3 Sensor comparison

All investigations were performed based on daily-averaged values from 1 June 2009 to 31 May 2011 focusing on the VWC obtained by applying the respective calibration function by the manufacturer. Because of their reported accuracy and the tested accuracy under laboratory conditions (e.g. Mittelbach et al., 2011) the TRIME-IT/-EZ sensors were taken as reference for the following analysis. As a quality check for the TRIME-IT/-EZ field measurements the relation to the lysimeter weight was taken into account. Given by a divergent behavior of the relation the time period 23 September 2010 to 15 April 2011 was excluded from the analysis. The measurements of the soil moisture sensors 10HS, CS616 ($CS616_{wT}$ and $CS616_{woT}$), and SISOMOP were compared with respect to the absolute daily VWC (m^3/m^3) and its anomalies relative to the average VWC over the investigated period. The RMSD and correlations with respect to VWC_{TRIME} were calculated for each measurement depth over the four seasons, winter (DJF), spring (MAM), summer (JJA), and fall (SON), as well as for the entire considered period. In addition, the absolute error of daily VWC dependent on the frequency distributed VWC_{TRIME} was analyzed. Therefore, the VWC_{TRIME} was merged over all depths and binned in 0.05 m^3/m^3 intervals and the difference between the tested sensor and the Furthermore, the effect of T_{soil} on the obtained daily VWC was assessed for each installation depth. By assuming TRIME-IT/-EZ as physically correct the test criterion was the difference in VWC to the other sensor types as used in (e.g. Verhoef et al., 2006):

$$\Delta VWC = (VWC_{test} - VWC_{TRIME} - \overline{(VWC_{test} - VWC_{TRIME}}. \qquad (3.6)$$

3.2.4 Comparison of change in integrated column water storage with evapotranspiration measurements from a lysimeter

As last criterion, the estimation of evapotranspiration (ET) using the soil water balance approach was evaluated using the lysimeter measurements available at the Rietholzbach site (Section 3.2.1). For precipitation-free periods and with the assumption of no drainage, ET over the considered time period can be approximately assumed to be equal to the change in weight of the lysimeter as well as to the change in absolute integrated column soil moisture storage S (mm) using soil moisture measurements. To minimize the effect of drainage, only drying periods starting on the fourth day after a precipitation event were taken into account. As reference, hourly data of weight and outflow from the weighing lysimeter at the Rietholzbach site were available. Three dry periods were investigated and are highlighted in Figure 1: 8 September to 13 September 2009 (6 days), 24 September to 5 October 2009 (12 days), and 25 June to 4 July 2010 (10 days). For each sensor type, S was calculated at an hourly time step by integrating the VWC measurements over the whole soil column z (from the surface down to 110 cm for TRIME-IT/-EZ, 10HS, CS616 and down to 80 cm for SISOMOP). As integration method, we used the trapezoidal method (e.g. Hupet et al., 2004) including an additional value VWC at the surface which is assumed to be equal to the measurement VWC in 5 cm:

$$S_t = \int_0^z VWC(z)dz \cong \sum_{i=1}^N \frac{VWC(t, z_i) + VWC(t, z_{i+1})}{2}(z_{i+1} - z_i). \qquad (3.7)$$

Where z indicates the depth, N the deepest measurement depth, the subscript i indicates the respective measurement level and t indicates the time. The change in absolute integrated column soil moisture storage S for these precipitation-free periods was estimated by the difference of the last (S(T)) and the first value (S(0)) over the considered time period:

$$\Delta S = S_{tend} - S_{t1}. \tag{3.8}$$

3.3 Results

While this paper intents to compare the VWC obtained by the sensor types and does not intent to characterize the permittivity and its relation to the VWC, it has to be acknowledged that a significant body of literature on exists focusing on issue involving different measurement techniques and its dependency on different factors, such as measurement frequency, temperature, soil texture, salinity, and VWC and its consequent impact on measurement accuracy (e.g. Wraith and Or, 1999; Kelleners et al., 2005; Blonquist et al., 2005; Evett et al., 2006; Escorihuela et al., 2007).

3.3.1 Volumetric water content and its anomalies

In the following analysis, daily VWC_{TRIME} measurements are used as reference. As displayed in Figure 3.1 VWC_{TRIME} is found to be most variable at 5 and 15 cm depth over the entire measurement period. VWC_{TRIME} has minimum values (in spring 2011) of about 0.25 and 0.32 m^3/m^3 with a measurement range of about 0.42 and 0.47 m^3/m^3 at these two depths. By contrast, VWC_{TRIME} at 25 cm depth shows a similar minimum at 0.31 m^3/m^3 but a strongly reduced measurement range of only about 0.09 m^3/m^3. At 25 cm depth and below, the VWC_{TRIME} measurements show a clear continuous decrease in variability with a nearly steady behavior for the whole observation period and similar VWC for all depths. The relatively shallow extent of soil moisture dynamics in Rietholzbach was also identified from long-term TDR measurements within the lysimeter (Seneviratne et al., 2011). Figure 3.1 shows further that the 10HS measurements do not exceed 0.40 m^3/m^3 independently of depth. In addition, the 10HS sensors do not capture the daily VWC fluctuations for moist conditions. This effect has the highest influence at 5 and 15 cm depth, where the VWC_{TRIME} shows highest variations. At 25 cm depth and below, the 10HS measurements are close to the VWC_{TRIME} measurements, but the soil moisture fluctuations are almost negligible at these depths. The $CS616_{wT}$ measurements display a higher variability than the 10HS measurements but tend to overestimate high water contents. Moreover, the $CS616_{wT}$ estimates, which use the temperature correction provided by the manufacturer (Section 3.2.3), present significant artifacts at 25 cm depth and below, with apparent variability in estimated VWC related to the measured soil temperature. These features appear erroneous compared to the VWC_{TRIME} measurements. In contrast, the $CS616_{woT}$ estimates, which do not use the temperature correction, reach values of up to 0.47 m^3/m^3 and show a lower VWC range. Nevertheless, the $CS616_{woT}$ performs reasonably well at 5 and 15 cm depths. The SISOMOP sensor shows an underestimation of VWC with an upper limit around 0.53 m^3/m^3, but indicates acceptable VWC variability at all depths.
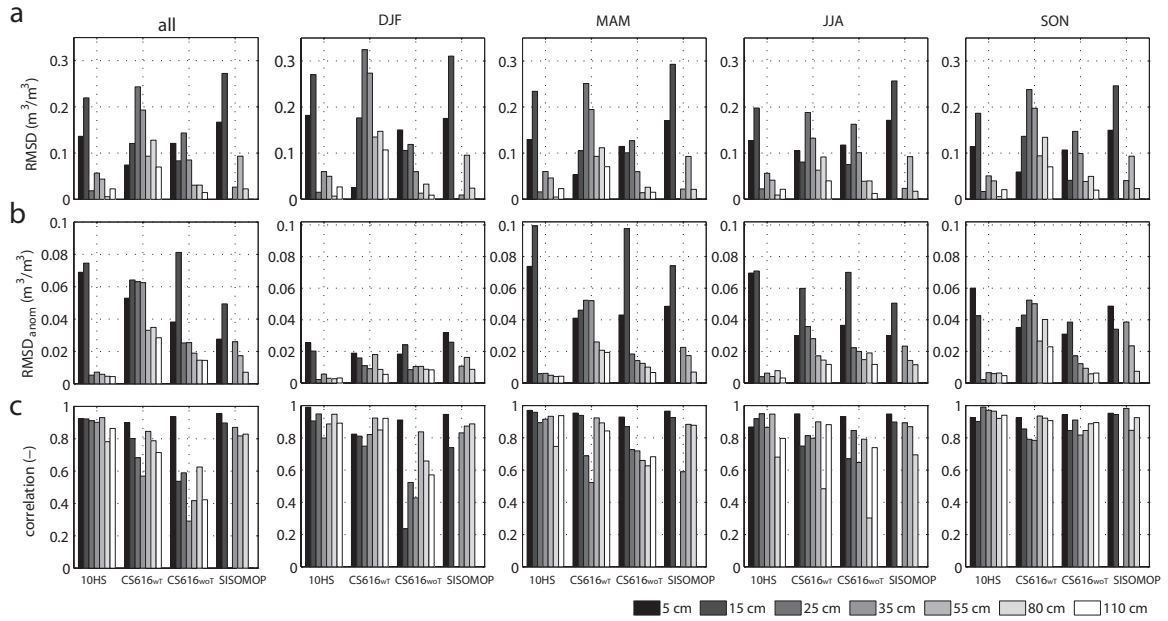
Figure 3.2: *RMSE (m³/m³) of (a) VWC measurements, (b) anomalies of VWC, and (c) the correlation between the sensor to be tested and the reference sensor (TRIME-IT/-EZ) in daily resolution for the seasons DJF, MAM, JJA and SON as well as for the whole period (1 June 2009 to 31 May 2011).*

The RMSD for the measured absolute and relative VWC and the correlation of the absolute VWC with respect to the VWC_{TRIME} values are shown in Figure 3.2 at seasonal scale and for the overall period. For all sensor types, the RMSD of the absolute VWC (Figure 3.2a) at the different measurement depths are overall lowest in JJA, when the lowest VWC_{TRIME} occur. For each sensor type, the highest RMSD are found at different depths with similar ranking for all seasons. The 10HS displays highest RMSD of about 0.18 to 0.27 m³/m³ at 5 and 15 cm depth, where the VWC_{TRIME} is highest and most variable. The lower and more steady VWC_{TRIME} at depths from 25 to 110 cm and similar behavior of the 10HS measurements leads to clearly smaller RMSD in absolute VWC in all seasons. The cumulative distribution function (cdf) for all measurement depths and over the whole measurement period (Figure 3.3a) confirms that the RMSD of the 10HS in 5 and 15 cm depth is mainly related to its limitation to measure VWC above 0.4 m³/m³. The probability of low VWC_{TRIME} agrees well with the probability of the TRIME-IT/-EZ. For VWC_{TRIME} above 0.3 m³/m³ the cdfs shows almost no flattening of the curve , which results in a underestimation. The $CS616_{wT}$ estimates show for all seasons the highest RMSD at 25 and 35cm depth with values of up to 0.32 and 0.27 m³/m³ (Figure 3.2a), respectively. The cdfs (Figure 3.3a) indicate that the RMSD in 15 to 110 cm represent an overestimation of the VWC. Furthermore, from 25 cm on the distribution results in a different shape displaying a larger measurement range of the $CS616_{wT}$. By contrast, the $CS616_{woT}$ estimates display a marked different behavior: The RMSD values for the absolute VWC are highest at 5 to 25 cm depth with values of up to 0.16 m³/m³ (Figure 3.2a) resulting in over- and underestimation of the VWC_{TRIME} (Figure 3.3a). The measurements at the other depths result in clearly smaller RMSD and display a good agreement with distribution of the reference sensors. Similar to the 10HS sensor, the SISOMOP sensor shows highest RMSD for the first

two measurement depths with values of up to 0.17-0.31 m^3/m^3 (Figure 3.2a). However, its cdfs display a similar shape as the reference sensor, but shifted to lower VWCs (Figure 3.3a).

The RMSD for the measured VWC anomalies (Figure 3.2b) display far smaller values compared to the RMSD of the absolute VWC for all tested sensor types. Note that the anomalies are computed with respect to the average VWC of the given analyzed time frames (i.e. whole time period for the annual values and respective seasonal values of the two years for the seasonal analyses). Furthermore, the ranking of depths with smallest RMSD is nearly the same for all four estimates and three sensor types. All show the highest error in the first two measurement depths where highest and most variable VWC_{TRIME} is found. Consequently, lowest RMSD are indicated in DJF with lowest VWC variability (temporal evolution of anomalies are visualized in the supplementary material). Largest differences can be identified with the $CS616_{wT}$ in all depths as well as for all of the tested sensor types in shallow depths (5 to 15 cm). Figure 3.3b displays the cdfs for the anomalies. Consistent with the Figure 3.2a,b it shows a better agreement between the measurements for the anomalies than for the absolute values (Figure 3.3a). The cdf of VWC_{TRIME} in 5 cm is well represented by $CS616_{wT}$, $CS616_{woT}$, and SISOMOP. Moreover, the probability of negative anomalies, indicating dry conditions, are captured well. In contrast, the 10HS does not capture extreme dry and wet conditions of the cdf at the uppermost two depths. As for the cdfs for the absolute VWC (Figure 3.3a), the $CS616_{wT}$ display a different shape than the VWC_{TRIME}.

The correlations between the TRIME-IT/-EZ measurements and the estimates derived from the three tested sensor types (Figure 3.2c) show high values (r>0.8) for the near surface depths. A clear linear relationship (r 0.6) is found for 10HS and SISOMOP in all depths for all seasons. The correlation for $CS616_{wT}$ is generally above 0.5 but displays more variations between the single depths and seasons. If the temperature correction is not applied ($CS616_{woT}$), the correlation is lower and more variable for the different depths and seasons.
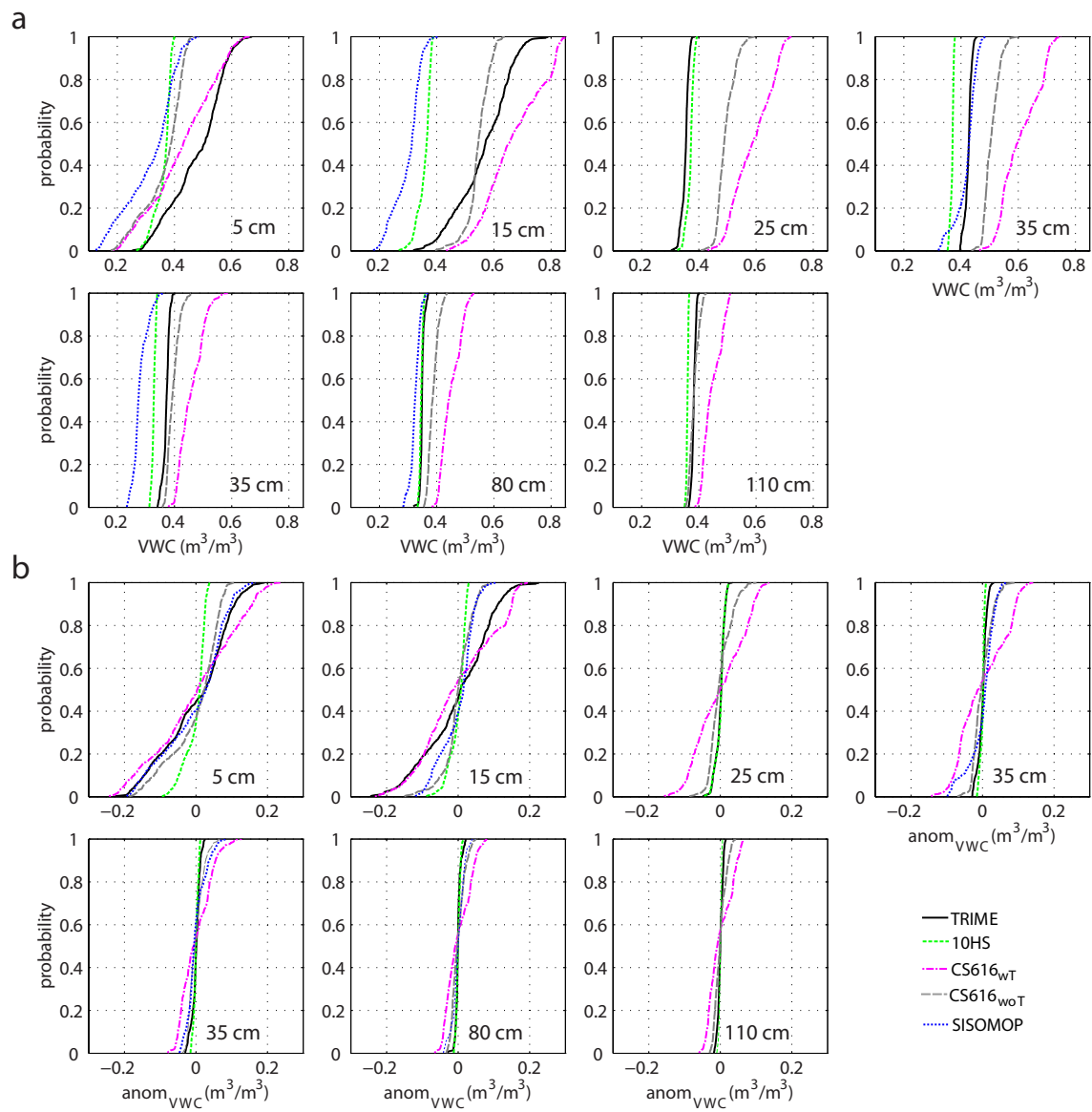
Figure 3.3: *Cumulative distribution function of the different sensors measurements at all depths of (a) VWC measurements and (b) anomalies of VWC.*

The absolute error of VWC for the tested sensors as a function of the measured VWC_{TRIME} as well as the frequency histogram of the respective VWC_{TRIME} values are displayed in Figure 3.4. A first striking feature is that the underestimation of actual VWC by the 10HS and SISOMOP sensors increases with increasing VWC. Nonetheless, for 74% of the data (VWC range of 0.30 to 0.45 m^3/m^3) the 10HS measurements underestimate the VWC_{TRIME} with a maximum error of about -0.06 m^3/m^3. Within the same measurement range, the absolute error of the SISOMOP sensor is around -0.16 m^3/m^3. By contrast the $CS616_{wT}$ and $CS616_{woT}$ measurements overestimate the VWC_{TRIME} within this VWC range by up to 0.15 m^3/m^3, and 0.06 m^3/m^3, respectively. Their absolute error decreases with increasing VWC and shifts to an underestimation for higher VWC values, which reaches at maximum around -0.08 m^3/m^3 and -0.18 m^3/m^3 for the $CS616_{wT}$ and $CS616_{woT}$ measurements, respectively. For higher VWC values ($\dot{\iota}$ 0.45 m^3/m^3), the 10HS and SISOMOP sensors underestimate the VWC_{TRIME} by up to -0.42 m^3/m^3.
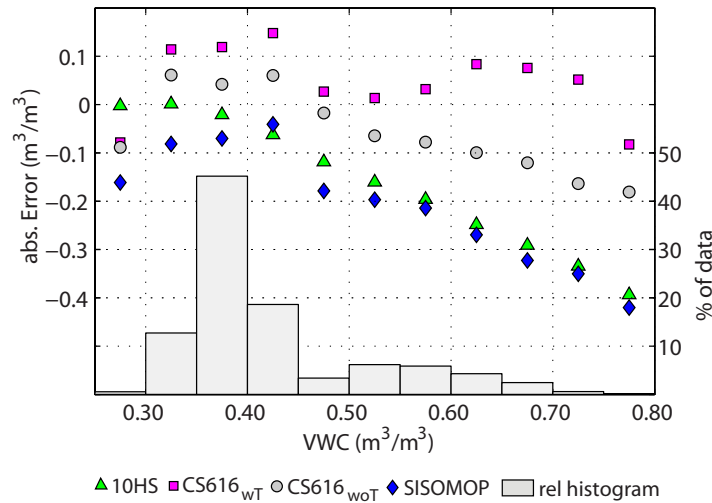
Figure 3.4: *Absolute errors of VWC measurements for the different sensor types and relative frequency distribution of VWC measured with TRIME-IT/-EZ. The error is calculated as the difference between the measurements of the respective sensor and those from the TRIME-IT/-EZ.*

3.3.2 Temperature dependency

In this section, we assess the temperature dependency of the soil moisture measurements performed with the different sensor types. Assuming the VWC measurements of TRIME-IT/-EZ to be physically correct we concentrate on the scatter plots of the differences of the tested sensor types to VWC_{TRIME} (ΔVWC) and soil temperature (Tsoil). Figure 3.5 provides the respective analysis by the single measurement depths. In general, the lowest errors are found at T_{soil} of 10 °C, and all low-cost sensor types switch at this temperature either from an over- to an underestimation or vice versa. The 10HS, $CS616_{woT}$, and SISOMOP display a positive relation between T_{soil} and ΔVWC at 5 and 15 cm depth, while at depths from 25 cm downwards the ΔVWC is close to zero with only a small slope. It is important to note that for the 10HS

and SISOMOP sensors the relation between ΔVWC and T_{soil} at 5 and 15 cm should be interpreted in sight of their limitations in measuring actual VWC values rather than be attributed to an effective temperature dependency. Both sensor types have highest RMSD in these depths (Figure 3.2a). Under the given conditions it is difficult to assess a temperature dependency for the measurements. Concerning the CS616$_{wT}$ a contrasting behavior compared to the previous mentioned sensors is identified, which is characterized by a strong negative relation with a similar slope at all depths.
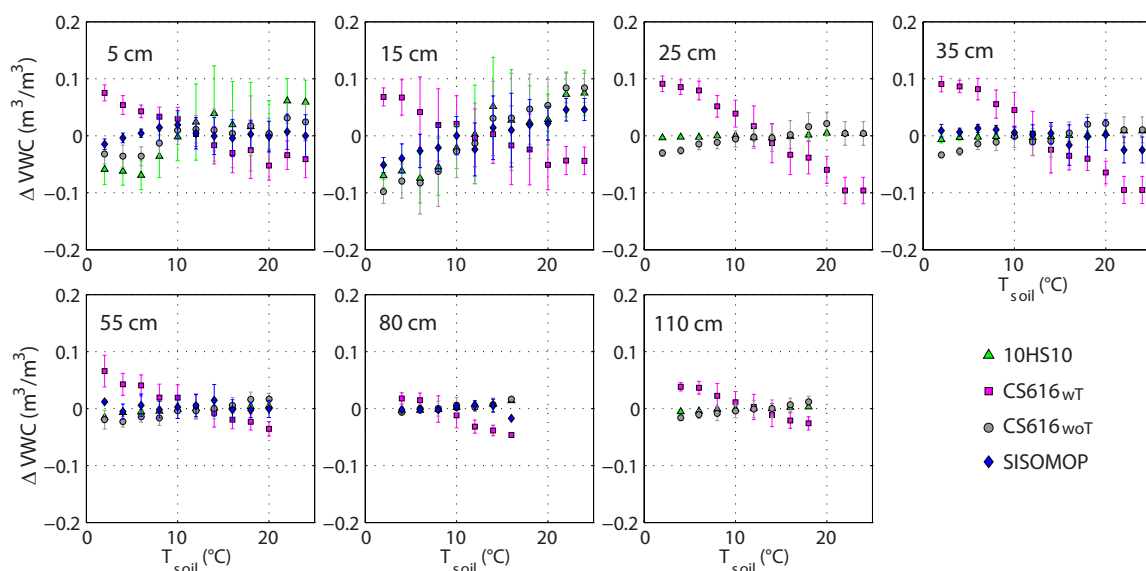
Figure 3.5: *Relation between soil temperature and difference in VWC (ΔVWC) for different installation depths. The data represent the mean and standard deviation using bins of $2°C$.*

3.3.3   Soil water storage estimation and comparison to lysimeter measurements

Figure 3.6 displays the changes in soil moisture over the whole soil column (mm) for three precipitation free periods (see Figure 3.1) by applying the soil water balance approach for each sensor type (see Section 3.2.4 for more details). The comparison with changes in lysimeter estimates shows that the TRIME-IT/-EZ performs best for the first two events (Figure 3.6a, b) with an overestimation of about 10 mm (11%) and underestimation of about 0.8 mm (4%), respectively. By contrast, for the third event (Figure 3.6c) the change in soil moisture is overestimated by about 15.5 mm (35%) with this sensor type. Nevertheless, this overestimation is likely related to the wetter initial conditions compared to events 1 and 2: The antecedent rainfall for the third event is 118 mm (10 days of rainfall) compared to 33 mm (5 days of rainfall) and 15 mm (7 days of rainfall) for the first and second event, respectively. Furthermore, the outflow from the lysimeter during the third event is higher and still continuously decreasing during the whole period. The initial conditions of the third event and the resulting non-steady outflow leads to the conclusion that the soil water balance approach to estimate evapotranspiration is not appropriate for this event. Hence, further comparisons focus on the first two events.

The 10HS sensor underestimates the evapotranspiration for the first and second event by 5.5 mm (48%) and 10.2 mm (58%), respectively. This can be mainly explained by the missing drying in the upper depths due to the small sensitivity of the 10HS under the given moisture conditions. The CS616 overestimates the first event by 2.6 mm (22%) but strongly underestimates the change in soil moisture by 11 mm (63%) for the second event. The strong underestimation of the second event is likely due to the temperature dependency of the CS616, which affects the measured changes in soil moisture for the rather steady VWC at depths below 25 cm. Furthermore, for the second event the daily change in soil temperature over the whole soil column (change in mean soil temperature over 5 to 110 cm relative to the duration of the event) is nearly three times higher and the event itself is twice as long as the first event. This induces an enhanced effect of the temperature dependency on the estimated change in soil moisture. By contrast the $CS616_{woT}$ estimates display an overestimation of 4.8 mm (42%) and 0.8 mm (5%), respectively for the two events. In the case of the SISOMOP sensor, one should take into account that the integration of VWC was only possible down to 80 cm with no measurement at 25 cm depth. Since the Rietholzbach site shows low variation in VWC for depths below 25 cm (Figure 3.1), the measurements of the SISOMOP sensor should nonetheless be comparable to those of the TRIME-IT/-EZ sensor. The analysis suggests that the SISOMOP sensor represents both events reasonably well with an overestimation of about 0.7 mm (6%) and an underestimation of about 2.5 mm (14%) for the first and second event, respectively.
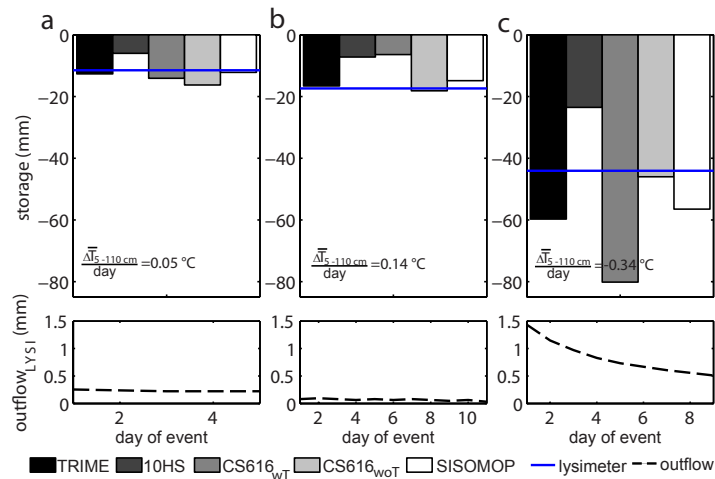
Figure 3.6: *Changes in absolute soil moisture and changes in temperature per day for the three precipitation-free periods (a) 8 September13 September 2009, (b) 24 September 5 October 2009, and (c) 25 June4 July 2010 for the TRIME-IT/-EZ, 10HS, $CS616_{wT}$, $CS616_{woT}$ and SISOMOP sensors. The blue line indicates the change by the lysimeter for each period. The bottom figures show the daily outflow of the lysimeter.*

3.4   Discussion

Two years of field measurements with a TDR sensor and three non-TDR low-cost sensor types operated side-by-side are used to evaluate the performance of the low-cost sensors using the respective calibration functions provided by the manufacturer. This study clearly shows that none of the investigated low-cost sensors can satisfactorily capture the actual VWC (VWC_{TRIME}) under the given conditions. With a RMSD of up to 0.3 m³/m³ in particular in near-surface layers, none of the sensors justifies the performance specified by the user manual. A seasonal dependency of the RMSD is found with smallest error in the summer season. Nonetheless, even in the summer season, this error can still be as large as 0.2 m³/m³. The large RMSD of the measurements is far larger than the requirements for the calibration and validation of e.g. passive remote sensing algorithms (Jackson et al., 2010). Previous studies concerning the evaluation of soil moisture sensors identified the measurement frequency to affect the determination of the permittivity and thus the performance of VWC measurements to a large part (see e.g. Blonquist et al., 2005; Escorihuela et al., 2007; Kizito et al., 2008). We find that each low-cost sensor has specific issues in accurately measuring VWC and that none clearly outperforms the others applying the calibration functions provided by the respective manufacturers.

The 10HS sensor has two main limitations: On the one hand, it fails to measure VWC above 0.4 m³/m³ and on the other hand it presents a decreasing sensitivity in measuring VWC with increasing VWC (see also Mittelbach et al., 2011). Both issues result in a poor ability of the sensor in representing the variability in VWC for moist conditions. This confirms the findings of (Mittelbach et al., 2011), where this dependency was shown to be induced by the lack of sensitivity of the sensor reading under these conditions. These limitations and the given moist conditions at the Rietholzbach site lead to an underestimation of changes in soil water storage for drying periods of around 50%. Furthermore, under moist conditions, it is barely possible to distinguish between the temperature dependency of the 10HS and its problems in measuring the VWC. Nevertheless, a temperature dependency of the 10HS is expected as it operates at a low measurement frequency (70 MHz) which affects the sensitivity of sensors measurements to temperature (Kelleners et al., 2005; Kizito et al., 2008). Furthermore, its forerunner model (EC-5) was shown to be sensitive to temperature variations (Bogena et al., 2007).

The $\mathrm{CS616}_{wT}$ estimates, i.e. the CS616 measurements with the applied temperature correction, are found to overcorrect (excessive increase) the original VWC estimates ($\mathrm{CS616}_{woT}$) under the given field conditions. In addition, the manufacturers correction superimpose an unrealistic strong seasonal soil temperature signal, which has a major influence for the $\mathrm{CS616}_{wT}$ estimates in depths with little VWC variation but significant soil temperature variations, and leads to an overestimation of VWC above 10 °C and an underestimation of VWC below 10 °C. Based on our analysis we identified this behavior as spurious temperature dependency, which is not directly related to effects on the permittivity, e.g. based on measurement frequency, soil texture, and electrical conductivity (e.g. Persson and Berndtsson, 1995; Kizito et al., 2008), but in this case is induced by the temperature correction of the manufacturer. By not considering this temperature correction, the $\mathrm{CS616}_{woT}$ is not able to represent the variability of the VWC and in addition, it shows the lowest correlation to the TDR measurements. Compared to the TDR-based sensor the $\mathrm{CS616}_{woT}$ showed a low temperature dependency, which

confirms findings from several studies. Blonquist et al. (2005) identified a similar behavior but under temperature-controlled test conditions. In their study, the over- to underestimation change point of the CS616 was found at 25 °C for a media with higher permittivity than at the Rietholzbach site. The identified temperature dependency for the clayey soil confirms the study by Benson and Wang (2006), which suggest a soil specific calibration with temperature compensation in particular for fine-grained soils. Rüdiger et al. (2010) established a general equation for the CS616 measurements including the soil type, based on the Australian soil classification. However, although the soil texture of the investigated site is known, it is based on another soil classification scheme (here USDA) and the soil type-specific parameters of the formula can thus only be estimated. Consequently the application of the equation results in inadequate values for the present measurements (not shown).

The performance of the SISOMOP sensor regarding the measured VWC and temperature dependency is of similar magnitude as for the other two (more commonly used) low-cost soil moisture sensors tested in this study. It thus seems to be an equivalent alternative within this type of sensors taking into account the overall limitations documented here.

The above discussion concerns the performance of the tested sensors in capturing the absolute VWC. In climate research, the VWC variability as well as extreme VWC conditions are generally more relevant than the absolute VWC (Seneviratne et al., 2010). With respect to the VWC anomalies, all low-cost sensors have in common strongly lower RMSD and more similar cdfs compared to those for the absolute values. Hence, they are found to perform better for long-term anomalies, i.e. to capture the dynamics of VWC. The maximum RMSD in summer is about 0.07 m^3/m^3 at depths of 5 and 15 cm. Our results confirm reported better performance of low-cost electromagnetic soil moisture sensors for dry conditions than for saturated conditions (e.g. Evett et al., 2006; Mittelbach et al., 2011). It has been suggested that the error in both the absolute VWC and its anomalies can be reduced for this sensor type with a site-specific calibration (e.g. Ventura et al., 2010). Nonetheless, also the actual sensitivity of the sensor needs to be considered and may impair such calibrations (Mittelbach et al., 2011).

The spurious temperature dependency of the daily data was particularly strong for the $CS616_{wT}$ estimates, and especially affects the evapotranspiration estimates derived with the water-balance approach in Section 3.3.3 (Figure 3.5), particularly for longer drying periods.

One should note that beside the accuracy of soil moisture sensors, also their design, and in particular their geometrical shape, is relevant for field applications (see Section 3.1). A first difficulty exists for sensors with long rods (e.g. CS616), which are in principle advantageous because of their larger measurement volume, but their installation in stony and clayey soil can be challenging. The second difficulty is found for sensors with relatively large and heavy sensor bodies (e.g. TRIME-IT/-EZ) whose centroid is not close to the sensor rods. The resulting pressure on the sensor rods can lead to a decreasing contact of the installed rods with the surrounding soil. We do not assess the impact of these effects on the measurements, but these could also explain some of the identified discrepancies.

3.5   Conclusion

This study is one of the first studies comparing the 10HS sensor with other frequently used soil moisture sensors over a more than one year measurement period. The results confirm the need for a site-specific calibration of low-cost sensors, including temperature corrections. This is in agreement with results from previous studies, which also used 10HS and CS616 sensors as well as their forerunner (EC-5 and CS615, respectively), but that were partly conducted under different soil and meteorological conditions (e.g. Benson and Wang, 2006; Bogena et al., 2007; Logsdon, 2009; Rüdiger et al., 2010; Mittelbach et al., 2011). For the temperature correction, one should note that parallel installed temperature sensors would be of advantage. If a site-specific calibration is established, low-cost sensors may be a viable alternative to TDR sensors for certain environmental applications (Seyfried and Murdock, 2004). Nonetheless, our results highlight significant weaknesses of these sensors such as (dependent on the sensor) a lack of sensitivity in moist soil moisture regimes or a spurious dependency on soil temperature. These imply intrinsic issues with the measurements derived with this type of instruments.

The results claim for a combination of high-accuracy and low-cost sensors in the design of soil moisture measurement networks and highlight the importance to evaluate and compare soil moisture sensors under different soil characteristics (texture, temperature, bulk density, and salinity) and under different moisture regimes. This would allow a better quantification of the accuracy of in-situ measurements. This consideration is particularly critical for a number of environmental, climate, and hydrological applications, including the assessment of remote sensing measurements and the evaluation of land surface, hydrological and climate models. In particular, the error ranges of the respective sensors should be assessed in such applications.

Acknowledgment

Supplementary Material
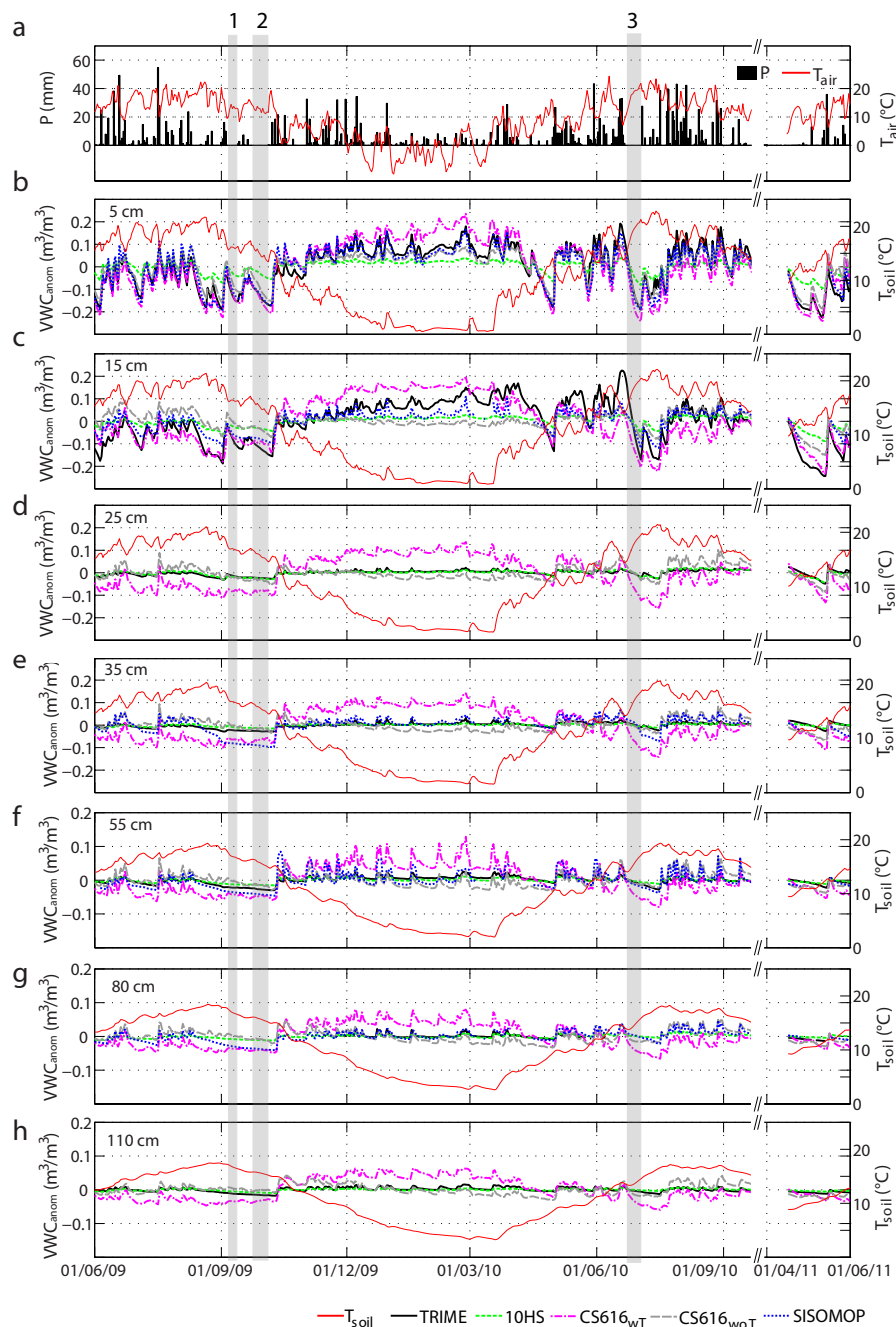
Figure 3.7: *Temporal evolution of (a) precipitation and 2-m air temperature and of (b to h) anomalies of soil moisture measurements (relative to the average VWC over the time period 1 June 2009 to 31 May 2011) of the different sensors and soil temperature measurements at the different depths at daily resolution. Dry down periods are indicated in grey and correspond to the following time frames: 8-13 September 2009 (1), 24 September - 05 October 2009 (2), and 25 June - 04 July 2010 (3). Note the different scale for the y-axis in plots f to h.*

Chapter 4

A new perspective on the spatio-temporal variability of soil moisture: Temporal dynamics versus time invariant contributions

A new perspective on
the spatio-temporal variability of soil moisture:
temporal dynamics versus time invariant contributions

Heidi Mittelbach[1] and S.I. Seneviratne[1]

(submitted to Hydrology and Earth System Sciences)

Abstract

Knowledge about the spatio-temporal variability of soil moisture is essential to understand and predict processes in climate science and hydrology. A significant body of literature exists on the characterization of the spatial variability and the ranks stability (also called temporal stability) of absolute soil moisture. Yet previous studies were generally based on short-term measurement campaigns and did not distinguish the respective contributions of time varying and time invariant components to these quantities. In this study, we investigate this issue using measurements from 14 grassland sites of the SwissSMEX soil moisture network (spatial extent of approx. 150×210 km) over the time period May 2010 to July 2011. We thereby decompose the spatial variance of absolute soil moisture over time in contributions from the spatial variance of the mean soil moisture at all sites (which is time invariant), and components that vary over time and are related to soil moisture dynamics. These include the spatial variance of the temporal soil moisture anomalies at all sites and the covariance between the sites' anomalies to the spatial mean at a given time step and those for the temporal mean values. The analysis demonstrates that the time invariant term contributes 50–160 % (on average 94 %) of the spatial soil moisture variance at any point in time, while the covariance term generally contributes negatively to the spatial variance. On the other hand the spatial variance of the temporal anomalies, which is overall most relevant for climate and hydrological applications because it is directly related to soil moisture dynamics, is relatively limited and constitutes at most 2–30 % (on average 9 %) of the total variance. Nonetheless, this term is not negligible compared to the temporal anomalies of the spatial mean. These results suggest that a large fraction of the spatial variability of soil moisture assessed from short-term campaign is time invariant. Moreover, we find that the rank (or "temporal") stability concept when applied to absolute soil moisture, mostly characterizes the time-invariant patterns. Indeed, sites that best represent the mean soil moisture dynamics of the network are not the same as those that best reflect mean soil moisture at any point in time. Overall this study shows that conclusions derived from the analysis of the spatio-temporal variability of absolute soil moisture do generally not apply to temporal soil moisture anomalies, and hence to soil moisture dynamics.

---

[1]Institute for Atmospheric and Climate Science, ETH Zurich, Switzerland

4.1   Introduction

Soil moisture is an essential variable in climate and hydrological science through its impact on the energy and water balance (see Seneviratne et al., 2010, for a review). Knowledge about soil moisture and its spatio-temporal variability, which is impacted by the heterogeneity of different characteristics, such as soil texture, vegetation, topography, and meteorological conditions, is essential to improve climate and hydrological modeling, remote sensing-based soil moisture estimates, and to optimize soil moisture monitoring networks (e.g. Vinnikov et al., 1996; Western et al., 2002; Jacobs, 2004; Koster et al., 2004; Seneviratne et al., 2006a; Robinson et al., 2008; Brocca et al., 2010).

Frequently used frameworks to investigate spatio-temporal variability of soil moisture patterns include geostatistical methods (Famiglietti et al., 2008; Western et al., 2004; Entin et al., 2000), the relationship between the spatial variance and the spatial mean soil moisture (e.g. Famiglietti et al., 1999; Brocca et al., 2010), and rank stability analyses (e.g. Vachaud et al., 1985; Martínez-Fernández and Ceballos, 2003; Tallon and Si, 2004; Zhou et al., 2007). These approaches are used to analyze and compare the spatial variability of soil moisture at multiple depths, across spatial scales and under different moisture conditions. Furthermore, several studies have analyzed the spatial variability of soil moisture and its relation to the spatial mean by using ground observations but also by stochastic analysis (e.g. Famiglietti et al., 1999; Teuling et al., 2006b; Vereecken et al., 2007). Investigations of the potential controls on soil moisture variability are for instance provided in Western et al. (1999); Albertson and Montaldo (2003); Cosh (2004); and Teuling and Troch (2005), and generally focus on parameters or variables such as soil texture, vegetation cover, topography, as well as land surface fluxes. The role of meteorological and climate forcing for spatial soil moisture variability has only be considered in few studies (Vinnikov et al., 1996; Robock et al., 1998; Entin et al., 2000). For its part, the concept of temporal stability proposed by Vachaud et al. (1985) aims at identifying the most representative soil moisture site within a given network and has been suggested to be relevant for improving monitoring strategies or for the upscaling of soil moisture (e.g. Kamgar et al., 1993; Guber et al., 2008; Brocca et al., 2009).

Most of the mentioned studies are based on data sets that were collected during short-term field campaigns. These studies often include observations for wet and dry conditions but no continuous long-term time series. However, already Bell et al. (1980) emphasized the need for long-term measurements to study the spatial variability over a large range of spatial mean moisture contents.

Long-term time series are essential to investigate soil moisture dynamics, i.e. variations of soil moisture in time. Previous analyses (Seneviratne, 2003; Seneviratne et al., 2004) indicated that temporal soil moisture variations may be more stable in space than absolute soil moisture. However, no extensive analyses were provided on this topic so far. In the present study we use continuous 15-month long soil moisture measurements from 14 sites of the SwissSMEX soil moisture network (Sect. 3.1), which cover a spatial extent of 150×210 km. The time series are decomposed in their temporal mean and anomalies. We apply the concepts of spatial variability and temporal stability to the decomposed time series, to assess to which extent they respectively contribute to the overall spatial soil moisture variability. In addition, we also in-

vestigate whether commonly applied concepts such as that of temporal stability are relevant from the point of view of soil moisture dynamics.

4.2 Methods

4.2.1 Framework to distinguish between time varying and time invariant contributors to spatial variability

Spatio-temporal variability of soil moisture is characterized by the spatial and temporal statistics of soil moisture. The spatial variability of soil moisture has been investigated in a number of previous studies using the relation between the spatial variance and the spatial mean of absolute soil moisture (e.g. Famiglietti et al., 1999; Brocca et al., 2007; Famiglietti et al., 2008). Here we propose a new approach, whereby we consider the respective contributions of time varying and time invariant factors to the overall spatial variability of soil moisture at any point in time.

For more clarity we will denote hereafter the mean μ, variance σ^2, and standard deviation σ with the subscript $\widehat{n}$ for the spatial statistics, and with the subscript $\widehat{t}$ for the temporal statistics. Let S_{tn} be the soil moisture of site $n \subset [1, ...N]$ at time $t \subset [1, ...T]$. Its spatial mean $\mu_{\widehat{n}}(S_{tn})$ and spatial variance $\sigma_{\widehat{n}}^2(S_{tn})$ at any time step t are defined as:

$$\mu_{\widehat{n}}(S_{tn}) = \frac{1}{N} \sum_{n=1}^{N} (S_{tn}), \tag{4.1}$$

$$\sigma_{\widehat{n}}^2(S_{tn}) = \frac{1}{N} \sum_{n=1}^{N} (S_{tn} - \mu_{\widehat{n}}(S_{tn}))^2. \tag{4.2}$$

Similarly, the temporal mean of soil moisture at any site n is defined as:

$$\mu_{\widehat{t}}(S_{tn}) = \frac{1}{T} \sum_{t=1}^{T} (S_{tn}) = m_n. \tag{4.3}$$

Note that of ease for notation we will use the symbol m_n to refer to the temporal mean $\mu_{\widehat{t}}(S_{tn})$.

Here we extend the classical framework that generally compares $\mu_{\widehat{n}}(S_{tn})$ and $\sigma_{\widehat{n}}^2(S_{tn})$ by decomposing S_{tn} into its temporal mean m_n and its temporal anomalies a_{tn}. This allows us to distinguish between spatio-temporal aspects that are time invariant and those related to soil moisture dynamics. Formally, this is expressed as follows:

$$S_{tn} = m_n + a_{tn}. \tag{4.4}$$

The corresponding equation for the mean of all sites is

$$\mu_{\widehat{n}}(S_{tn}) = \mu_{\widehat{n}}(m_n) + \mu_{\widehat{n}}(a_{tn}) = m_{\widehat{n}} + a_{t\widehat{n}}. \tag{4.5}$$

Using Equations (4.4) and (4.5), it is possible to decompose $\sigma_{\widehat{n}}^2(S_{tn})$ in time varying and time invariant components by resolving Equations (4.4) and (4.5) into Equations (4.1) and (4.2):

$$\sigma_{\widehat{n}}^2(S_{tn}) = \frac{1}{N} \sum_{n=1}^{N} [(m_n + a_{tn}) - (m_{\widehat{n}} + a_{t\widehat{n}})]^2. \tag{4.6}$$

Equation (4.6) can then be reexpressed as follows:

$$\sigma_{\widehat{n}}^2(S_{tn}) = \frac{1}{N} \sum_{n=1}^{N} [(m_n - m_{\widehat{n}})^2 + 2\mathrm{cov}(m_n - m_{\widehat{n}})(a_{tn} - a_{t\widehat{n}}) + (a_{tn} - a_{t\widehat{n}})^2], \tag{4.7}$$

resulting in the following Equation:

$$\sigma_{\widehat{n}}^2(S_{tn}) = \sigma_{\widehat{n}}^2(m_n) + 2\mathrm{cov}(m_n, a_{tn}) + \sigma_{\widehat{n}}^2(a_{tn}), \tag{4.8}$$

where $\sigma_{\widehat{n}}^2(m_n)$ is the spatial variance of temporal mean soil moisture, $\sigma_{\widehat{n}}^2(a_{tn})$ is the spatial variance of anomalies, and $\mathrm{cov}(m_n, a_{tn})$ is the spatial covariance between the temporal mean soil moisture of a site and its respective anomaly.

Note that Equation (4.8) can also be expressed as follows:

$$\sigma_{\widehat{n}}^2(S_{tn}) = \sigma_{\widehat{n}}^2(m_n) + 2\rho(m_n, a_{tn})\sigma(m_n)\sigma(a_{tn}) + \sigma_{\widehat{n}}^2(a_{tn}), \tag{4.9}$$

where $\rho(m_n, a_{tn})$ refers to the temporal correlation between m_n and a_{tn}.

Equation (4.8) allows to analyze the spatio-temporal variability of soil moisture considering its temporal mean m_n state and its dynamics a_{tn}. Furthermore, the temporal evolution of the spatial variance and the contribution of its single components can be investigated. Note that $\sigma_{\widehat{n}}^2(m_n)$ is time invariant, while $\sigma_{\widehat{n}}^2(a_{tn})$ and $\mathrm{cov}(m_n, a_{tn})$ vary over time.

4.2.2 Relating the rank stability concept to time varying and time invariant soil moisture components

The concept of temporal stability, proposed by Vachaud et al. (1985) is used in several previous studies to identify sites where soil moisture is considered to be most representative of the spatial mean soil moisture within a network (e.g. Kamgar et al., 1993; Teuling et al., 2006b; Brocca et al., 2010). Following Vachaud et al. (1985), the difference ΔS_{tn} between the soil moisture S_{tn} and the spatial mean soil moisture $\mu_{\widehat{n}}(S_{tn})$ is defined as:

$$\Delta S_{tn} = S_{tn} - \mu_{\widehat{n}}(S_{tn}). \tag{4.10}$$

Its relative difference is:

$$\delta S_{tn} = \frac{\Delta S_{tn}}{\mu_{\widehat{n}}(S_{tn})}, \tag{4.11}$$

and its temporal mean $\mu_{\widehat{t}}(\delta S_{tn})$ and temporal standard deviation $\sigma_{\widehat{t}}(\delta S_{tn})$ are estimated as:

$$\mu_{\widehat{t}}(\delta S_{tn}) = \frac{1}{T} \sum_{t=1}^{T} (\delta S_{tn}), \tag{4.12}$$

$$\sigma_{\hat{t}}(\delta S_{tn}) = \sqrt{\frac{1}{T} \sum_{t=1}^{T} (\delta S_{tn} - \mu_{\hat{t}}(\delta S_{tn}))^2}. \tag{4.13}$$

The $\mu_{\hat{t}}(\delta S_{tn})$ or $\mu_{\hat{t}}(\Delta S_{tn})$ of the sites are ranked from the smallest to the largest difference. Sites closest to $\mu_{\hat{n}}(S_{tn})$, i.e. $\mu_{\hat{t}}(\delta S_{tn}) \approx 0$ are considered to be the most representative of the overall network.

Using Equation (4.4), the temporal stability analyses (Equations 4.10–4.13) can be extended by including the different contributors to absolute soil moisture. As a_{tn} can have negative values the absolute value of the difference for a_{tn} and m_n are used:

$$|\Delta a_{tn}| = |a_{tn} - \mu_{\hat{n}}(a_{tn})|, \tag{4.14}$$

$$|\Delta m_n| = |m_n - \mu_{\hat{n}}(m_n)|. \tag{4.15}$$

The temporal mean and standard deviation of the anomalies $\mu_{\hat{t}}(\Delta a_{tn})$ and $\sigma_{\hat{t}}(\Delta a_{tn})$ can be analyzed to provide a ranking of the sites according to their respective deviation from the overall mean. Similarly, the absolute deviation of the temporal mean Δm can also provide a ranking. To relate the new ranking to the ranking of the overall soil moisture, the framework by Vachaud et al. (1985) is adapted here by considering the absolute terms $|\delta S|$ and $|\Delta S|$, respectively.

In this study, we are interested in the ranking of the single sites and not in the differences themself. The comparison of the rank of the absolute soil moisture S_{tn} with the ranks of its decomposed parts m_n and a_{tn} allows us to make a statement on how the framework of rank stability (Vachaud et al., 1985) incorporates the soil moisture dynamics.

4.3 Application to the SwissSMEX network

4.3.1 Studied network and data

The Swiss Soil Moisture Experiment (SwissSMEX) network (http://www.iac.ethz.ch/url/research/SwissSMEX) has a spatial extent of about 150×210 km and consists of overall 19 sites, covering different land use and climatic regimes of Switzerland. For further information about the set up and instrumentation of the network see Mittelbach et al. (2011). In the present study 14 grassland sites with no slope are included. Their location, respective climatic region (Müller, 1980), and average soil texture over 50 cm are shown in Figure 4.1. At each site, measurements of volumetric water content (VWC) at 5, 10, 30, and 50 cm depth as well as precipitation (P) and 2-m air temperature (T_{air}) are available. The VWC at the different depths were integrated over 50 cm using the trapezoidal method (e.g. Hupet et al., 2004) including an additional value of VWC at the surface, which is set equal to the measurement in 5 cm depth. The analysis is based on daily aggregated data for the time period 1 May 2010 to 31 July 2011, including the particular dry months April and May 2011.
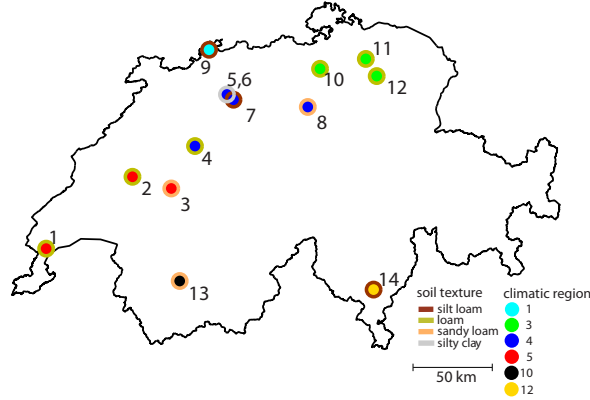
Figure 4.1: *Map of Switzerland showing the location, climatic region, and soil texture (according to USDA taxonomy and averaged over 50 cm depth) of the 14 investigated grassland sites of the SwissSMEX network. The indicated climate regions are based on the classification of Müller (1980).*

4.3.2 Relation between spatial variance and spatial mean

Brocca et al. (2007) investigate the relation between $\sigma_{\hat{n}}^2(S_{tn})$ and $\mu_{\hat{n}}(S_{tn})$, as well as the relation between the coefficient of variation ($CV = \sigma(S_{tn})/\mu_{\hat{n}}(S_{tn})$) and $\mu_{\hat{n}}(S_{tn})$, based on measurements from several networks. Based on these data they identified an increasing spatial variability with decreasing mean soil moisture for humid climates. The corresponding relation for the measurements used in the current study with their temporal occurrence is shown in Figure 4.2a and b. Similar to Brocca et al. (2007) an increasing variability with decreasing spatial mean is found. However, the values of spatial variability scatter more widely when spatial mean soil moisture decreases (Figure 4.2a). The nearly steady spatial variability with decreasing spatial mean soil moisture for April and May 2011 is particularly seen for $\sigma_{\hat{n}}^2(S_t)$.

The relation for the anomalies (Figure 4.2c) shows the behavior of soil moisture, when the temporal mean state of each site is removed and only its dynamics are considered. A parabolic shape with expected smallest variability for moisture conditions close to the spatial mean $m_{\hat{n}}$, with $\mu_{\hat{n}}(a_{tn}) \approx 0$, is found. Interestingly, the dry period of April and May 2011 is not as outstanding for the soil moisture anomalies (Figure 4.2c) as when considering the absolute soil moisture (Figure 4.2a, b), given that it shows an increase in variability similar to that seen in July and August 2010.

For both absolute soil moisture as well as its anomalies, a temporal dependency in the sequence of the relation is found. Indeed, for the absolute soil moisture, highest spatial mean related to lowest spatial variance, e.g. for the DJF season, and lowest spatial mean related to highest spatial variance, e.g. for May to August, are found. On the other hand, the relation of the anomalies reflect the longer dry period from July 2010 to the beginning of August 2010 and the particularly dry April and May 2011 (see Figure 4.3a for the spatial P and T_{air} during these periods).
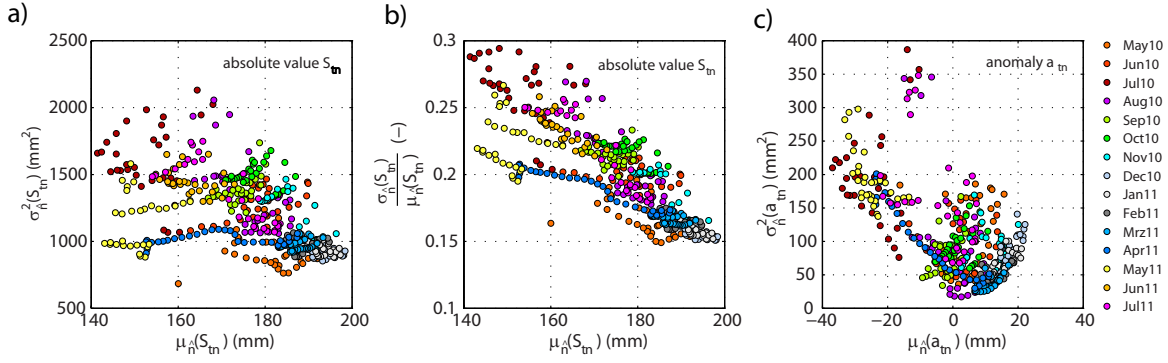
Figure 4.2: *Scatter plots of (a) the spatial mean ($\mu_{\widehat{n}}(S_{tn})$) vs. spatial variance ($\sigma^2_{\widehat{n}}(S_{tn})$) of daily absolute soil moisture, (b) the coefficient of variation ($\sigma_{\widehat{n}}(S_{tn})/\mu_{\widehat{n}}(S_{tn})$) vs. the spatial mean ($\mu_{\widehat{n}}(S_{tn})$) of daily absolute soil moisture, as well as (c) the spatial mean ($\mu_{\widehat{n}}(a_{tn})$) vs. spatial variance ($\sigma^2_{\widehat{n}}(a_{tn})$) of daily anomalies. The different colors indicate daily data of the single months.*

4.3.3 Time series of spatial variability

Figure 4.3 displays the time series of the spatial mean and spatial standard deviation for P and T_{air} (Figure 4.3a), which show a higher and more fluctuating variability in P and a more spatially homogeneous T_{air}. Figure 4.3b shows the spatial mean $\mu_{\widehat{n}}(S_{tn})$ and spatial standard deviation $\sigma_{\widehat{n}}(S_{tn})$ of absolute soil moisture. The term $\mu_{\widehat{n}}(S_{tn})$ is positively related to P and negatively related to T_{air} and shows smallest variability during the winter months. While the time series of spatial mean of the anomalies $\mu_{\widehat{n}}(a_{tn})$ (Figure 4.3c) show a similar behavior to $\mu_{\widehat{n}}(S_{tn})$, its standard deviation $\sigma_{\widehat{n}}(a_{tn})$ (Figure 4.3c, grey band) displays a higher variability than $\sigma_{\widehat{n}}(S_{tn})$. A notable increase in $\sigma_{\widehat{n}}(a_{tn})$ is visible during longer-lasting periods with no rain over the whole network, such as in July to August 2010 and April to May 2011, but also during longer lasting periods with rain at all sites, such as the end of August 2010.

4.3.4 Time series of decomposed spatial variability

The temporal evolution of the spatial variance of absolute soil moisture and its components according to Equation (8) are shown in Figure 4.3d. Their respective percentage is shown in Figure 4.3e and summarized over the DJF, MAM, JJA, and SON seasons in Figure 4.4a. As indicated in Figure 4.3c, $\sigma^2_{\widehat{n}}(S_{tn})$ displays clear lower variability for the winter and spring months compared with the summer and autumn seasons. The time invariant $\sigma^2_{\widehat{n}}(m_n)$ contributes most to $\sigma^2_{\widehat{n}}(S_{tn})$ with percentages ranging from about 50 to 160 %, with largest percentages and exceedance of $\sigma^2_{\widehat{n}}(S_{tn})$ during the DJF and MAM seasons, but also during particularly wet or dry conditions, such as in May 2010 as well as in April and May 2011. This exceedance is compensated by the time variant contributors $\sigma^2_{\widehat{n}}(a_{tn})$ and $\mathrm{cov}(m_n, a_{tn})$, and reflects a negative contribution of $\mathrm{cov}(m_n, a_{tn})$ of about 50 % during these periods. The contribution of $\sigma^2_{\widehat{n}}(a_{tn})$ is smallest and ranges between about 2 to 30 % and is highest for MAM and JJA with an average percentage of 10 % (Figure 4.4a). Interestingly, $\sigma^2_{\widehat{n}}(a_{tn})$ shows an increase during particularly dry periods, such as in July 2010 as well as in April and the mid of May 2011, which are not seen in $\sigma^2_{\widehat{n}}(S_{tn})$. Summarized by seasons (Figure 4.4a), the smallest percentages
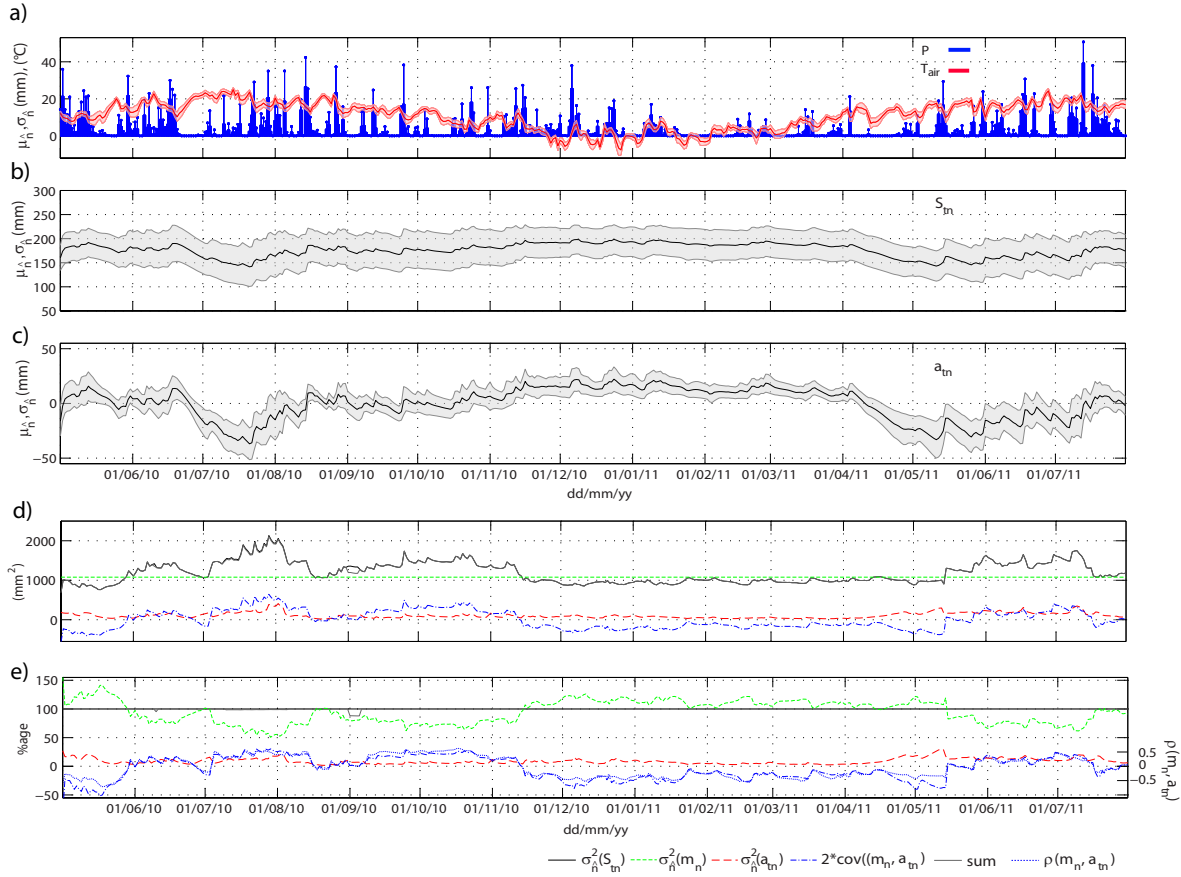
Figure 4.3: *Time series of spatial mean and spatial standard deviation (shaded areas) for (a) precipitation and 2-m air temperature, (b) absolute soil moisture, and (c) anomalies of absolute soil moisture. Decomposition of spatial variance of absolute soil moisture into its contributors according to Equation (7) expressed (d) in mm^2 and (e) as percentage.*

of $\sigma_{\hat{n}}^2(m_n)$ and highest percentages of the summed $\sigma_{\hat{n}}^2(a_{tn})$ and $\text{cov}(m_n, a_{tn})$ are found for the summer season (JJA). This indicates that the soil moisture dynamics has the largest impact on the spatial variability in this season. Figure 4.4b confirms that the spatial variance of absolute soil moisture is equal to the sum of the single terms in Equation (4.8). The discrepancies from the 1:1 line correspond to missing values at single sites.

The relation between the single contributors can be seen in the scatter plots of Figure 4.5. The scatter plot between $\sigma_{\hat{n}}^2(a_{tn})$ and $\sigma_{\hat{n}}^2(S_{tn})$ (Figure 4.5a) shows a general positive relation between these two terms. However, for $\sigma_{\hat{n}}^2(S_{tn}) < \sigma_{\hat{n}}^2(m_n)$ the data scatters more widely, and moreover, the particular dry May enhances this scatter, indicating the above mentioned dynamics, which is not found in the total soil moisture variance. A positive, mostly linear, relation between $\text{cov}(m_n, a_{tn})$ and $\sigma_{\hat{n}}^2(S_{tn})$ is identified in Figure 4.5b. The contribution of $\text{cov}(m_n, a_{tn})$ results in positive but also negative values, where negative values occur for $\sigma_{\hat{n}}^2(S_{tn}) < \sigma_{\hat{n}}^2(m_n)$. The different sign of $\text{cov}(m_n, a_{tn})$ for $\sigma_{\hat{n}}^2(S_{tn})$ above or below $\sigma_{\hat{n}}^2(m_n)$ implies a change in the relation between $\sigma_{\hat{n}}^2(m_n)$ and $\sigma_{\hat{n}}^2(a_{tn})$, which depends on the structure of anomalies, as the variability in the mean stays the same over time.
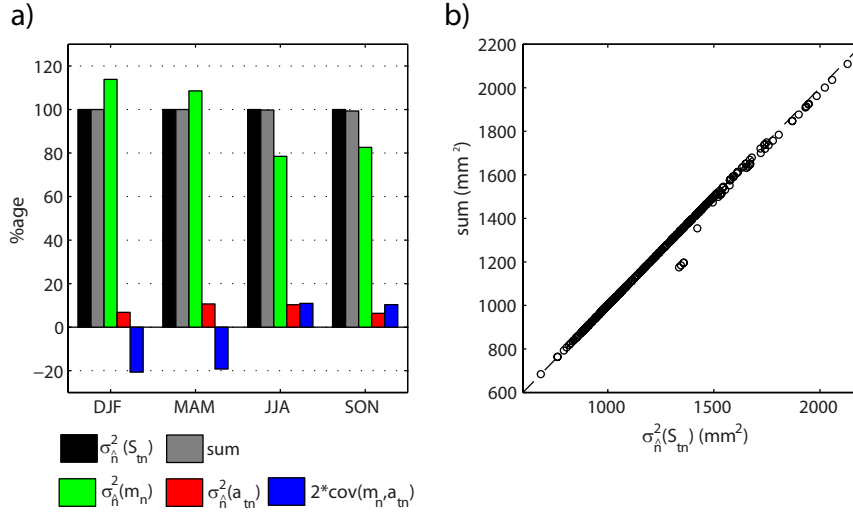
Figure 4.4: *(a) Percentage of the single contributors to the spatial variance of absolute soil moisture ($\sigma^2_{\hat{n}}(m_n)$, $\sigma^2_{\hat{n}}(a_{tn})$ and $2 * \mathrm{cov}(m_n, a_{tn})$) averaged over the seasons DJF, MAM, JJA, and SON. (b) Scatter plot of the spatial variance of absolute soil moisture vs. the sum of the single contributors.*
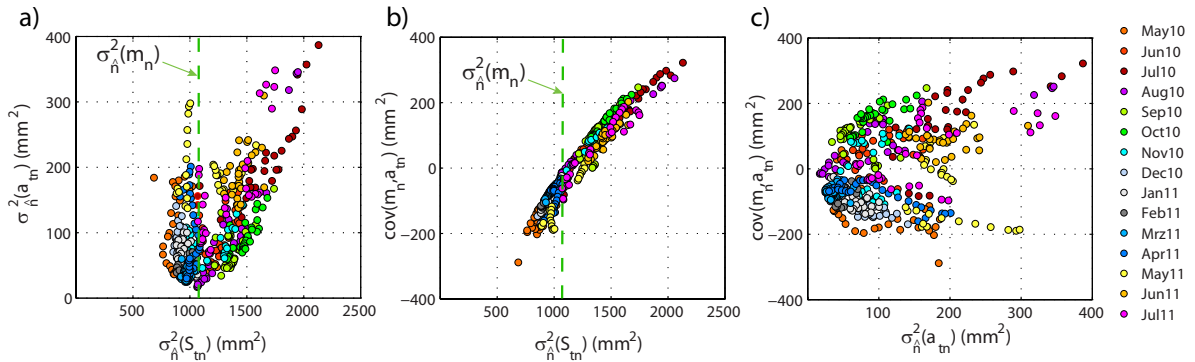
Figure 4.5: *Scatter plots of (a) the spatial variance of absolute soil moisture ($\sigma^2_{\hat{n}}(S_{tn})$) vs. spatial variance of anomalies ($\sigma^2_{\hat{n}}(a_{tn})$), (b) spatial variance of absolute soil moisture vs. spatial covariance of mean and anomalies $2*\mathrm{cov}(m_n, a_{tn})$, and of (c) spatial variance of anomalies vs. the spatial covariance between the mean and anomalies. The green dotted line represents the variance of spatial temporal mean ($\sigma^2_{\hat{n}}(m_n)$).*

4.3.5 Temporal stability of absolute soil moisture and its dynamics

The rank ordered temporal mean of relative difference δS_{tn} as well as of absolute difference ΔS_{tn} after Vachaud et al. (1985) with one standard deviation is shown in Figure 4.6a, b. The temporal mean of δS_{tn} varies between $-35\,\%$ and $39\,\%$, its standard deviation varies between $3\,\%$ and $10\,\%$. These values are comparable to values found in the literature using observations from networks with a smaller spatial extent (see e.g. Brocca et al., 2009, for a summary of the characteristics of temporal stabilty of different studies).

The rank ordered absolute value of differences for the total and decomposed soil moisture ($|\mu_{\hat{t}}(\delta S_{tn})|, |\mu_{\hat{t}}(\Delta S_{tn})|, \ |\Delta m_n|,$ and $\mu_{\hat{t}}(|\Delta a_{tn}|))$ with one standard deviation, are shown in

Figure 4.6c, d and Figure 4.7, respectively. As expected, the ranks of $|\mu_{\hat{t}}(\delta S_{tn})|$ and $|\mu_{\hat{t}}(\Delta S_{tn})|$ have the same order. In this study we focus on the ordered ranks of $|\mu_{\hat{t}}(\Delta S_{tn})|$ and we analyze their relation to the time-varying and time-invariant contributions by comparing the ranks of $|\mu_{\hat{t}}(\Delta S_{tn})|$ (Figure 4.6d) with the ranks of the absolute differences of the decomposed soil moisture $|\Delta m_n|$ and $\mu_{\hat{t}}(|\Delta a_{tn}|)$ (Figure 4.7a, b). Considering the ranks of the decomposed S_{tn} (Figure 4.7), it is seen that the ranks of $|\mu_{\hat{t}}(\Delta S_{tn})|$ (Figure 4.6d) are mostly reflected by the ranks of $|\Delta m_n|$ (Figure 4.7a). The ranks of the temporal mean of the anomalies $\mu_{\hat{t}}(|\Delta a_n|)$ (Figure 4.7b) show a contrasting sequence for the sites. The scatter plots of Figure 4.8 indicate that the rank stability of S_{tn} contains information about the temporal mean of soil moisture, but is not related to the dynamics of soil moisture. Hence, this suggests that the evaluation of the stability of the rank ordering of $\mu_{\hat{t}}(\delta S_{tn})$ proposed by Vachaud et al. (1985) is a measure of the rank stability of mean soil moisture conditions within the SwissSMEX network but does not provide information on the varying spatio-temporal characteristics of the network.
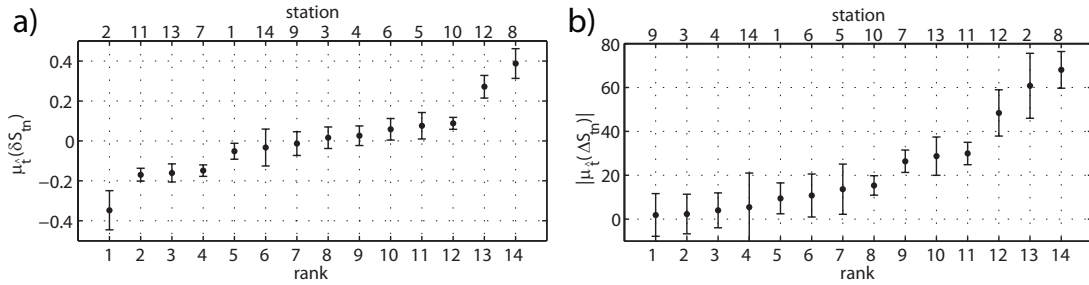
Figure 4.6: *Rank stability plots of (a) the temporal mean of relative difference of absolute soil moisture $\mu_{\hat{t}}(\delta S_{(tn)})$, (b) the temporal mean of difference of absolute soil moisture ($\mu_{\hat{t}}(\Delta S_{tn})$), (c) the absolute values of temporal mean of the relative difference of absolute soil moisture $|\mu_{\hat{t}}(\delta S_{(tn)})|$, and (d) the absolute values of temporal mean of difference of absolute soil moisture $|\mu_{\hat{t}}(\Delta S_{(tn)})|$. The vertical lines represent $\pm$ one standard deviation. The sites have been ranked according to their mean differences.*
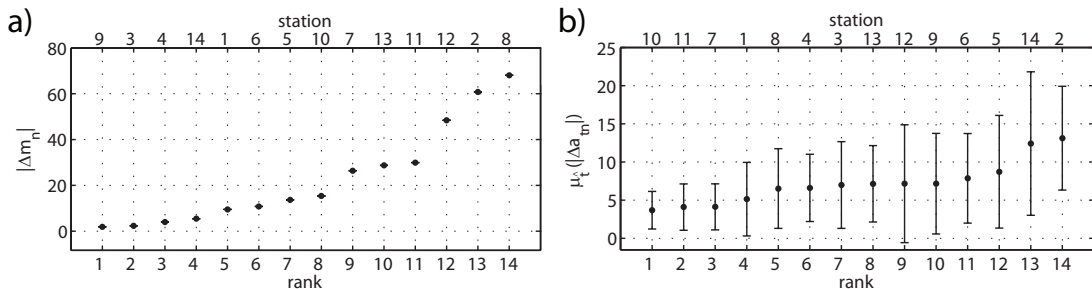
Figure 4.7: *Rank stability plots of (a) the absolute value of temporal mean ($|m_n|$), and (b) the temporal mean of the absolute values of differences of anomalies ($\mu_{\hat{t}}(|\Delta a_{tn}|)$). The vertical lines represent $\pm$ one standard deviation. The sites have been ranked according to their mean differences.*
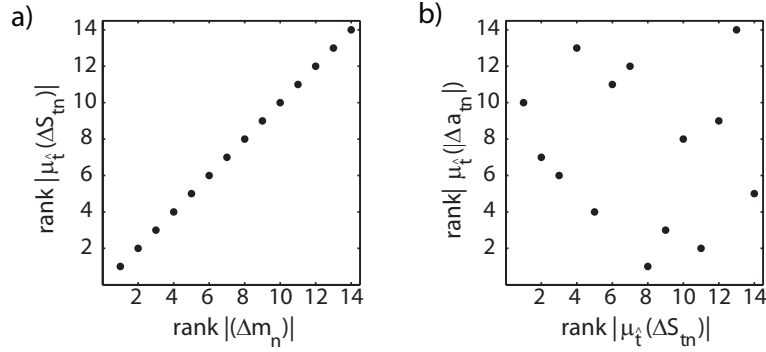
Figure 4.8: *Scatter plots of (a) the rank of absolute value of temporal mean ($|m_n|$) vs. the rank of absolute values of temporal mean difference of absolute soil moisture ($|\mu_{\hat{t}}(\Delta S_{tn})|$) and (b) the rank of absolute values of temporal mean difference of absolute soil moisture vs. the rank of temporal mean of absolute values of differences of anomalies ($\mu_{\hat{t}}(|\Delta a_{tn}|)$).*

4.4 Discussion

In this study we expand frequently used hydrological frameworks for the analysis of the spatio-temporal variability of soil moisture within a given network to distinguish between the contribution of the temporal mean and anomalies of soil moisture. Furthermore, we focus on how the dynamics of soil moisture is represented in these frameworks. Previous studies on related topics (e.g. Kamgar et al., 1993; Famiglietti et al., 1999; Teuling et al., 2006b; Brocca et al., 2007) were mostly based on non-continuous observations or short-term campaigns and focused on the investigation of absolute soil moisture values. By contrast, this study is based on 15-months long continuous soil moisture measurements from 14 grassland sites of the SwissSMEX network. It analyzes the decomposed absolute soil moisture, including its time invariant temporal mean and its time variant dynamics, expressed as anomalies. The time invariant term is influenced by factors, that do not significantly change over time, such as the topography, soil texture, and land cover, while the time variant dynamics are controlled by factors that change at synoptic scale, such as climate variables. Another aspect contributing to the time invariant component is the climate regime over the considered time frame, which strictly speaking could be time varying if the analyzed time series spanned a longer time period, such as several years or decades. The decomposition enables us to investigate the spatio-temporal variability of absolute soil moisture with a focus on the contribution of its single components. Using long-term measurements provides furthermore the possibility to analyze the temporal evolution of the spatial variability of soil moisture.

First comparisons of the relation between the spatial variance and the spatial mean absolute soil moisture as well as for the temporal stability indicates an overall behavior that is consistent with previous reports from the literature (see Brocca et al., 2007, 2010, for a summary). Regarding the relation between the spatial variance and spatial mean absolute soil moisture, the relation for absolute soil moisture and its anomalies, respectively, are analyzed. Comparing both relations, a different variability is mainly found for average dry moisture contents. The particularly dry 2011 spring shows almost constant absolute soil moisture during the recession of the spatial mean moisture content, while the variability of the anomalies indicates an in-

creased variability during this period.

Regarding the temporal evolution of the spatial variability of absolute soil moisture and the contribution of its time varying and time invariant parts, the results reveal that the variance of the time invariant mean is with 50 to 160 % the largest contributor to the overall spatial variability. The variance of temporal anomalies contributes by about 5 to 30 %. The covariance term of the temporal mean and anomalies results in correlations of both negative and positive signs, including periods of almost no correlation. For the DJF season the relation is continously negative with low variability over the whole period, whereas in the other seasons the correlation changes between positive and negative values, influenced by the meteorological conditions, with mainly positive values for JJA and SON. For periods with particularly wet but also particularly dry soil moisture conditions, as in the case of the dry 2011 spring, the correlation results in negative values and appears to get more negative with longer lasting duration. This implies that the sequence of the sites with respect to their mean status is not the same for their anomalies. Indeed, for the studied period the particularly dry 2011 spring shows the strongest increase of a negative correlation between the spatial variance of absolute soil moisture and anomalies, resulting in different potential controls of spatial variability during such periods. Furthermore, this suggests that the dynamics can vary strongly for the different sites, while their mean state stays similar. Findings of the rank stability analyses confirm that the ordered ranks of the temporal mean absolute soil moisture are similar to the ranks of its mean state, while the ranks of the soil moisture dynamics are not consistent with this ranking. Indeed, sites which are identified as being most representative for the spatial mean do not correspond to the sites that are most representative for the soil moisture dynamics within the network.

4.5 Conclusions

From the analyses of this study, we conclude that frequently used frameworks assessing spatio-temporal characteristics of soil moisture networks do generally not apply to temporal soil moisture anomalies. For the investigated data set, the analyses of the decomposed soil moisture reveals a small contribution of the dynamics to the overall variability of soil moisture. Reversely, this indicates a smaller spatial variability of the temporal dynamics than possibly inferred from the spatial variability of the mean soil moisture. Although the spatial variability of anomalies contributes with a smaller percentage to the whole spatial variance, its contribution is nonetheless not negligible compared to the actual values of the temporal anomalies. Based on our results we strongly encourage further analyses investigating the spatio-temporal characteristics of temporal soil moisture anomalies, in addition to those assessing temporal mean or absolute soil moisture. This is essential for investigations focusing on soil moisture dynamics e.g. on runoff generation, drought development, and land-atmosphere interactions (e.g. Entekhabi et al., 1996; Seneviratne et al., 2010), weather and seasonal forecasting (e.g. Beljaars et al., 1996; Koster et al., 2010a; Weisheimer et al., 2011) or climate change applications. To our knowledge this is the first study focusing on the spatio-temporal variability of soil moisture that provides a separate analysis for its time varying and time invariant components. The presented framework could be easily applied to further long-term data sets to investigate the spatial and temporal variability of soil moisture and its dynamics under various climate conditions.

Acknowledgement

Chapter 5

Soil moisture and soil temperature development across different land cover types

Soil moisture and soil temperature development across different land cover types

5.1 Introduction

As mentioned in Chapter 1, soil moisture is among other factors affected by land cover with consequent impact on e.g. evapotranspiration and temperature. The characteristics of vegetation such as albedo, friction, stomatal resistance, rooting depth, density, as well as phenology contribute strongly to variations in soil moisture, soil temperature and air temperature. Several studies investigated variations in surface exchanges with land cover and the consequences of land use change for climate change (e.g. Fu et al., 2003; Teuling et al., 2010b; Zha et al., 2010; Peel et al., 2010; Venkatesh et al., 2011; Renaud and Rebetez, 2009). Beside soil moisture and air temperature, also the behavior of soil temperature is of interest, as it influences e.g. the activity of soil fauna, seed germination, and the mineralization of nitrogen.

The SwissSMEX-*Veg* equipment project, which was started in 2010, allowed an extension of the SwissSMEX network to forest sites (see Section 1.4.1). In this chapter a first investigation of the role of land cover (grassland and forest) for soil moisture and soil temperature dynamics is provided. The analyses build upon the BSc thesis of Henschel (2011), and provide a comparison of soil temperature and soil moisture time series, with a focus on the recession of soil moisture during precipitation free periods.

5.2 Investigated sites

Henschel (2011) compared three of four paired SwissSMEX sites. Each pair consists of a grassland and a forest site and is located in a different climate region of Switzerland (Müller, 1980, see also Appendix A for more details). The pairs are Changins/Lausanne (CHN/LAU), Cadenazzo/Novaggio (CAD/NOV), and Taenikon/Laegern (TAE/LAE), whereas the first listed site corresponds to the grassland and the second to the forest site. The site, location, and pictures are shown in Figure 5.1, while their site specific characteristics are listed in Table 5.1. Daily measurements of volumetric water content and soil temperature at 5, 10, 30 and 50 cm depth are available for all sites. Almost no measurements of volumetric water content are available at CHN in 30 cm depth due to a broken sensor. The time series at the forest sites LAU and NOV include data gaps due to irregular power failures. Column soil moisture S over 0 to 50 cm is estimated by the integration of the volumetric water content at 5, 10, 30, and 50 cm depth using the trapezoidal method (e.g. Hupet et al., 2004), and by assuming that surface volumetric water content is equal to that measured in 5 cm depth. Meteorological variables are available from nearby stations operated by MeteoSwiss for the grassland sites, by WSL for the forest sites LAU and NOV, and by the Grassland Science group of the Institute of Agricultural Sciences at ETH Zurich for the LAG site. Daily data of precipitation, 2-m air temperature, and relative humidity were used for the analyses. The meteorological variables for the forest sites

NOV and LAU are measured below the canopy, whereas for the LAG site they are measured above the canopy from a 45 m high FLUXNET tower.

The analyses include daily aggregated measurements over different time periods: CHN/LAU 25 June 2010 to 28 February 2011, CAD/NOV 02 July 2010 to 28 February 2011, and TAE/LAG 01 May 2010 to 28 February 2011.
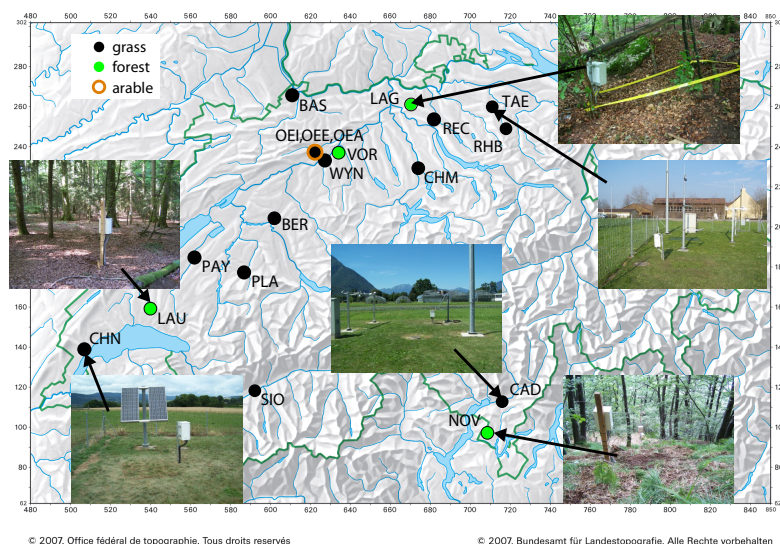
Figure 5.1: *SwissSMEX network with the investigated paired grassland and forest SwissSMEX/-Veg sites CHN/LAU, CAD/NOV, and TAE/LAG.*

Table 5.1: *Basic characteristics of the investigated sites.*

Site	Land use	Elevation (m a.s.l.)	Soil texture (USDA taxonomy)	slope (%)	aspect
CHN	grassland	430	loam	0	none
LAU	deciduous forest	800	sandy loam	7	NE
CAD	grassland	197	silt loam	0	none
NOV	deciduous forest	950	loamy sand	68	S
TAE	grassland	536	loam	0	none
LAG	mixed forest	682	clay	27	S

5.3 Results and discussion

5.3.1 Meteorological conditions at paired sites

Figure 5.2 shows the Spearman correlation between the different sites for the meteorological variables 2-m air temperature, precipitation, and relative humidity at daily time scales. All correlations are significant at the 5% level. It can be seen that the correlation of air temperature is high (>0.90) between all sites. In contrast, precipitation and relative humidity show higher heterogeneity between the sites, indicating a higher spatial variabilty than air temperature. For
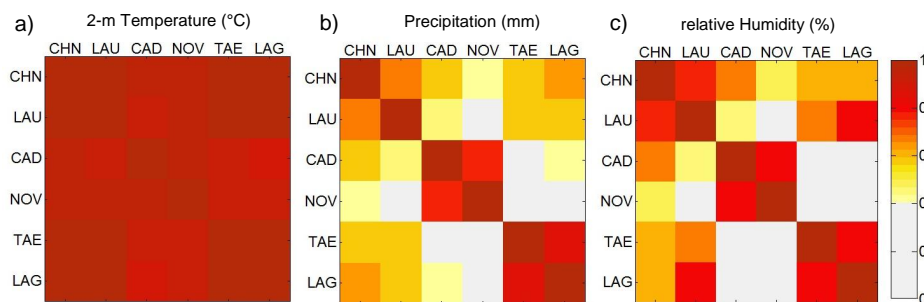
Figure 5.2: *Spearman correlation of (a) 2-m air temperature, (b) precipitation, and (c) relative humidity. Correlations <0.4 are gray. All correlations are significant with $\alpha = 5\%$.*

precipitation highest correlation are found between the paired grassland/forest sites with a correlation of 0.68 for CHN/LAU, 0.75 CAD/NOV and 0.86 for TAE/LAG. Clear low correlation (<0.4) are indicated between the paired sites (TAE/LAG) and CAD/NOV. A similar signal is found for relative humidity, suggesting a possible link of its temporal evolution to precipitation.

The cumulative distribution functions (cdf) for air temperature, precipitation, and relative humidity at each site pair are shown in Figure 5.3. The similarity of the underlying distributions within the site pairs is tested with the Kolmogorov-Smirnov test at a significance level of 5%. The cdfs of precipitation and air temperature indicate CAD/NOV to be the wettest paired site and CAD to be the warmest site. The distributions show similar shapes for air temperature and precipitation within the paired sites. In addition, the probability of a specific precipitation amount within the paired sites is similar. Although the cdfs of air temperature show similar shape at the grassland and forest sites, they display different temperature ranges, especially for CHN/LAU and CAD/NOV. The curve of the forest sites is shifted towards lower air temperature, which can be largely explained by the difference in elevation at these two pairs of 370 m and 753 m, respectively. To take this fact into account, the time series of air temperature is additionally corrected by a lapse rate of 0.65 K/100 m. With this correction, the air temperature distribution of the paired sites are similar, except for CAD/NOV. The cdfs of relative humidity display larger differences between the grassland and forest sites (except for CHN/LAU).

The comparison of the meteorological conditions shows that the paired soil moisture sites are characterized by similar meteorological conditions while different meteorological conditions between the paired sites exists. This is expected, as they are located in different climate regions of Switzerland (Müller, 1980).

5.3.2 Air temperature and soil temperature

The monthly statistics of daily average and maximal 2-m air temperature, corrected by a lapse rate of 0.65 K/100 m, as well as the difference between the grassland and forest sites are displayed in Figure 5.4. Note that at LAU and NOV air temperature is measured below the canopy. For all sites, an annual cycle of the average and maximal air temperature is visible with highest values in July. As suggested by the analyses of the cdfs (Figure 5.3), the corrected temperature
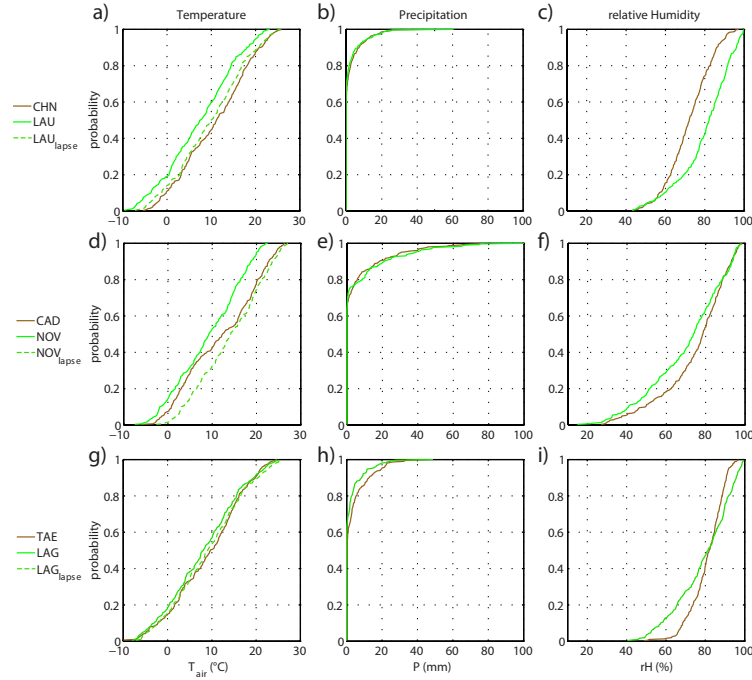
Figure 5.3: *Cumulative probability function of (a,d,g) 2-m air temperature, (b,e,h) precipitation, and (c,f,i) relative humidity for the paired sites (a-c) CHN/LAU, (d-f) CAD/NOV, and (g-i) TAE/LAG. The dashed green line refer to the 2-m air temperature corrected with a lapse rate of 0.65 K/100 m. The grassland sites are illustrated in brown and the forest sites are illustrated in green.*

values are similar for both land cover types, with slightly lower values for the forest especially for maximal daily temperatures. An exception is CAD/NOV, which display from September on a higher temperature for the forest sites possible due to the southern expect with steep slopes of the NOV site (see Table 5.1 for site characteristics).

The similar lapse rate-corrected temperatures suggest that the differences in daily temperature is mostly affected by elevation. For further detailed analyses, e.g. of the variability and diurnal cycle if temperature, an impact of the canopy is suggested through different insulation of the surface layer. Furthermore, this effect is expected to change over the seasons due to the phenology of deciduous and mixed forests (Ferrez et al., 2011).

The mean time delay Δt between the peak in daily air temperature to soil temperature over the whole period is shown in Figure 5.5. Henschel (2011) estimated the mean time delay simplified using the temporal occurrence of maximum soil temperature at the depths z of 5, 10, and 30 cm and the time of daily maximum of air temperature by:

$$\Delta t_z = t(max(T_{soil_z})) - t(max(T_{air})). \tag{5.1}$$

This analysis illustrates that the peak soil temperature lagged that of air temperature by increasingly large amounts with increasing depth, which is obviously expected when taking into account heat diffusion in the soil (Hillel, 2007). For grassland the penetration of heat down to 5 and 10 cm takes about 2 and 4 hours, respectively. The time delay for 5 cm depth is for the forest site nearly twice as long as for the grassland site. This gives also an indication of
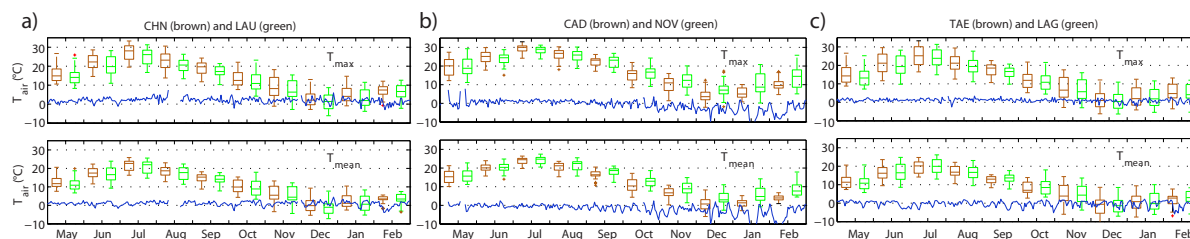
Figure 5.4: *Monthly boxplots for daily maximum 2-m air temperature (T_{max}) and daily mean 2-m air temperature (T_{mean}) for the paired sites (a) CHN/LAU, (b) CAD/NOV, and (c) TAE/LAG. The temperature was corrected with a lapse rate of 0.65 K/100 m. The grassland sites are illustrated in brown and the forest sites in green. The blue lines show the difference between the temperature of the grassland and the temperature of the forest sites. Note that the 2-m air temperature of the LAG site is measured above the canopy.*

a slower propagation of soil heat flux for forest. The large delay in soil temperature seems to be present only for the uppermost soil layer, as the difference nearly disappears at 30 cm depth. The magnitude of the time delay varies for different meteorological conditions and soil moisture.
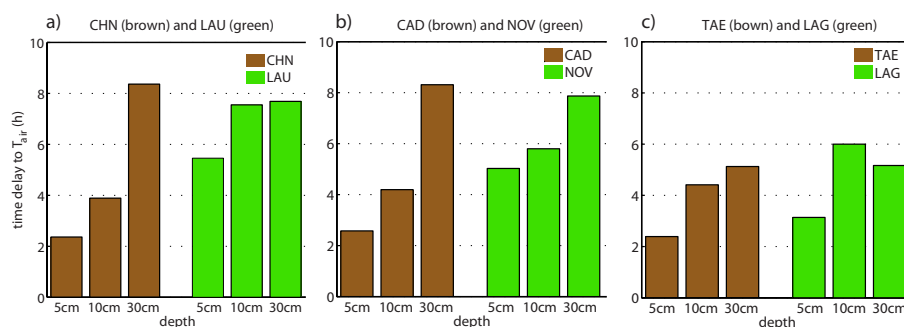
Figure 5.5: *Time delay of soil temperature with respect to the 2-m air temperature for the different paired sites (a) CHN/LAU, (b) CAD/NOV, and (c) TAE/LAG. The grassland sites are illustrated in brown and the forest sites are illustrated in green.*

5.3.3 Absolute volumetric water content and its anomalies

The absolute volumetric water content and its anomalies at 5, 10, 30 and 50 cm depths are shown in Figure 5.6 and Figure 5.7. Their statistics are summarized in Table 5.2 and Table 5.3, respectively. The reaction of volumetric water content to precipitation and to air temperature is visible independent of the vegetation cover, whereas the grassland sites react more intensively. Highest values of mean volumetric water content are found for the LAG site, which is characterized by clayey soil texture. In general, the mean volumetric water content is increasing with increasing depth, while its variability is decreasing with increasing depth, with very low variability at the deepest soil layer at all sites (Table 5.2).

Table 5.2: *Mean, standard deviation, minimum, and maximum of absolute volumetric water content (m^3/m^3) at the different measurement depths and for the column soil moisture (mm) for the investigated sites.*

		depth						depth				
		5 cm	10 cm	30 cm	50 cm	column SM		5 cm	10 cm	30 cm	50 cm	column SM
mean	CHN	0.31	0.33		0.36	170.35	LAU	0.29	0.30	0.31	0.31	151.40
stdv		0.05	0.06		0.03	22.16		0.02	0.01	0.03	0.02	10.01
max		0.39	0.42		0.40	202.66		0.33	0.33	0.41	0.38	183.78
min		0.22	0.23		0.32	134.38		0.26	0.27	0.27	0.28	135.10
range		0.17	0.18		0.08	68.29		0.07	0.06	0.14	0.10	48.69
mean	CAD	0.30	0.35	0.36	0.39	177.09	NOV	0.28	0.33	0.29	0.26	147.73
stdv		0.07	0.05	0.04	0.03	23.32		0.02	0.02	0.01	0.01	7.53
max		0.46	0.43	0.44	0.43	219.09		0.36	0.40	0.32	0.30	169.20
min		0.13	0.18	0.22	0.29	104.37		0.23	0.29	0.26	0.23	129.37
range		0.33	0.25	0.22	0.15	114.73		0.13	0.11	0.06	0.06	39.82
mean	TAE	0.29	0.31	0.27	0.36	150.08	LAG	0.40	0.47	0.37	0.36	197.09
stdv		0.03	0.03	0.03	0.01	11.79		0.03	0.02	0.01	0.01	7.16
max		0.34	0.33	0.31	0.37	164.47		0.47	0.52	0.39	0.38	217.01
min		0.18	0.20	0.17	0.33	108.19		0.30	0.41	0.32	0.32	168.78
range		0.16	0.13	0.13	0.04	56.28		0.17	0.11	0.08	0.06	48.23

Table 5.3: *Standard deviation, minimum, and maximum of anomalies of absolute volumetric water content (m^3/m^3) at the different measurement depths and for the column soil moisture (mm) for the investigated sites.*

		depth						depth				
		5 cm	10 cm	30 cm	50 cm	column SM		5 cm	10 cm	30 cm	50 cm	column SM
stdv	CHN	0.05	0.06		0.03	22.16	LAU	0.02	0.01	0.03	0.02	10.01
max		0.08	0.08		0.04	32.31		0.04	0.03	0.10	0.07	32.38
min		-0.09	-0.10		-0.04	-35.98		-0.03	-0.02	-0.04	-0.03	-16.30
range		0.17	0.18		0.08	68.29		0.07	0.06	0.14	0.10	48.69
stdv	CAD	0.07	0.05	0.04	0.03	23.32	NOV	0.02	0.02	0.01	0.01	7.53
max		0.17	0.08	0.08	0.05	42.00		0.08	0.06	0.03	0.03	21.47
min		-0.17	-0.18	-0.14	-0.10	-72.72		-0.05	-0.05	-0.03	-0.03	-18.35
range		0.33	0.25	0.22	0.15	114.73		0.13	0.11	0.06	0.06	39.82
stdv	TAE	0.03	0.03	0.03	0.01	11.79	LAG	0.03	0.02	0.01	0.01	7.16
max		0.05	0.03	0.04	0.01	14.38		0.07	0.06	0.02	0.03	19.92
min		-0.12	-0.10	-0.10	-0.03	-41.90		-0.10	-0.06	-0.05	-0.04	-28.31
range		0.16	0.13	0.13	0.04	56.28		0.17	0.11	0.08	0.06	48.23
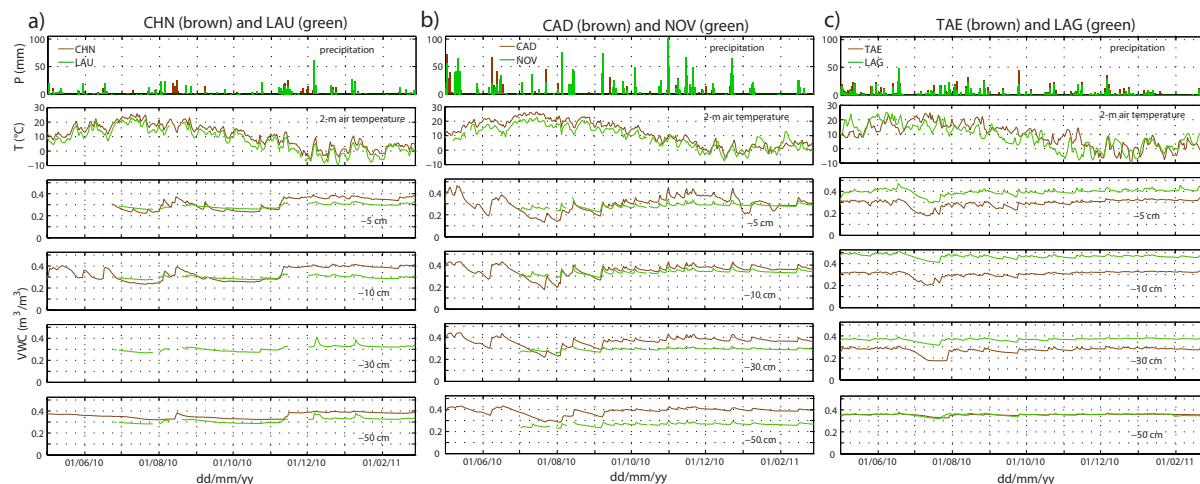
Figure 5.6: *Temporal evolution of precipitation, 2-m air temperature and of absolute soil moisture measurements at the different depths of the paired sites (a) CHN/LAU, (b) CAD/NOV, and (c) TAE/LAG. The grassland sites are illustrated in brown and the forest sites are illustrated in green.*
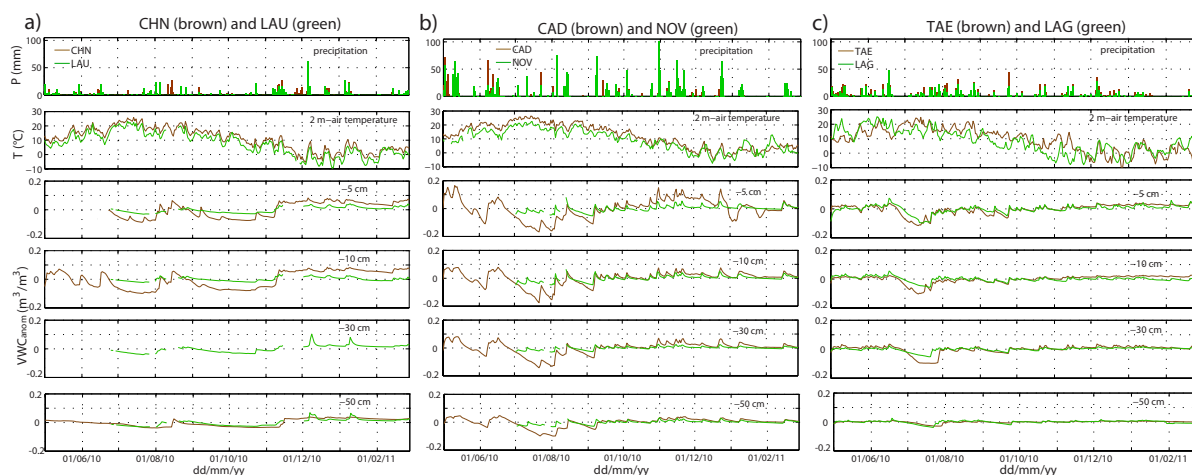
Figure 5.7: *Temporal evolution of precipitation, 2-m air temperature and of anomalies of soil moisture measurements (relative to the average VWC) at the different depths of the paired sites (a) CHN/LAU, (b) CAD/NOV, and (c) TAE/LAG. The grassland sites are illustrated in brown and the forest sites are illustrated in green.*

Regarding the paired sites CHN/LAU and CAD/NOV, the grassland sites show a higher variability than the forest sites, mainly for the near-surface soil layers, with a consequently stronger variability of the column soil moisture most distinctive for CAD/NOV. In contrast at the site pair TAE/LAG, the variability of volumetric water content and column soil moisture displays similar values (Table 5.2).

An increasing variability of volumetric water content results from precipitation, which displays similar timing and amount at the paired sites. However, the precipitation is less visible at the forest sites, possible due to the greater interception of precipitation as well as to the insulation by litter, which both lead to a reduced infiltration. The recession of volumetric water content,

which is related to infiltration, drainage, and evapotranspiration, is also higher at the grassland sites. The stronger recession of volumetric water content at the near-surface layer can be related to the better connection between the land surface and the atmosphere due to a better mixing of the air over grassland as well as to a higher insulation effect at the forest sites due to litter and due to not managed grass. Furthermore, the deeper rooting depth of the trees results in a more constant water availability. In addition, the presence of slope at the forest sites (see Figure 5.1 and Table 5.1) influence the infiltration and drainage of water into deeper soil layers, leading to a higher complexity of volumetric water content patterns.

5.3.4   Recession of column soil moisture

As already seen in Figures 5.6 and 5.7, the recession of volumetric water content differs for grassland and forest, with apparently lower recession at the forest sites. To investigate these differences, the column soil moisture S over 50 cm depth is further analyzed and related to the soil water balance. The soil water balance can be expressed by (e.g. Fernandez-Galvez et al., 2007):

$$\frac{dS(t)}{dt} = P(t) - I(t) - R(t) - D(t) - ET(t), \tag{5.2}$$

where dS(t)/dt is the change in S over time, P is the precipitation, I is the interception, R is the surface runoff, D is the drainage, and ET is the evapotranspiration. Here we focus on the recession of column soil moisture during dry-down events, where these events are defined as precipitation-free days starting from the fourth day after a precipitation event (see also Teuling et al., 2006a). Within such periods ET can be approximately assumed to be the dominant flux and Equation 5.2 is reduced to:

$$\frac{dS(t)}{dt} = -ET(t). \tag{5.3}$$

Using Equation 5.3, the recession of column soil moisture can be related to evapotranspiration. For precipitation-free periods the evapotranspiration can be assumed to be proportional to the column soil moisture following the typical Budyko approach (e.g. Budyko, 1956; Manabe, 1969):

$$ET(t) = cS(t), \tag{5.4}$$

where c is the proportionality constant, indicating the sensitivity of evapotranspiration for column soil moisture, which is described by an exponential decay. By combining Equation (5.3) and (5.4) the recession of column soil moisture can be defined as:

$$S(t) = S_0 exp(-\frac{t - t_0}{\lambda}), \tag{5.5}$$

where S_0 is S at t=t_0 and λ(=1/c) is the e-folding time controlling the temporal evolution of S. The parameter λ can be estimated from linear regression of ln(S) on t (Teuling et al., 2006a). To estimate the strength of the linear regression the adjusted R^2 is also considered here. For the comparison of the paired sites, only recession periods over common periods are analyzed. Because we relate the change in column soil moisture to the evapotranspiration, only the period 1 May 2010 to 31 October 2010 is investigated. To obtain as possible long time periods without having a major impact of precipitation on the soil moisture evolution, precipitation free-days

are defined as days with precipitation $\leq$5 mm.

Figure 5.8 displays the characteristics of the single dry-down events and the meteorological boundary conditions for the whole investigated time period. Table 5.4 includes the duration of the dry-down events as well as the adjusted R^2 for the respective linear regressions. A R2>0.9 for almost all events indicate a linear decay of the soil water storage and confirm the relation of column soil moisture to evapotranspiration. In general, the recession of column soil moisture $1/\lambda$ at the grassland sites is faster than at the forest sites (except for CHN/LAU event 4). Moreover, the decay is always about twice as fast at the grassland sites, resulting in an e-folding time for the forest sites which is twice as long than for the grassland sites.
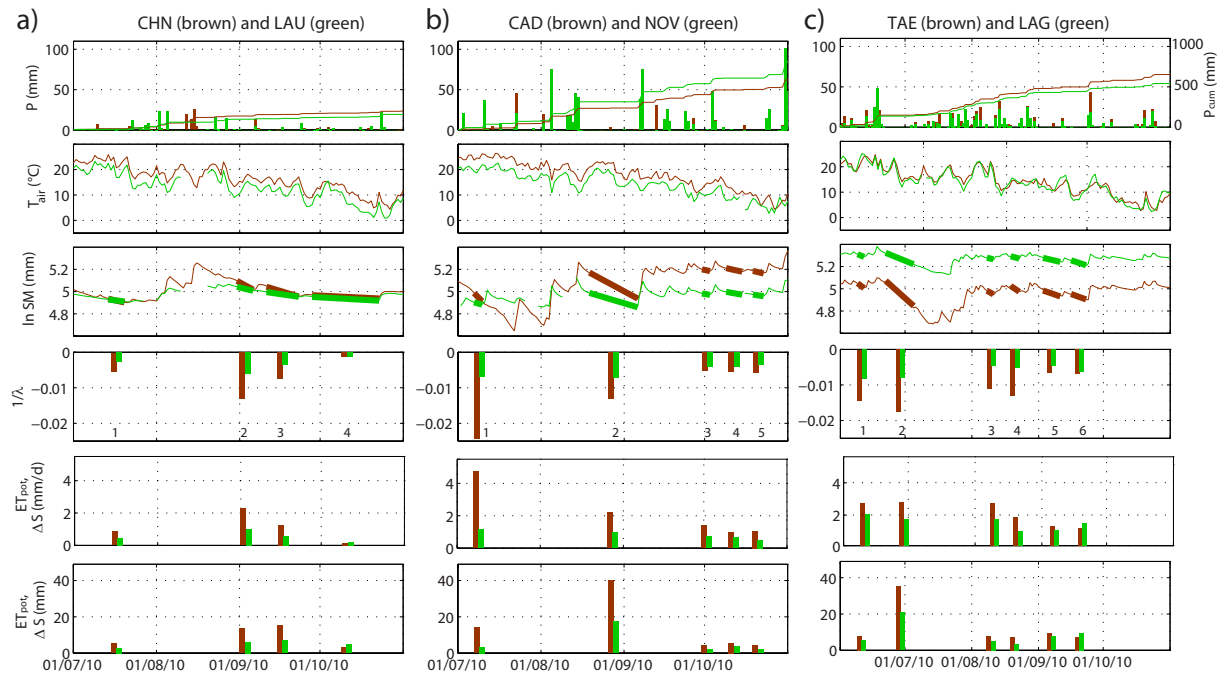
Figure 5.8: *Precipitation (P) with cumulative precipitation P_{cum}, 2-m air temperature T_{air}, logarithmic column soil moisture (SM) with highlighted recession for dry-down events, slope of recession (1/λ) of soil moisture recession for the dry-down events, difference in soil moisture (Δ S) per day, as well as over the whole period for the dry-down events, for the different paired sites (a) CHN/LAU, (b) CAD/NOV, and (c) TAE/LAG. The grassland sites are illustrated in brown and the forest sites are illustrated in green. Note that the time period for the paired site TAE/LAG is different than for the other two paired sites.*

**Table 5.4:** *Duration of the single events and adjusted R^2 of the recession analysis.*

Event	Duration (d)	CHN	LAU	Duration (d)	CAD	NOV	Duration (d)	TAE	LAG
1	6	0.97	0.97	3	0.99	0.99	3	0.98	0.99
2	6	0.99	0.99	18	0.99	0.90	13	0.98	0.99
3	12	0.98	0.99	3	0.98	0.96	3	0.98	0.57
4	25	0.79	0.91	6	0.99	0.99	4	0.99	0.94
5				4	0.98	0.99	8	0.82	0.90
6							7	0.98	0.99

Comparing the e-folding time within sites with the same vegetation cover, and thus in different Swiss climatic regions, similar values are found during common time periods. Most striking are the events 2 of CHN and CAD and event 3 to 5 of TAE, and for their respective forest sites, which occur in August and beginning of September 2010. As a consequence, the daily soil moisture loss for these events are similar at all three grassland sites with values of 2 mm/d, and are also similar for the forest sites with values of about about 1 mm/d only half of those a the grassland sites.

The level of soil moisture recession is found to be related to the daily evaporation rate. Fastest recession, resulting in shorter e-folding time, are observed for events with maximal daily evaporation rate. Consequently, the e-folding time is expected to have seasonal characteristics due to the seasonality in the meteorological forcing. For the investigated events this seasonality is more enhanced for the grassland sites. As with the chosen approach and with the strong linear recession (Table 5.4) the soil moisture loss is directly associated to evapotranspiration. Consequently, we find the evapotranspiration to be higher over the grassland sites. Beside the effect of difference in elevation (Table 5.1) and the insulation by litter at the forest sites, the difference in daily evaporation rate can mainly be related to the difference in canopy structure of forest compared to grassland (Kelliher et al., 1993). This is furthermore in agreement with the findings by Teuling et al. (2010b), showing higher latent heat over grassland sites than over forest sites for average climate conditions.

By using distant paired grassland/forest sites with similar meteorological but different topographically characteristics within the pairs, we suggest that the recession of soil moisture during dry-down events and thus the evapotranspiration is strongly related to the characteristics of canopy.

5.4 Conclusions

In the current chapter first measurements of soil moisture and soil temperature from paired grassland/forest sites are used to compare the behavior of these variables across the different land cover. Already using the available short measurement period and their aggregation to daily mean data yields interesting results. Although the paired sites are different with respect to topography and soil texture, general variations in 2-m air temperature, soil temperature, and soil moisture between grassland and forest are observed. For the observed time period, the lapse-rate corrected air temperature indicated that air temperature is mostly affected by the difference in elevation. On the other hand, the absolute values and variability of soil temperature and soil moisture is found to depended more on the characteristics of the canopy, litter, as well as rooting depth, than on the topographical characteristics of the sites. The vegetation cover and litter affects the insulation and therefore the exchange of the surface with the atmosphere, which is reflected by the soil temperatures and soil moisture. Furthermore, the variability of soil moisture reflects not only the effect of land cover on evapotranspiration, but also on precipitation reaching the surface as input of the water balance. Precipitation is influenced through interception, which is strongly dependent on canopy, litter and land management. Here, we compare the forest with managed grassland, meaning that the later is frequently cut and thus has fairly no change in phenology over the whole year. The deciduous and mixed forest with

its understory on the other hand have a relative strong phenology, affecting the insulation of the near surface and depth of the litter. Relating the recession of soil moisture during dry-down events to evapotranspiration we confirm that also this surface flux is mainly impacted by vegetation cover and the corresponding rooting depths, already for normal dry-down conditions. For the comparison to other studies one should take into account that the meteorological conditions of the forest sites are measured below the canopy. Above canopy conditions would be different and possibly lead to different results and conclusions.

The identified strong influence of vegetation cover rises interest for more investigations on this issue. Continuous multi-year measurements for both grassland and forest, will provide larger measurement ranges for soil moisture and soil temperatures and will lead to further opportunities to investigate the identified processes in more detail. The analysis of e.g. the diurnal cycle under different meteorological conditions would lead to more precise conclusions for average climate conditions but also for the behavior during dry extremes. With the findings of this study we conclude that it is important to conduct soil moisture and soil temperature measurements across different land covers to better understanding land-climate interactions for both average and extreme climate conditions.

Chapter 6

Conclusions and outlook

6.1 Conclusions

The results of this dissertation are based on the new SwissSMEX soil moisture data set, which was also set up as part of this PhD thesis. Several scientific and technical questions are addressed within this research. Chapter 2 and 3 evaluate the accuracy of the employed low-cost soil moisture sensors. Chapter 4 and 5 include first analyses of this data set with respect to the spatio-temporal variability of soil moisture and the comparison of soil moisture across different land covers. The following overall conclusions can be drawn based on this research:

- **New data set of soil moisture and soil temperature for Switzerland:** The setup of the SwissSMEX soil moisture network allowed the initiation of a high-quality large-scale and long-term soil moisture data set covering a significant regional spatial extent. For each site detailed information about vegetation cover, topography, soil characteristics (texture, organic fraction, pH value) for the soil horizons, as well as measurement of the main meteorological variables are available. Measurements for soil moisture and soil temperature at 5, 10, 30, and 50 cm depth are available at all sites, whereby most of the sites provide additional measurements down to 120 cm. This enables the comparison of soil moisture across Switzerland for the upper 50 cm, where strongest dynamics are expected to take place.

- **Setup and design of soil moisture measurement sites:** Two main questions are often raised: First, is the soil disturbed too much during the setup and consequently, do the measurements represent natural conditions? And second, how representative is the measurement site, if the soil is heterogeneous already on a small scale? Regarding the first question it cannot be denied that the soil is disturbed. For that reason, the digging of each hole was performed by hand with extreme caution by measuring the location and thickness of the removed soil layers to enable a refilling of the soil as close as possible to the original conditions. During later visits of the sites, the location of "disturbance" was not visible anymore. Furthermore, the measurements do represent the natural conditions, as the sensor are installed into the undisturbed wall. The answer to the second question is given in the different spatial scales of soil moisture dynamics. The SwissSMEX network is a large-scale network, which intends to provide data as basis for the investigation

of land surface-atmosphere interactions. Thus, the focus is more on the meteorological than on the land surface scale. Furthermore, soil moisture anomalies, which are most relevant for climate science, are expected to be more homogeneous than absolute values of soil moisture (Seneviratne, 2003). This result is confirmed in the present analyses and is validating the chosen setup.

- **Evaluation of low-cost soil moisture sensors for climate research:** The comparison of the performance of low-cost vs high-cost soil moisture sensors include the representation of absolute soil moisture and its anomalies, as well as the performance of the sensors for climate and hydrological applications (Chapter 2 and 3). The studies confirm the need of site-specific calibration of low-cost sensors for the applied sensors under the given soil and meteorological conditions. For the SwissSMEX network, the low-cost sensor 10HS (Decagon Devices, USA) is used for the basic installation. This sensor type was introduced on the market as a successor of a frequently used low-cost sensor onto the market when the project was started. To my knowledge, this thesis provides the first scientific evaluation of the 10HS sensor. These analyses reveal the need for site-specific calibration of this sensor and the fact that this sensor performs poorly at high moisture contents. Nonetheless, the performance of the sensor is found to be adequate with low and medium soil moisture ranges.

- **New perspective on spatio-temporal variability of soil moisture:** So far, little is known about the temporal evolution of spatial variability of absolute soil moisture and the contribution of its temporal mean and temporal anomalies. This issue is the focus of Chapter 4. For the given conditions, the time invariant temporal mean is indicated to be the most relevant contributor to spatial variability of absolute soil moisture, while the time variant anomaly contribute less. It is furthermore found that the rank stability of absolute soil moisture is mostly affected by the rank stability of the temporal mean and does not reflect the rank stability of anomalies. This suggest that conclusions derived from analyses of the spatio-temporal variability of absolute soil moisture do not apply generally to soil moisture anomalies.

- **Soil moisture across different land covers:** The development of soil moisture for grassland and nearby forest sites show a different behavior (Chapter 5) in amount and variation of soil moisture. Although the grassland and respective forest sites show differences in 2-m air temperature due to the difference in elevation, soil moisture is found to depend on canopy, litter, and rooting depth. The recession of soil moisture is found to be constantly about twice as fast for the grassland sites. Consequently, the evapotranspiration rate for dry-down periods, which can be related to soil moisture recession during these periods, is twice as much for grassland than for forest. Thus, even under the normal meteorological conditions, the impact of vegetation on land surface-climate interactions through soil moisture and evapotranspiration can be detected.

- **Long-term soil moisture measurements:** Advantage is taken of long-term soil moisture measurements from the SwissSMEX network. Already the continuous time series of soil moisture over the available time (for 14 grassland sites since May 2010), led to analyses

which would not have been possible with commonly available short-term data sets. In particular, analyses are performed separately for the temporal mean of soil moisture and its anomalies. This approach is used for the evaluation of low-cost sensors (Chapter 2) as well as for the analyses of the spatial variability and temporal stability of soil moisture (Chapter 4).

Overall, this thesis substantially contributes to the evaluation of soil moisture dynamics in Switzerland, ranging from the setup of an extensive soil moisture network, all the way to the evaluation and calibration of the applied soil moisture sensors, and to in-depth analyses of the collected data. Furthermore, the large-scale SwissSMEX network will continue to provide long-term soil moisture measurements that will help to investigate land surface-atmosphere interactions and can be used for numerous applications and scientific projects in the fields of climate research, hydrology, agriculture science, and remote sensing.

6.2 Outlook

The analyses conducted in this PhD thesis raise a series of questions which may be investigated in further studies. They in particular concern the following points:

- **Potential controls of spatio-temporal variability of soil moisture and its dynamics using the SwissSMEX data set:** The spatio-temporal variability of soil moisture should be further investigated considering variations depending on the climate conditions, i.e. for dry and wet events. This includes on the one hand the temporal evolution of the decomposed spatial variability and how the percentage of temporal mean and anomalies change for different moisture conditions, and on the other hand the comparison of the rank stability for these conditions. Thereby, the impact of initial moisture conditions and potential controls can be investigated and would contribute to the further understanding of the spatial and temporal scales of soil moisture dynamics. For the SwissSMEX data set this is of particular interest, as there are large variations in meteorological forcing over the spatial extent of the network. Cluster analyses using the characteristics of the single SwissSMEX sites will be useful to identify similarities between the sites.

- **Apply the tested approach for the analysis of the spatio-temporal variability of soil moisture to other networks:** The application of the tested approach, which allows to distinguish effects either in to time-invariant respectively time varying components of soil moisture dynamics, to other long-term, large-scale but also small-scale networks in different climates would be extremely useful. Consequently, potential controls under mean and extreme climates could be investigated. In addition, the significance of this perspective could be further assessed by using long-term networks with a larger ratio between the number of site and the spatial extent.

- **Geostatistical analyses using SwissSMEX data set:** Due to the limited number of soil moisture sites and their irregular distribution over a large spatial extent, geostatistical analyses using the SwissSMEX network are challenging. One possible solution to estimate geostatistical parameters, such as correlation length, from variogram analyses might

be to focus on the Swiss Plateau. By excluding Sion and Cadenazzo from this analyses, the 2-D variogram could be projected on a 1-D line and thus geostatistical parameters can be estimated.

- **Extend analyses with newer data:** All the analyses of this thesis should be extended by considering newer data. This will not only allow the consideration of longer record, but will also include particular interesting events, namely the strong 2011 spring drought in Switzerland. Furthermore, the winter 2010/11 is characterized by below average precipitation and the spring 2011 had a large precipitation deficit and is the warmest spring recorded by MeteoSwiss since 1864. Although in July above average precipitation amounts were recorded, August to October 2011 is characterized by longer warm and dry periods until the end of October 2011 (http://www.meteoschweiz.admin.ch/web/en/climate/climate_today.html). This will thus provide the possibility to further analyses soil moisture dynamics for extreme conditions.

Beside the highlighted points there are a large number of questions that could be considered with the SwissSMEX data set. The existence of the new data set with the given spatial and temporal resolution and available site specific characteristics will lead to a number further applications concerning a wide range of research fields:

- The comparison of soil moisture flux and evapotranspiration using Swiss FluxNet data.

- The investigation of the micro-climate for grassland and forest sites.

- The investigation of soil moisture dynamics and its controls on the land surface scale.

- The assessment of temporal variability of soil moisture and its link to main climate drivers.

- The validation of land surface and climate models with regard to soil moisture representation.

- The investigation of regionalization approaches.

- The calibration and evaluation of indirect soil moisture techniques and approaches.

To conclude, the data set put together within this thesis as well as the analyzed approach will allow significant investigations in the research area of land surface-atmosphere interactions in the coming years.

Appendix A

Climatic regions of Switzerland according to Müller (1980)

The climatic regions after Müller (1980) consist of 12 large and 60 smaller regions of Switzerland. They were worked out in the context of the measurement concept MK1980 for the observational system of MeteoSwiss. Detailed information (in German) of the climatic characteristics are shown in Begert et al. (2007).
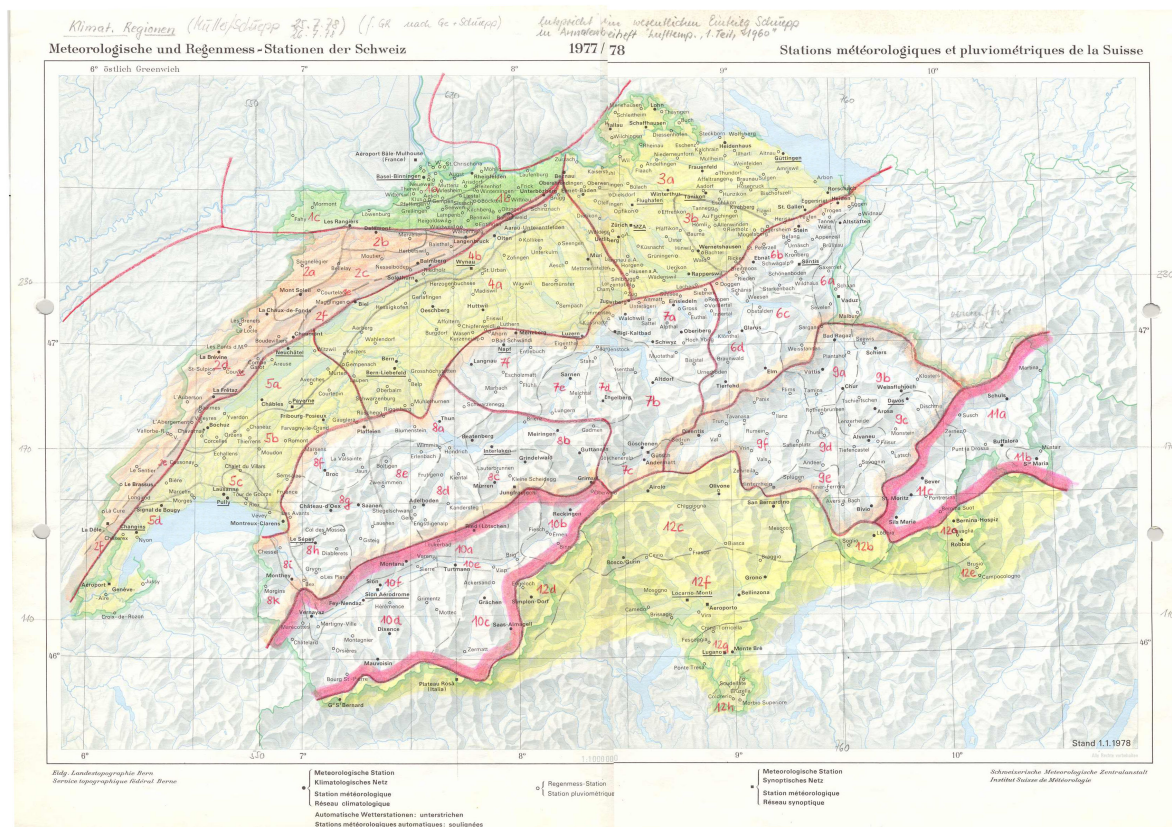
Figure A.1: *Climatic Region of Switzerland according to Müller (1980).*

Appendix B

Site characteristics of the SwissSMEX network

This Appendix provides information of the site characteristics of the SwissSMEX soil moisture network. Section B.1 gives an overall overview for the whole network. Section B.2 to B.20 provide detailed information of the soil characteristics and sensor installation of the single sites.

B.1 Overview of the SwissSMEX sites
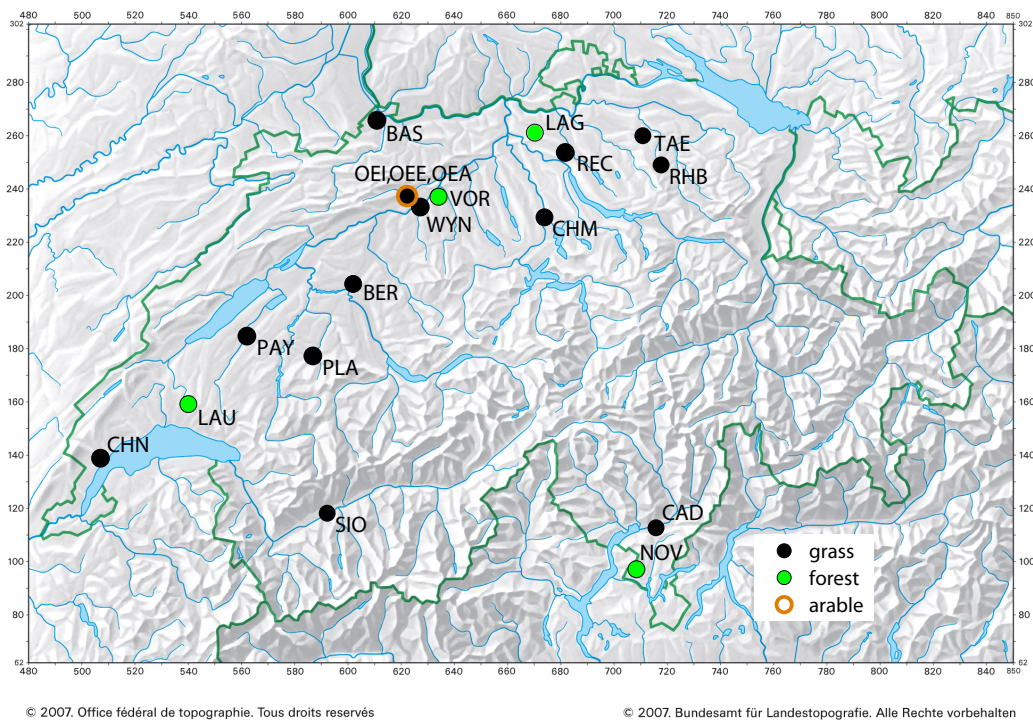
Figure B.1: *Map of Switzerland showing the location and land use of the SwissSMEX/-Veg soil moisture monitoring sites.*

Table B.1: *General characteristics of the SwissSMEX sites.*

Site	Site code		Swiss grid y coord	Swiss grid x coord	Land use	Elevation (m a.s.l.)	Aspect	Slope (%)	Texture[a][b]	Region[c]	Data since	Installed at
Changins	1	CHN	507280	139170	grass	430	-	-	loam	5	08.07.2009	MeteoSwiss
Payerne	2	PAY	562150	184855	grass	490	-	-	loam	5	15.08.2008	MeteoSwiss
Plaffeien	3	PLA	586850	177400	grass	1042	-	-	sandy loam	5	29.04.2010	MeteoSwiss
Bern	4	BER	601935	204410	grass	553	-	-	loam	4	20.07.2009	MeteoSwiss
Oensingen intensiv	5	OEI	622200	237220	grass	450	-	-	silty clay loam	4	15.08.2008	Fluxnet
Oensingen extensiv	6	OEE	622210	237220	grass	450	-	-	silty clay loam	4	15.08.2008	Fluxnet
Wynau	7	WYN	626400	233860	grass	422	-	-	silt loam	4	16.04.2010	MeteoSwiss
Chamau	8	CHM	673635	229265	grass	400	-	-	sandy loam	4	31.07.2009	Fluxnet
Basel	9	BAS	610850	265620	grass	316	-	-	silt loam	1	17.07.2009	MeteoSwiss
Reckenholz	10	REC	681425	253555	grass	443	-	-	loam	3	18.07.2009	MeteoSwiss
Taenikon	11	TAE	710500	259820	grass	536	-	-	loam	3	24.04.2010	MeteoSwiss
Rietholzbach	12	RHB	717400	248900	grass	754	-	-	loam	3	07.05.2009	IAC ETH
Sion	13	SIO	592200	118625	grass	482	-	-	sandy loam	10	09.07.2009	MeteoSwiss
Cadenazzo	14	CAD	715475	113162	grass	197	-	-	silt loam	12	06.08.2009	MeteoSwiss
Lausanne	15	LAU	540175	159445	deciduous forest	800	NE	7	sandy loam	5	25.06.2010	LWF
Vordemwald	16	VOR	633925	236995	mixed forest	480	NW	14	loam	4	01.06.2010	LWF
Laegern	17	LAG	670000	261000	mixed forest	868	S	27	clay	4	24.08.2008	Fluxnet
Novaggio	18	NOV	708090	97695	deciduous forest	950	S	68	loamy sand	12	02.07.2010	LWF
Oensingen arable	19	OEA	622590	237450	arable	450	-	-	silty clay loam	4	15.08.2008	Fluxnet

a   Averaged over the whole soil column.
b   According to USDA taxonomy.
c   Climatic regions according to Müller (1980); see Appendix A.

B.2 Changins CHN - grassland

Table B.2: *Soil characteristics of the SwissSMEX site CHN.*

Sensor depth (cm)	Layer depth (cm)	Bulk density (g/cm^3)	Sample depth (cm)	Particle size distribution[a](%)			Texture[b]	Organic fraction[c] (%)	pH
				Clay ($<2\ \mu$m)	Silt ($2-63\ \mu$m)	Sand ($>63\ \mu$m)			
5	4 to 27	1.11	0 to 4	25.0	44.9	30.1	loam	2.7	6.9
10	4 to 27	1.11	20	26.7	47.7	25.6	loam	2.2	7.1
30	4 to 27	1.11	40	29.7	46.0	24.3	clay loam	0.5	7.3
50	27 to 50	1.39	40	29.7	46.0	24.3	clay loam	0.5	7.3
80	50 to 90	1.47	75	23.0	51.1	25.9	silt loam	0.2	7.5

[a] Using pipette method (Scott, 2000) after organic matter was removed by oxidation with hydrogen peroxide.

[b] According to USDA taxonomy.

[c] Using dichromat oxidation method (Margesin and Schinner, 2005).

Table B.3: *Installed soil temperature and soil moisture[a] sensors of the SwissSMEX site CHN.*

Depth[b] (cm)	Soil temperature		Soil moisture (capacitance-based)		Soil moisture (TDR-based)	
	Quantity	Serial number	Quantity	Serial number	Quantity	Serial number
5	1	60	1	76	-	-
10	1	61	2	75, 77	1	30327*
30	1	62	1	78	-	-
50	1	63	1	79	-	-
80	1	64	1	80	1	30279*
5[+]	-	-	1	154	1	32275*
10[+]	-	-	1	155	1	32276*
30[+]	-	-	1	156	1	32277*
50[+]	-	-	1	157	1	32278*

[a] Asterisk (*) indicates additionally measurement of soil temperature.

[b] Plus (+) indicates sites, which are installed within the equipment project SwissSMEX-*Veg*.

B.3   Payerne PAY - grassland

Table B.4: *Soil characteristics of the SwissSMEX site PAY.*

Sensor depth (cm)	Layer depth (cm)	Bulk density (g/cm^3)	Sample depth (cm)	Particle size distribution[a](%)			Texture[b]	Organic fraction[c] (%)	pH
				Clay ($<2\ \mu$m)	Silt ($2-63\ \mu$m)	Sand ($>63\ \mu$m)			
5	0 to 30	1.49	0 to 30	5.9	41.8	52.3	sandy loam	1.5	
10	0 to 30	1.49	0 to 30	5.9	41.8	52.3	sandy loam	1.5	
30	30 to 100	1.49	30 to 100	19.0	41.7	39.3	loam	0.4	
50	30 to 100	1.49	30 to 100	19.0	41.7	39.3	loam	0.4	
80	30 to 100	1.49	30 to 100	19.0	41.7	39.3	loam	0.4	

[a]   Using pipette method (Scott, 2000) after organic matter was removed by oxidation with hydrogen peroxide.

[b]   According to USDA taxonomy.

[c]   Using dichromat oxidation method (Margesin and Schinner, 2005).

Table B.5: *Installed soil temperature and soil moisture sensors of the SwissSMEX site PAY.*

Depth (cm)	Soil temperature		Soil moisture (capacitance-based)		Soil moisture (TDR-based)	
	Quantity	Serial number	Quantity	Serial number	Quantity	Serial number
5	1	11	1	24	1	15253
10	1	12	1	25	1	15256
30	1	13	1	26	1	15273
50	1	14	1	27	1	15269
80	1	15	1	28	1	15265

B.4   Plaffeien PLA - grassland

Table B.6: Soil characteristics of the SwissSMEX site PLA.

Sensor depth (cm)	Layer depth (cm)	Bulk density (g/cm^3)	Sample depth (cm)	Particle size distribution[a](%)			Texture[b]	Organic fraction[c] (%)	pH
				Clay ($<2\ \mu$m)	Silt ($2-63\ \mu$m)	Sand ($>63\ \mu$m)			
5			0 to 30	10.0	40.0	60.0	loam		
10			0 to 30	10.0	40.0	60.0	loam		
30			0 to 30	10.0	40.0	60.0	loam		
50			30 to 70	5.0	35.0	65.0	sandy loam		
80			70 to 120	5.0	5.0	95.0	sand		
120			70 to 120	5.0	5.0	95.0	sand		

[a] Using pipette method (Scott, 2000) after organic matter was removed by oxidation with hydrogen peroxide.

[b] According to USDA taxonomy.

[c] Using dichromat oxidation method (Margesin and Schinner, 2005).

Table B.7: Installed soil temperature and soil moisture[a] sensors of the SwissSMEX site PLA.

Depth[b] (cm)	Soil temperature		Soil moisture (capacitance-based)		Soil moisture (TDR-based)	
	Quantity	Serial number	Quantity	Serial number	Quantity	Serial number
5[+]	1	85	1	108	-	-
10[+]	1	86	1	109	1	31175[*]
30[+]	1	-	1	110	1	31171[*]
50[+]	1	87	1	111	-	-
80[+]	1	88	1	112	1	31172[*]
120[+]	1	-	1	113	-	-

[a] Asterisk (*) indicates additionally measurement of soil temperature.

[b] Plus ($^+$) indicates sites, which are installed within the equipment project SwissSMEX-*Veg*.

B.5   Bern BER - grassland

Table B.8: Soil characteristics of the SwissSMEX site BER.

Sensor depth (cm)	Layer depth (cm)	Bulk density (g/cm^3)	Sample depth (cm)	Particle size distribution[a](%)			Texture[b]	Organic fraction[c] (%)	pH
				Clay ($<2\ \mu$m)	Silt ($2-63\ \mu$m)	Sand ($>63\ \mu$m)			
5	0 to 23	1.13	0 to 20	16.2	32.1	51.7	loam	2.1	4.7
10	0 to 23	1.13	0 to 20	16.2	32.1	51.7	loam	2.1	4.7
30	0 to 23	1.13	20 to 40	18.6	22.8	58.6	sandy loam	0.5	4.8
50	23 to 96	1.27	40 to 75	20.5	12.4	67.1	sandy clay loam	0.3	5.1
80	23 to 96	1.3	40 to 75	20.5	12.4	67.1	sandy clay loam	0.3	5.1
120	96 to 120	1.3	75 to 120	27.7	53.5	18.8	silty clay loam	0.6	5.5

[a] Using pipette method (Scott, 2000) after organic matter was removed by oxidation with hydrogen peroxide.

[b] According to USDA taxonomy.

[c] Using dichromat oxidation method (Margesin and Schinner, 2005).

Table B.9: Installed soil temperature and soil moisture[a] sensors of the SwissSMEX site BER.

Depth (cm)	Soil temperature		Soil moisture (capacitance-based)		Soil moisture (TDR-based)	
	Quantity	Serial number	Quantity	Serial number	Quantity	Serial number
5	1	35	1	51	-	-
10	1	36	1	52	1	30323[*]
30	1	37	1	53	-	-
50	1	38	1	54	-	-
80	1	39	1	55	1	30277[*]
120	1	40	1	56	-	-

[a] Asterisk (*) indicates additionally measurement of soil temperature.

B.6   Oensingen OEI - intensive managed grassland

Table B.10: *Soil characteristics of the SwissSMEX site OEI.*

Sensor depth (cm)	Layer depth (cm)	Bulk density (g/cm^3)	Sample depth (cm)	Particle size distribution[a](%)			Texture[b]	Organic fraction[c] (%)	pH
				Clay ($<2\ \mu$m)	Silt ($2-63\ \mu$m)	Sand ($>63\ \mu$m)			
5	0 to 25	1.39	0 to 25	28.2	57.9	13.9	silty clay loam	3.4	
10	0 to 25	1.39	0 to 25	28.2	57.9	13.9	silty clay loam	3.4	
30	25 to 75	1.49	25 to 75	25.8	56.3	17.9	silt loam	2.2	
50	25 to 75	1.49	25 to 75	25.8	56.3	17.9	silt loam	2.2	
80	75 to 95		75 to 95				gravel layer		
120	95 to 120	1.45	95 to 120	30.2	62.5	7.3	silty clay loam	1.4	

[a] Using pipette method (Scott, 2000) after organic matter was removed by oxidation with hydrogen peroxide.

[b] According to USDA taxonomy.

[c] Using dichromat oxidation method (Margesin and Schinner, 2005).

Table B.11: *Installed soil temperature and soil moisture sensors of the SwissSMEX site OEI.*

Depth (cm)	Soil temperature		Soil moisture (capacitance-based)		Soil moisture (TDR-based)	
	Quantity	Serial number	Quantity	Serial number	Quantity	Serial number
5	1	22	1	35	1	15257
10	1	23	1	36	1	15254
30	1	24	1	37	1	15272
50	1	25	1	38	1	15314
75	1	26	1	39	1	15264
120	1	27	1	40	1	15263

B.7   Oensingen OEE - extensive managed grassland

Table B.12: Soil characteristics of the SwissSMEX site OEE.

Sensor depth (cm)	Layer depth (cm)	Bulk density (g/cm^3)	Sample depth (cm)	Particle size distribution[a](%)			Texture[b]	Organic fraction[c] (%)	pH
				Clay (<2 μm)	Silt (2−63 μm)	Sand (>63 μm)			
5	0 to 25	1.43	0 to 25	27.3	62.3	10.4	silty clay loam		
10	0 to 25	1.43	0 to 25	27.3	62.3	10.4	silty clay loam		
30	25 to 73	1.55	25 to 73	26.7	52.1	21.2	silt loam		
50	25 to 73	1.55	25 to 73	26.7	52.1	21.2	silt loam		
80	73 to 90		73 to 90				gravel layer		
120	90 to 120	1.41	90 to 120	44.9	46.0	9.2	silty clay		

[a] Using pipette method (Scott, 2000) after organic matter was removed by oxidation with hydrogen peroxide.

[b] According to USDA taxonomy.

[c] Using dichromat oxidation method (Margesin and Schinner, 2005).

Table B.13: Installed soil temperature and soil moisture sensors of the SwissSMEX site OEE.

Depth (cm)	Soil temperature		Soil moisture (capacitance-based)		Soil moisture (TDR-based)	
	Quantity	Serial number	Quantity	Serial number	Quantity	Serial number
5	1	16	1	29	-	-
10	1	17	1	30	-	-
30	1	18	1	31	-	-
50	1	19	1	32	-	-
75	1	20	1	33	-	-
120	1	21	1	34	-	-

B.8 Wynau WYN - grassland

Table B.14: Soil characteristics of the SwissSMEX site WYN.

Sensor depth (cm)	Layer depth (cm)	Bulk density (g/cm³)	Sample depth (cm)	Particle size distribution[a](%)			Texture[b]	Organic fraction[c] (%)	pH
				Clay (<2 μm)	Silt (2−63 μm)	Sand (>63 μm)			
5			0 to 14	15.0	75.0	10.0	silt loam		
10			14 to 30	20.0	60.0	20.0	silt loam		
25			14 to 30	20.0	60.0	20.0	silt loam		
50			30 to 67	20.0	30.0	50.0	loam		

[a] Using pipette method (Scott, 2000) after organic matter was removed by oxidation with hydrogen peroxide.

[b] According to USDA taxonomy.

[c] Using dichromat oxidation method (Margesin and Schinner, 2005).

Table B.15: Installed soil temperature and soil moisture[a] sensors of the SwissSMEX site WYN.

Depth[b] (cm)	Soil temperature		Soil moisture (capacitance-based)		Soil moisture (TDR-based)	
	Quantity	Serial number	Quantity	Serial number	Quantity	Serial number
5[+]	1	77	1	93	-	-
10[+]	1	78	2	94, 95	1	31173[*]
25[+]	1	79	2	96, 97	1	31167[*]
50[+]	1	80	1	98	1	31168[*]

[a] Asterisk (*) indicates additionally measurement of soil temperature.

[b] Plus (+) indicates sites, which are installed within the equipment project SwissSMEX-*Veg*.

B.9   Basel BAS - grassland

Table B.16: Soil characteristics of the SwissSMEX site BAS.

| Sensor depth (cm) | Layer depth (cm) | Bulk density (g/cm^3) | Sample depth (cm) | Particle size distribution[a](%) | | | Texture[b] | Organic fraction[c] (%) | pH |
				Clay (<2 μm)	Silt (2−63 μm)	Sand (>63 μm)			
5	0 to 30	1.41	8	26.2	66.0	7.8	silt loam	2.7	7.1
10	0 to 30	1.41	8	26.2	66.0	7.8	silt loam	2.7	7.1
30	30 to 60	1.61	38	22.7	64.6	12.7	silt loam	1.4	7.2
50	30 to 60	1.61	38	14.9	76.6	8.5	silt loam	0.5	7.4
80	60 to 120	1.36	80	19.5	73.5	7.0	silt loam	0.5	7.4
120	60 to 120	1.36	120	13.5	77.9	8.6	silt loam	0.4	7.3

[a] Using pipette method (Scott, 2000) after organic matter was removed by oxidation with hydrogen peroxide.
[b] According to USDA taxonomy.

[c] Using dichromat oxidation method (Margesin and Schinner, 2005).

Table B.17: Installed soil temperature and soil moisture[a] sensors of the SwissSMEX site BAS.

| Depth (cm) | Soil temperature | | Soil moisture (capacitance-based) | | Soil moisture (TDR-based) | |
	Quantity	Serial number	Quantity	Serial number	Quantity	Serial number
5	1	53	1	69	-	-
10	1	54	1	70	1	30330[*]
30	1	55	1	71	-	-
50	1	56	1	72	-	-
80	1	57	1	73	1	30282[*]
120	1	58	1	74	-	-

[a] Asterisk (*) indicates additionally measurement of soil temperature.

B.10   Chamau CHM - grassland

Table B.18: Soil characteristics of the SwissSMEX site CHM.

Sensor depth (cm)	Layer depth (cm)	Bulk density (g/cm^3)	Sample depth (cm)	Particle size distribution[a](%)			Texture[b]	Organic fraction[c] (%)	pH
				Clay (<2 μm)	Silt (2−63 μm)	Sand (>63 μm)			
5	0 to 25	1.18	0 to 23	22.4	34.9	42.7	Loam	3.2	4.6
10	0 to 25	1.18	0 to 23	22.4	34.9	42.7	Loam	3.2	4.6
30	25 to 65	1.25	23 to 40	36.2	30.1	33.7	Clay Loam	1.1	5.1
50	25 to 65	1.25	40 to 55	19.7	43.8	36.5	Loam	1.1	5.1
80	65 to 75	1.41	55 to 85	8.8	7.3	83.9	Loamy Sand	0.4	5.6
120	75 to 90	1.56	55 to 85	8.8	7.3	83.9	Loamy Sand	0.2	5.4

[a] Using pipette method (Scott, 2000) after organic matter was removed by oxidation with hydrogen peroxide.

[b] According to USDA taxonomy.

[c] Using dichromat oxidation method (Margesin and Schinner, 2005).

Table B.19: Installed soil temperature and soil moisture[a] sensors of the SwissSMEX site BER.

Depth (cm)	Soil temperature		Soil moisture (capacitance-based)		Soil moisture (TDR-based)	
	Quantity	Serial number	Quantity	Serial number	Quantity	Serial number
5	1	41	1	57	-	-
10	1	42	1	58	1	30324[*]
30	1	43	1	59	-	-
50	1	44	1	60	-	-
80	1	45	1	61	1	30278[*]
120	1	46	1	62	-	-

[a] Asterisk (*) indicates additionally measurement of soil temperature.

B.11   Reckenholz REC - grassland

Table B.20: *Soil characteristics of the SwissSMEX site REC.*

Sensor depth (cm)	Layer depth (cm)	Bulk density (g/cm^3)	Sample depth (cm)	Particle size distribution[a](%)			Texture[b]	Organic fraction[c] (%)	pH
				Clay (<2 μm)	Silt (2−63 μm)	Sand (>63 μm)			
5	0 to 38	1.33	10	15.0	35.7	49.3	loam	2.2	4.5
10	0 to 38	1.33	10	15.0	35.7	49.3	loam	2.2	4.5
30	38 to 130	1.49	40	18.8	36.0	45.2	loam	0.6	5.0
50	38 to 130	1.49	80	29.5	41.4	29.1	clay loam	0.4	5.2
80	38 to 130	1.49	115	22.6	40.5	36.9	loam	0.7	5.4
150	150	1.41	130	13.0	29.7	57.3	sandy loam	0.3	7.3

[a]   Using pipette method (Scott, 2000) after organic matter was removed by oxidation with hydrogen peroxide.

[b]   According to USDA taxonomy.

[c]   Using dichromat oxidation method (Margesin and Schinner, 2005).

Table B.21: *Installed soil temperature and soil moisture[a] sensors of the SwissSMEX site REC.*

Depth (cm)	Soil temperature		Soil moisture (capacitance-based)		Soil moisture (TDR-based)	
	Quantity	Serial number	Quantity	Serial number	Quantity	Serial number
5	1	47	1	63	-	-
10	1	49	1	64	1	30328[*]
30	1	50	1	65	-	-
50	1	51	1	66	-	-
80	1	52	1	67	1	30283[*]
150	1	48	1	68	-	-

[a]   Asterisk (*) indicates additionally measurement of soil temperature.

B.12   Taenikon TAE - grassland

Table B.22: *Soil characteristics of the SwissSMEX site TAE.*

Sensor depth (cm)	Layer depth (cm)	Bulk density (g/cm^3)	Sample depth (cm)	Particle size distribution[a](%) Clay (<2 μm)	Silt (2−63 μm)	Sand (>63 μm)	Texture[b]	Organic fraction[c] (%)	pH
5	0 to 23			28.0	13.0	59.0	sandy clay loam		
10	23 to 37			21.0	38.0	41.0	loam		
30	23 to 37			21.0	38.0	41.0	loam		
50	37 to 50			20.0	35.0	45.0	loam		

[a]   Using pipette method (Scott, 2000) after organic matter was removed by oxidation with hydrogen peroxide.

[b]   According to USDA taxonomy.

[c]   Using dichromat oxidation method (Margesin and Schinner, 2005).

Table B.23: *Installed soil temperature and soil moisture[a] sensors of the SwissSMEX site TAE.*

Depth[b] (cm)	Soil temperature Quantity	Serial number	Soil moisture (capacitance-based) Quantity	Serial number	Soil moisture (TDR-based) Quantity	Serial number
5[+]	1	81	1	99	-	-
10[+]	1	82	2	100, 101	1	31174[*]
30[+]	1	83	2	104, 106	1	31169[*]
50[+]	1	84	1	107	1	31170[*]

[a]   Asterisk (*) indicates additionally measurement of soil temperature.

[b]   Plus (+) indicates sites, which are installed within the equipment project SwissSMEX-*Veg*.

B.13   Rietholzbach RHB - grassland

Table B.24: Soil characteristics of the SwissSMEX site RHB.

Sensor Depth (cm)	Soil horizon		Depth (cm)	Particle size distribution[a](%)			Texture[b]	Organic fraction[c] (%)	pH
	Depth (cm)	Bulk density (g/cm^3)		Clay ($<2\,\mu$m)	Silt ($2-63\,\mu$m)	Sand ($>63\,\mu$m)			
5	0 to 15	1.08	0 to 15	30.6	35.9	33.5	clay loam	4.7	6.9
15	0 to 15	1.08	0 to 15	30.6	35.9	33.5	clay loam	4.7	6.9
25	15 to 23	1.37	15 to 23	30.8	31.0	38.2	clay loam	2.5	7.0
35	23 to 70	1.5	23 to 70	25.6	32.7	41.7	loam	1.3	7.1
55	23 to 70	1.5	23 to 70	25.6	32.7	41.7	loam	1.3	7.1
80	23 to 70	1.5	23 to 70	25.6	32.7	41.7	loam	1.3	7.1
110	70 to 120	1.5	70 to 120	26.9	34.4	38.7	loam	1.7	7.1

[a] Using pipette method (Scott, 2000) after organic matter was removed by oxidation with hydrogen peroxide.
[b] According to USDA taxonomy.
[c] Using dichromat oxidation method (Margesin and Schinner, 2005).

Table B.25: Installed soil temperature and soil moisture sensors of the SwissSMEX site RHB.

Depth (cm)	Soil temperature		Soil moisture (capacitance-based)		Soil moisture (TDR-based)	
	Quantity	Serial number	Quantity	Serial number	Quantity	Serial number
5	1	28	1	44	1	15259
15	1	29	1	45	1	15258
25	1	30	1	46	1	15270
35	1	31	1	47	1	15261
55	1	32	1	48	1	15271
80	1	33	1	49	1	15268
110	1	34	1	50	1	15260

B.14 Sion SIO - grassland

Table B.26: Soil characteristics of the SwissSMEX site SIO.

| Sensor depth (cm) | Layer depth (cm) | Bulk density (g/cm^3) | Sample depth (cm) | Particle size distribution[a](%) | | | Texture[b] | Organic fraction[c] (%) | pH |
				Clay (<2 μm)	Silt (2−63 μm)	Sand (>63 μm)			
5	5	0.94	5	10.2	51.6	38.2	silt loam	4.2	6.5
10	9 to 34	1.09	17	7.3	52.9	39.8	silt loam	2.6	7.0
30	9 to 34	1.09	34 to 95	6.4	62.2	31.4	silt loam	1.4	7.4
50	34 to 95	1.47	34 to 95	6.4	62.2	31.4	silt loam	1.4	7.4
80	34 to 95	1.47	100	2.3	6.8	90.9	sand	0.2	7.4
120	110 to 130	1.22	120	7.0	54.7	38.3	silt loam	1.6	7.4

[a] Using pipette method (Scott, 2000) after organic matter was removed by oxidation with hydrogen peroxide.

[b] According to USDA taxonomy.

[c] Using dichromat oxidation method (Margesin and Schinner, 2005).

Table B.27: Installed soil temperature and soil moisture[a] sensors of the SwissSMEX site SIO.

| Depth[b] (cm) | Soil temperature | | Soil moisture (capacitance-based) | | Soil moisture (TDR-based) | |
	Quantity	Serial number	Quantity	Serial number	Quantity	Serial number
5	1	65	1	81	-	-
10	1	66	1	82	1	30326[*]
30	1	67	1	83	-	-
50	1	68	1	84	-	-
80	1	69	1	85	1	30280[*]
120	1	70	1	86	-	-
5[+]	-	-	1	158	1	31962[*]
10[+]	-	-	1	159	1	32279[*]
30[+]	-	-	1	160	1	32280[*]
50[+]	-	-	1	161	1	32229[*]

[a] Asterisk (*) indicates additionally measurement of soil temperature.

[b] Plus (+) indicates sites, which are installed within the equipment project SwissSMEX-*Veg*.

B.15   Cadenazzo CAD - grassland

Table B.28: *Soil characteristics of the SwissSMEX site CAD.*

Sensor depth (cm)	Layer depth (cm)	Bulk density (g/cm^3)	Sample depth (cm)	Particle size distribution[a](%)			Texture[b]	Organic fraction[c] (%)	pH
				Clay ($<2\ \mu$m)	Silt ($2-63\ \mu$m)	Sand ($>63\ \mu$m)			
5	5 to 35	0.998	5 to 35	9.8	57.9	32.3	silt loam	4.0	4.3
10	5 to 35	0.998	5 to 35	9.8	58.6	31.6	silt loam	1.4	4.5
30	5 to 35	0.998	5 to 35	9.8	58.6	31.6	silt loam	1.4	4.5
50	35 to 63	1.72	35 to 63	8.3	62.4	29.3	silt loam	1.2	4.5
80	63 to 85	1.69	63 to 85	2.2	8.9	88.9	sand	0.3	4.7

[a]   Using pipette method (Scott, 2000) after organic matter was removed by oxidation with hydrogen peroxide.

[b]   According to USDA taxonomy.

[c]   Using dichromat oxidation method (Margesin and Schinner, 2005).

Table B.29: *Installed soil temperature and soil moisture[a] sensors of the SwissSMEX site CAD.*

Depth[b] (cm)	Soil temperature		Soil moisture (capacitance-based)		Soil moisture (TDR-based)	
	Quantity	Serial number	Quantity	Serial number	Quantity	Serial number
5	1	71	2	87, 88	-	-
10	1	72	2	90, 91	-	-
30	1	73	2	92, 102	-	-
50	1	74	1	103	1	30329[*]
80	1	75	-	-	1	30281[*]
5[+]	-	-	1	162	1	32306[*]
10[+]	-	-	1	163	1	32356[*]
30[+]	-	-	1	164	1	32357[*]
50[+]	-	-	1	165	1	32358[*]

[a]   Asterisk (*) indicates additionally measurement of soil temperature.

[b]   Plus ($^+$) indicates sites, which are installed within the equipment project SwissSMEX-*Veg*.

B.16   Lausanne LAU - deciduous forest

Table B.30: *Soil characteristics of the SwissSMEX site LAU.*

Sensor depth (cm)	Layer depth (cm)	Bulk density (g/cm^3)	Sample depth (cm)	Particle size distribution[a](%)			Texture[b]	Organic fraction[c] (%)	pH
				Clay (<2 μm)	Silt (2$-$63 μm)	Sand (>63 μm)			
5	5	1.20	5	13	25	62	sandy loam		
10	10	1.33	10	14	26	60	sandy loam		
30	20	1.28	20	18	31	51	loam		
50	50	1.39	50	17	32	52	loam		
80	110	1.58	110	16	27	57	sandy loam		
120	110	1.58	110	16	27	57	sandy loam		

[a]   Using pipette method (Scott, 2000) after organic matter was removed by oxidation with hydrogen peroxide.

[b]   According to USDA taxonomy.

[c]   Using dichromat oxidation method (Margesin and Schinner, 2005).

Table B.31:   *Installed soil temperature and soil moisture[a] sensors of the SwissSMEX site LAU.*

Depth[b] (cm)	Soil temperature		Soil moisture (capacitance-based)		Soil moisture (TDR-based)	
	Quantity	Serial number	Quantity	Serial number	Quantity	Serial number
5[+]	1	95	2	126, 132	-	-
10[+]	1	96	2	127, 133	1	31185[*]
30[+]	1	97	2	128, 134	2	31186[*] 31182[*]
50[+]	1	98	2	129, 135	-	-
80[+]	1	99	2	130, 136	2	31187[*] 31182[*]
120[+]	1	100	2	131, 137	-	-

[a]   Asterisk (*) indicates additionally measurement of soil temperature.

[b]   Plus ($^+$) indicates sites, which are installed within the equipment project SwissSMEX-*Veg*.

B.17   Vordemwald VOR - mixed forest

Table B.32: *Soil characteristics of the SwissSMEX site VOR.*

Sensor depth (cm)	Layer depth (cm)	Bulk density (g/cm^3)	Sample depth (cm)	Particle size distribution[a](%)			Texture[b]	Organic fraction[c] (%)	pH
				Clay (<2 μm)	Silt (2−63 μm)	Sand (>63 μm)			
5	5	0.67	5	11	47	43	loam		
10	10	0.93	10	19	59	22	silt loam		
30	20	1.21	20	20	61	19	silt loam		
50	60	1.25	60	20	62	18	silt loam		
80	60	1.25	60	20	62	18	silt loam		
120	100	1.51	100	19	57	24	silt loam		

[a]   Using pipette method (Scott, 2000) after organic matter was removed by oxidation with hydrogen peroxide.

[b]   According to USDA taxonomy.

[c]   Using dichromat oxidation method (Margesin and Schinner, 2005).

Table B.33: *Installed soil temperature and soil moisture[a] sensors of the SwissSMEX site VOR.*

Depth[b] (cm)	Soil temperature		Soil moisture (capacitance-based)		Soil moisture (TDR-based)	
	Quantity	Serial number	Quantity	Serial number	Quantity	Serial number
5[+]	1	89	2	114, 120	-	-
10[+]	1	90	2	115, 121	2	31176[*] 31179[*]
30[+]	1	91	2	116, 122	2	31177[*] 31180[*]
50[+]	1	92	2	117, 123	-	-
80[+]	1	93	2	118, 124	2	31178[*] 31181[*]
120[+]	1	94	2	119, 125	-	-

[a]   Asterisk (*) indicates additionally measurement of soil temperature.

[b]   Plus (+) indicates sites, which are installed within the equipment project SwissSMEX-*Veg*.

B.18   Laegern LAG - mixed forest

Table B.34: Soil characteristics of the SwissSMEX site LAG.

| Sensor depth (cm) | Layer depth (cm) | Bulk density (g/cm^3) | Sample depth (cm) | Particle size distribution[a](%) | | | Texture[b] | Organic fraction[c] (%) | pH |
				Clay (<2 μm)	Silt (2−63 μm)	Sand (>63 μm)			
5	0 to 10	1.07	0 to 10	49.2	22.7	28.1	clay	4.7	6.0
10	0 to 10	1.07	0 to 10	49.2	22.7	28.1	clay	4.7	6.0
30	10 to 40	1.41	10 to 40	51.4	19.4	29.2	clay	2.1	6.1
45	10 to 40	1.41	10 to 40	51.4	19.4	29.2	clay	2.1	6.1

[a]   Using pipette method (Scott, 2000) after organic matter was removed by oxidation with hydrogen peroxide.
[b]   According to USDA taxonomy.

[c]   Using dichromat oxidation method (Margesin and Schinner, 2005).

Table B.35: Installed soil temperature and soil moisture sensors of the SwissSMEX site LAG.

| Depth (cm) | Soil temperature | | Soil moisture (capacitance-based) | | Soil moisture (TDR-based) | |
	Quantity	Serial number	Quantity	Serial number	Quantity	Serial number
5	1	1	2	16, 20	-	-
10	1	2	2	17, 21	1	15255
30	1	3	2	18, 22	-	-
45	1	4	2	19, 23	1	15267

B.19   Novaggio NOV - deciduous forest

Table B.36: *Soil characteristics of the SwissSMEX site NOV.*

Sensor depth (cm)	Layer depth (cm)	Bulk density (g/cm^3)	Sample depth (cm)	Particle size distribution[a](%)			Texture[b]	Organic fraction[c] (%)	pH
				Clay (<2 μm)	Silt (2−63 μm)	Sand (>63 μm)			
5	5		5	14	18	69	sandy loam		
10	10		10	12	19	69	sandy loam		
30	20		20	11	19	71	sandy loam		
50	55		55	2	18	79	loamy sand		
80	90		90	2	13	84	loamy sand		
100	90		90	2	13	84	loamy sand		

[a]   Using pipette method (Scott, 2000) after organic matter was removed by oxidation with hydrogen peroxide.

[b]   According to USDA taxonomy.

[c]   Using dichromat oxidation method (Margesin and Schinner, 2005).

Table B.37: *Installed soil temperature and soil moisture[a] sensors of the SwissSMEX site NOV.*

Depth[b] (cm)	Soil temperature		Soil moisture (capacitance-based)		Soil moisture (TDR-based)	
	Quantity	Serial number	Quantity	Serial number	Quantity	Serial number
5[+]	1	101	2	138, 144	-	-
10[+]	1	102	2	139, 145	2	31188[*], 31191[*]
30[+]	1	103	2	140, 146	2	31189[*], 31192[*]
50[+]	1	104	2	141, 147	-	-
80[+]	1	105	1 (profil1)	142, 148	1 (profil2)	31190[*], 31193[*]
100[+]	1	106	1	143	-	-

[a]   Asterisk (*) indicates additionally measurement of soil temperature.

[b]   Plus (+) indicates sites, which are installed within the equipment project SwissSMEX-*Veg*.

B.20   Oensingen OEA- arable

Table B.38: Soil characteristics of the SwissSMEX site OEA.

Sensor depth (cm)	Layer depth (cm)	Bulk density (g/cm^3)	Sample depth (cm)	Particle size distribution[a](%)			Texture[b]	Organic fraction[c] (%)	pH
				Clay ($<2\ \mu$m)	Silt ($2-63\ \mu$m)	Sand ($>63\ \mu$m)			
5	0 to 40	1.41							
10	0 to 40	1.41							
30	0 to 40	1.41							
50	40 to 120	1.60							
80	40 to 120	1.60							
100	40 to 120	1.60							

[a]   Using pipette method (Scott, 2000) after organic matter was removed by oxidation with hydrogen peroxide.

[b]   According to USDA taxonomy.

[c]   Using dichromat oxidation method (Margesin and Schinner, 2005).

Table B.39: Installed soil temperature and soil moisture sensors of the SwissSMEX site OEA.

Depth (cm)	Soil temperature		Soil moisture (capacitance-based)		Soil moisture (TDR-based)	
	Quantity	Serial number	Quantity	Serial number	Quantity	Serial number
5	1	5	1	10	-	-
10	1	6	1	11	-	-
30	1	7	1	12	-	-
50	1	8	1	13	-	-
80	1	9	1	14	-	-
120	1	10	1	15	-	-

Bibliography

Albergel, C., et al., 2008: From near-surface to root-zone soil moisture using an exponential filter: an assessment of the method based on in-situ observations and model simulations. *Hydrology and Earth System Sciences*, **12 (6)**, 1323–1337.

Albertson, J. D. and N. Montaldo, 2003: Temporal dynamics of soil moisture variability: 1. Theoretical basis. *Water Resources Research*, **39 (10)**, doi:127410.1029/2002wr001616.

Andersen, O. B., 2005: GRACE-derived terrestrial water storage depletion associated with the 2003 European heat wave. *Geophysical Research Letters*, **32 (18)**, 2–5, doi:10.1029/2005GL023574.

Bassara, J. and T. Crawford, 2000: Improved Installation Procedures for Deep-Layer Soil Moisture Measurements. *Journal of Atmospheric and Oceanic Technology*, **17**, 879–884.

Baumhardt, R. L., R. J. Lascano, and S. R. Evett, 2000: Soil material, temperature, and salinity effects on calibration of multisensor capacitance probes. *Soil Science Society of America Journal*, **64 (6)**, 1940–1946.

Begert, M., G. Seiz, N. Foppa, T. Schlegel, C. Appenzeller, and G. Müller, 2007: *Die Überführung der klimatologischen Referenzstationen der Schweiz in das Swiss National Basic Climatological Network (Swiss NBCN)*. Bundesamt für Meteorologie und Klimatologie, MeteoSchweiz, URL http://www.meteoschweiz.admin.ch/web/de/forschung/publikationen/alle_publikationen/ab-215.Par.0001.DownloadFile.tmp/arbeitsbericht215.pdf.

Beljaars, A. C. M., P. Viterbo, M. J. Miller, and A. K. Betts, 1996: The Anomalous Rainfall over the United States during July 1993: Sensitivity to Land Surface Parameterization and Soil Moisture Anomalies. *Monthly Weather Review*, **124 (3)**, 362–383, doi:10.1175/1520-0493(1996)124⟨0362:TAROTU⟩2.0.CO;2.

Bell, K. R., B. J. Blanchard, T. J. Schmugge, and M. W. Witczak, 1980: Analysis of surface moisture variations within large-field sites. *Water Resources Research*, **16 (4)**, 796–810, doi:10.1029/WR016i004p00796.

Benson, C. H. and X. Wang, 2006: Temperature-compensating calibration procedure for Water Content Reflectometers. *TDR 2006*, Paper ID 50, 16p.

Betts, A. K., 2004: Understanding hydrometeorology using global models. *Bulletin of the American Meteorological Society*, **85 (11)**, 1673–+, doi:10.1175/bams-85-11-1673.

Blonquist, J. M., S. B. Jones, and D. A. Robinson, 2005: Standardizing characterization of electromagnetic water content sensors: Part 2. Evaluation of seven sensing systems. *Vadose Zone Journal*, **4 (4)**, 1059–1069, doi:10.2136/vzj2004.0141.

Bogena, H. R., J. A. Huisman, C. Oberdorster, and H. Vereecken, 2007: Evaluation of a low-cost soil water content sensor for wireless network applications. *Journal of Hydrology*, **344**, 32–42, doi:10.1016/j.jhydrol.2007.06.032.

Brocca, L., F. Melone, T. Moramarco, and R. Morbidelli, 2009: Soil moisture temporal stability over experimental areas in Central Italy. *Geoderma*, **148 (3-4)**, 364–374, doi:10.1016/j.geoderma.2008.11.004.

Brocca, L., F. Melone, T. Moramarco, and R. Morbidelli, 2010: Spatial-temporal variability of soil moisture and its estimation across scales. *Water Resources Research*, **46**, doi:W0251610.1029/2009wr008016.

Brocca, L., R. Morbidelli, F. Melone, and T. Moramarco, 2007: Soil moisture spatial variability in experimental areas of central Italy. *Journal of Hydrology*, **333 (2-4)**, 356–373, doi:10.1016/j.jhydrol.2006.09.004.

Budyko, M. I., 1956: *The heat balance of the earths surface*. U.S. Dept of Commerce, Washington,, Leningrad, 255 pp.

C, R., et al., 2007: Goulburn River experimental catchment data set. *Water Resources Research*, **43**, 1–10.

Chahine, M. T., 1992: The hydrological cycle and its influence on climate. *Nature*, **359**, 373–379.

Cosh, M. H., 2004: Variability of surface soil moisture at the watershed scale. *Water Resources Research*, **40 (12)**, 1–9, doi:10.1029/2004WR003487.

Czarnomski, N., G. W. Moore, T. G. Pypker, J. Licata, and B. J. Bond, 2005: Precision and accuracy of three alternative instruments for measuring soil water content in two forest soils of the Pacific Northwest. *Canadian Journal of Forest Research-Revue Canadienne De Recherche Forestiere*, **35 (8)**, 1867–1876.

de Jeu, R. A. M., W. Wagner, T. R. H. Holmes, A. J. Dolman, N. C. van de Giesen, and J. Friesen, 2008: Global Soil Moisture Patterns Observed by Space Borne Microwave Radiometers and Scatterometers. *Surveys in Geophysics*, **29 (4-5)**, 399–420, doi:10.1007/s10712-008-9044-0.

Dean, T., J. Bell, and A. Baty, 1987: Soil moisture measurement by an improved capacitance technique, Part I. Sensor design and performance. *Journal of Hydrology*, **93 (1-2)**, 67–78, doi:10.1016/0022-1694(87)90194-6.

Decagon, D., 2009: 10HS Soil Moisture Sensor Operatorâs Manual, Version 2.0.

Diffenbaugh, N. S., J. S. Pal, F. Giorgi, and X. J. Gao, 2007: Heat stress intensification in the Mediterranean climate change hotspot. *Geophysical Research Letters*, **34 (11)**, 6, doi: L1170610.1029/2007gl030000.

Dirmeyer, P. A., R. D. Koster, and Z. C. Guo, 2006: Do global models properly represent the feedback between land and atmosphere? *Journal of Hydrometeorology*, **7 (6)**, 1177–1198.

Dorigo, W. A., et al., 2011: The International Soil Moisture Network: a data hosting facility for global in situ soil moisture measurements. *Hydrology and Earth System Sciences*, **15 (5)**, 1675–1698, doi:10.5194/hess-15-1675-2011.

Entekhabi, D. and I. Rodriguez-Iturbe, 1994: Analytical framework for the characterization of the space-time variability of soil moisture. *Advances in Water Resources*, **17 (1-2)**, 35–45, doi:10.1016/0309-1708(94)90022-1.

Entekhabi, D., I. Rodriguez-iturbe, and F. Castelli, 1996: Mutual interaction of soil moisture state and atmospheric processes. *Journal of Hydrology*, **184**, 3–17.

Entin, J. K., A. Robock, K. Y. Vinnikov, S. E. Hollinger, S. X. Liu, and A. Namkhai, 2000: Temporal and spatial scales of observed soil moisture variations in the extratropics. *Journal of Geophysical Research-Atmospheres*, **105 (D9)**, 11 865–11 877, doi:10.1029/2000jd900051.

Escorihuela, M. J., P. De Rosnay, Y. H. Kerr, and J. C. Calvet, 2007: Influence of bound-water relaxation frequency on soil moisture measurements. *IEEE Transactions on Geoscience and Remote Sensing*, **45 (12)**, 4067–4076, doi:10.1109/tgrs.2007.906090.

Evett, S. R., J. A. Tolk, and T. A. Howell, 2006: Soil profile water content determination: Sensor accuracy, axial response, calibration, temperature dependence, and precision. *Vadose Zone Journal*, **5 (3)**, 894–907, doi:10.2136/vzj2005.0149.

Famiglietti, J. S., D. Ryu, A. A. Berg, M. Rodell, and T. J. Jackson, 2008: Field observations of soil moisture variability across scales. *Water Resources Research*, **44 (1)**, W01 423, doi: 10.1029/2006wr005804.

Famiglietti, J. S., et al., 1999: Ground-based investigation of soil moisture variability within remote sensing footprints during the Southern Great Plains 1997 (SGP97) Hydrology Experiment. *Water Resources Research*, **35 (6)**, 1839–1851, doi:10.1029/1999wr900047.

FAO, 2008: *Terrestrial Essential Climate Variables for Climate Change Assessment, Mitigation and Adaptation, Biennial report supplement*. Rome, Italy, 5 pp., URL http://www.fao.org/gtos/doc/pub52.pdf.

Fernandez-Galvez, J., A. Verhoef, and E. Barahona, 2007: Estimating soil water fluxes from soil water records obtained using dielectric sensors. *Hydrological Processes*, **21 (20)**, 2785–2793, doi:10.1002/hyp.6494.

Ferrez, J., A. Davison, and M. Rebetez, 2011: Extreme temperature analysis under forest cover compared to an open field. *Agricultural and Forest Meteorology*, **151 (7)**, 992–1001, doi: 10.1016/j.agrformet.2011.03.005.

Findell, K. L., P. Gentine, B. R. Lintner, and C. Kerr, 2011: Probability of afternoon precipitation in eastern United States and Mexico enhanced by high evaporation. *Nature Geoscience*, **4 (7)**, 434–439, doi:10.1038/ngeo1174.

Fischer, E. M., S. I. Seneviratne, D. Luthi, and C. Schar, 2007a: Contribution of land-atmosphere coupling to recent European summer heat waves. *Geophysical Research Letters*, **34 (6)**, 6, doi:L0670710.1029/2006gl029068.

Fischer, E. M., S. I. Seneviratne, P. L. Vidale, D. Luthi, and C. Schar, 2007b: Soil moisture - Atmosphere interactions during the 2003 European summer heat wave. *Journal of Climate*, **20 (20)**, 5081–5099, doi:10.1175/jcli4288.1.

Fu, B., J. Wang, L. Chen, and Y. Qiu, 2003: The effects of land use on soil moisture variation in the Danangou catchment of the Loess Plateau, China. *Catena*, **54 (1-2)**, 197–213, doi: 10.1016/s0341-8162(03)00065-1.

Granier, A., et al., 2007: Evidence for soil water control on carbon and water dynamics in European forests during the extremely dry year: 2003. *Agricultural and Forest Meteorology*, **143 (1-2)**, 123–145, doi:10.1016/j.agrformet.2006.12.004.

Guber, A. K., T. J. Gish, Y. A. Pachepsky, M. T. Van Genuchten, C. S. T. Daughtry, T. J. Nicholson, and R. E. Cady, 2008: Temporal stability in soil water content patterns across agricultural fields. *Catena*, **73 (1)**, 125–133, doi:10.1016/j.catena.2007.09.010.

Haarsma, R. J., F. Selten, B. V. Hurk, W. Hazeleger, and X. L. Wang, 2009: Drier Mediterranean soils due to greenhouse warming bring easterly winds over summertime central Europe. *Geophysical Research Letters*, **36**, 7, doi:L0470510.1029/2008gl036617.

Hasted, J., 1973: *Aqueous Dielectrics*. Chapman and Hall, London, 8 pp.

Henschel, F., 2011: Untersuchung der zeitlichen und räumlichen Variabilität der Bodenfeuchte in der Schweiz für verschiedene Landnutzung. Bachelor thesis, ETH Zurich, Zurich, Switzerland.

Hillel, D., 2007: *Soil in the environment: crucible of terrestiral life*. Elsevier/Academic Press, Oxford, 221–231 pp.

Hirschi, M., et al., 2011: Observational evidence for soil-moisture impact on hot extremes in southeastern Europe. *Nature Geoscience*, **4 (1)**, 17–21, doi:10.1038/ngeo1032.

Hohenegger, C., P. Brockhaus, C. S. Bretherton, and C. Schär, 2009: The Soil Moisture–Precipitation Feedback in Simulations with Explicit and Parameterized Convection. *Journal of Climate*, **22 (19)**, 5003–5020, doi:10.1175/2009JCLI2604.1.

Hollinger, S. E. and S. A. Isard, 1994: A soil moisture climatology of Illinois. *Journal of Climate*, **7 (5)**, 822–833.

Hupet, F., P. Bogaert, and M. Vanclooster, 2004: Quantifying the local-scale uncertainty of estimated actual evapotranspiration. *Hydrological Processes*, **18 (17)**, 3415–3434, doi:10. 1002/hyp.1504.

IMKO, 2006: TRIME-EZ /-EZC /-IT /-ITC, User Manual.

Jackson, T., 2002: Remote sensing of soil moisture: implications for groundwater recharge. *Hydrogeology Journal*, **10 (1)**, 40–51, doi:10.1007/s10040-001-0168-2.

Jackson, T. J., 2005: Estimation of surface soil moisutre using microwave sensors. John Wiley & Sons, Ltd., 799–810 pp.

Jackson, T. J., et al., 2010: Validation of Advanced Microwave Scanning Radiometer Soil Moisture Products. *IEEE Transactions on Geoscience and Remote Sensing*, **48 (12)**, 4256–4272, doi:10.1109/tgrs.2010.2051035.

Jacobs, J., 2004: SMEX02: Field scale variability, time stability and similarity of soil moisture. *Remote Sensing of Environment*, **92 (4)**, 436–446, doi:10.1016/j.rse.2004.02.017.

Jaeger, E. B. and S. I. Seneviratne, 2011: Impact of soil moisture-atmosphere coupling on European climate extremes and trends in a regional climate model. *Climate Dynamics*, **36 (9-10)**, 1919–1939, doi:10.1007/s00382-010-0780-8.

Jones, S. B., J. M. Blonquist, D. A. Robinson, V. P. Rasmussen, and D. Or, 2005: Standardizing characterization of electromagnetic water content sensors: Part 1. Methodology. *Vadose Zone Journal*, **4 (4)**, 1048–1058, doi:10.2136/vzj2004.0140.

Joshi, C. and B. P. Mohanty, 2010: Physical controls of near-surface soil moisture across varying spatial scales in an agricultural landscape during SMEX02. *Water Resources Research*, **46 (12)**, 1–21, doi:10.1029/2010WR009152.

Jung, M., et al., 2010: Recent decline in the global land evapotranspiration trend due to limited moisture supply. *Nature*, **467 (7318)**, 951–954, doi:10.1038/nature09396.

Kamgar, A., J. W. Hopmans, W. Wallender, and O. Wendroth, 1993: Plotsize and sample number for neutron probe measurements in small field trials. *Soil Science*, 213–224.

Kelleners, T. J., D. A. Robinson, P. J. Shouse, J. E. Ayars, and T. H. Skaggs, 2005: Frequency dependence of the complex permittivity and its impact on dielectric sensor calibration in soils. *Soil Science Society of America Journal*, **69 (1)**, 67–76.

Kelliher, M., R. Leuning, and D. Schulze, 1993: Oecologia Review article and grasslands. *Oecologia*, **95**, 153–163.

Kizito, F., C. S. Campbell, G. S. Campbell, D. R. Cobos, B. L. Teare, B. Carter, and J. W. Hopmans, 2008: Frequency, electrical conductivity and temperature analysis of a low-cost capacitance soil moisture sensor. *Journal of Hydrology*, **352 (3-4)**, 367–378, doi:10.1016/j. jhydrol.2008.01.021.

Koster, R. D., S. P. P. Mahanama, B. Livneh, D. P. Lettenmaier, and R. H. Reichle, 2010a: Skill in streamflow forecasts derived from large-scale estimates of soil moisture and snow. *Nature Geoscience*, **3 (9)**, 613–616, doi:10.1038/ngeo944.

Koster, R. D. and P. C. D. Milly, 1997: The interplay between transpiration and runoff formulations in land surface schemes used with atmospheric models. *Journal of Climate*, **10 (7)**, 1578–1591.

Koster, R. D., et al., 2004: Regions of strong coupling between soil moisture and precipitation. *Science*, **305 (5687)**, 1138–1140.

Koster, R. D., et al., 2010b: Contribution of land surface initialization to subseasonal forecast skill: First results from a multi-model experiment. *Geophysical Research Letters*, **37**, 6, doi:L0240210.1029/2009gl041677.

Krauss, L., C. Hauck, and C. Kottmeier, 2010: Spatio-temporal soil moisture variability in Southwest Germany observed with a new monitoring network within the COPS domain. *Meteorologische Zeitschrift*, **19 (6)**, 523–537, doi:10.1127/0941-2948/2010/0486.

Larson, K. M., E. E. Small, E. D. Gutmann, A. L. Bilich, J. J. Braun, and V. U. Zavorotny, 2008: Use of GPS receivers as a soil moisture network for water cycle studies. *Geophysical Research Letters*, **35 (24)**, 5, doi:L2440510.1029/2008gl036013.

Ledieu, J., P. Deridder, P. Declerck, and S. Dautrebande, 1986: A method of measuring soil moisture by time domain reflectometry. *Journal of Hydrology*, **88 (3-4)**, 319–328.

Lehner, I., A. J. Teuling, J. Gurtz, and S. I. Seneviratne, 2010: Long-term water balance in the prealpine Rietholzbach catchment: First comparison of evapotranspiration estimates. IAHS publ. 336.

Loew, A., T. Holmes, and R. de Jeu, 2009: The European heat wave 2003: Early indicators from multisensoral microwave remote sensing? *Journal of Geophysical Research-Atmospheres*, **114**, 14, doi:D0510310.1029/2008jd010533.

Logsdon, S. D., 2009: CS616 Calibration: Field versus Laboratory. *Soil Science Society of America Journal*, **73 (1)**, 1, doi:10.2136/sssaj2008.0146.

Lorenz, R., E. B. Jaeger, and S. I. Seneviratne, 2010: Persistence of heat waves and its link to soil moisture memory. *Geophysical Research Letters*, **37**, doi:L0970310.1029/ 2010gl042764.

Manabe, S., 1969: Climate and the ocean circulation 1. the atmospheric circulation and the hydrology of the earth's surface. *Monthly Weather Review*, **97 (11)**.

Margesin, R. and F. Schinner, 2005: *Manual for Soil Analysisâ Monitoring and Assessing Soil Bioremediation*. Springer, Berlin, 366 pp.

Martínez-Fernández, J. and A. Ceballos, 2003: Temporal stability of soil moisture in a large-field experiment in Spain. *Soil Science Society of America Journal*, **67**, 1647–1656.

Martinez-Fernandez, J. and A. Ceballos, 2005: Mean soil moisture estimation using temporal stability analysis. *Journal of Hydrology*, **312 (1-4)**, 28–38, doi:10.1016/j.jhydrol.2005.02.007.

Mittelbach, H., F. Casini, I. Lehner, A. J. Teuling, and S. I. Seneviratne, 2011: Soil moisture monitoring for climate research: Evaluation of a low-cost sensor in the framework of the Swiss Soil Moisture Experiment (SwissSMEX) campaign. *Journal of Geophysical Research-Atmospheres*, **116**, doi:D0511110.1029/2010jd014907.

Müller, G., 1980: *Die Beobachtungsnetze der Schweizerischen Meteorologischen Anstalt. Konzept 1980*. Arbeitsbericht der Schweizerischen Meteorologischen Anstalt, Zurich.

Oki, T. and S. Kanae, 2006: Global hydrological cycles and world water resources. *Science*, **313 (5790)**, 1068–1072, doi:10.1126/science.1128845.

Or, D. and S. B. Jones, 2002: Time Domain Reflectometry (TDR) Applications in Earth Science. *IEEE*.

Pal, J. S. and E. A. B. Eltahir, 2003: A feedback mechanism between soil-moisture distribution and storm tracks. *Quarterly Journal of the Royal Meteorological Society*, **129 (592)**, 2279–2297, doi:10.1256/qj.01.201.

Peel, M. C., T. a. McMahon, and B. L. Finlayson, 2010: Vegetation impact on mean annual evapotranspiration at a global catchment scale. *Water Resources Research*, **46 (9)**, 1–16, doi:10.1029/2009WR008233.

Persson, M. and R. Berndtsson, 1995: Texture and Electrial Conductivity Effects on Temperature Dependency in Time Domain Reflectometry. *Soil Science Society of America Journal*, **62**, 887–893.

Plauborg, F., B. V. Iversen, and P. E. Laerke, 2005: In situ comparison of three dielectric soil moisture sensors in drip irrigated sandy soils. *Vadose Zone Journal*, **4 (4)**, 1037–1047, doi:10.2136/vzj2004.0138.

Polyakov, V., A. Fares, and M. H. Ryder, 2005: Calibration of a capacitance system for measuring water content of tropical soil. *Vadose Zone Journal*, **4 (4)**, 1004–1010, doi:10.2136/vzj2005.0028.

Ramillien, G., J. S. Famiglietti, and J. Wahr, 2008: Detection of Continental Hydrology and Glaciology Signals from GRACE: A Review. *Surveys in Geophysics*, **29 (4-5)**, 361–374, doi:10.1007/s10712-008-9048-9.

Renaud, V. and M. Rebetez, 2009: Comparison between open-site and below-canopy climatic conditions in Switzerland during the exceptionally hot summer of 2003. *Agricultural and Forest Meteorology*, **149 (5)**, 873–880, doi:10.1016/j.agrformet.2008.11.006.

Robinson, D. A., S. B. Jones, J. M. Wraith, D. Or, and S. P. Friedman, 2003: A Review of Advances in Dielectric and Electrical Conductivity Measurement in Soils Using Time Domain Reflectometry. *Vadose Zone Journal*, **2 (4)**, 444–475.

Robinson, D. A., et al., 2008: Soil moisture measurement for ecological and hydrological watershed-scale observatories: A review. *Vadose Zone Journal*, **7 (1)**, 358–389, doi:10.2136/vzj2007.0143.

Robock, A., A. Schlosser, K. Y. Vinnikov, N. A. Speranskaya, and J. K. Entin, 1998: Evaluation of AMIP soil moisture simulations. *Global and Planetary Change*, **19**, 181–208.

Robock, A., K. Y. Vinnikov, G. Srinivasan, J. K. Entin, S. E. Hollinger, N. A. Speranskaya, S. X. Liu, and A. Namkhai, 2000: The Global Soil Moisture Data Bank. *Bulletin of the American Meteorological Society*, **81 (6)**, 1281–1299.

Roth, K., R. Schulin, H. Fluhler, and W. Attinger, 1990: Calibration of time domain reflectometry for water content measurements using a composite dielectric approach. *Water Resources Research*, **26 (10)**, 2267–2273.

Rüdiger, C., A. W. Western, J. P. Walker, A. B. Smith, J. D. Kalma, and G. R. Willgoose, 2010: Towards a general equation for frequency domain reflectometers. *Journal of Hydrology*, **383 (3-4)**, 319–329, doi:10.1016/j.jhydrol.2009.12.046.

Schmugge, T. J., T. J. Jackson, and H. L. McKim, 1980: Survey of methods for soil moisture determination. *Water Resources Research*, **16 (6)**, 961–979.

Schmugge, T. J., W. P. Kustas, J. C. Ritchie, T. J. Jackson, and A. Rango, 2002: Remote sensing in hydrology. *Advances in Water Resources*, **25 (8-12)**, 1367–1385.

Scott, H. D., 2000: *Soil Physics: Agricultural and Environmental Applications*. Iowa State Univ. Press, Ames, 421 pp.

Seneviratne, S. I., 2003: *Terrestrial Water Storage: A Critical Variable for Mid-latitude Climate and Climate Change*. Ph.D. thesis, ETH Zurich, Zurich, Switzerland, 136 pp.

Seneviratne, S. I., T. Corti, E. L. Davin, M. Hirschi, E. B. Jaeger, I. Lehner, B. Orlowsky, and A. J. Teuling, 2010: Investigating soil moisture-climate interactions in a changing climate: A review. *Earth-Science Reviews*, **99 (3-4)**, 125–161, URL http://www.elsevier.com.

Seneviratne, S. I., D. Luthi, M. Litschi, and C. Schar, 2006a: Land-atmosphere coupling and climate change in Europe. *Nature*, **443 (7108)**, 205–209, doi:10.1038/nature05095.

Seneviratne, S. I., P. Viterbo, D. Lüthi, and C. Schär, 2004: Inferring Changes in Terrestrial Water Storage Using ERA-40 Reanalysis Data: The Mississippi River Basin. *Journal of Climate*, **17 (11)**, 2039–2057.

Seneviratne, S. I., et al., 2006b: Soil moisture memory in AGCM simulations: Analysis of global land-atmosphere coupling experiment (GLACE) data. *Journal of Hydrometeorology*, **7 (5)**, 1090–1112.

Seyfried, M. S. and M. D. Murdock, 2004: Measurement of soil water content with a 50-MHz soil dielectric sensor. *Soil Science Society of America Journal*, **68 (2)**, 394–403.

Shukla, J. and Y. Mintz, 1982: Influence of Land-Surface Evapotranspiration on the Earth's Climate. *Science*, **215 (4539)**, 1498–501, doi:10.1126/science.215.4539.1498.

Steele-Dunne, S. C., M. M. Rutten, D. M. Krzeminska, M. Hausner, S. W. Tyler, J. Selker, T. a. Bogaard, and N. C. van de Giesen, 2010: Feasibility of soil moisture estimation using passive distributed temperature sensing. *Water Resources Research*, **46 (3)**, 1–12, doi:10.1029/2009WR008272.

Tallon, L. K. and B. Si, 2004: Representative Soil Water Benchmarking for Environmental Monitoring. *Journal of Environmental Informatics*, **4 (1)**, 31–39, doi:10.3808/jei.200400034.

Tapley, B. D., S. Bettadpur, J. C. Ries, P. F. Thompson, and M. M. Watkins, 2004: GRACE measurements of mass variability in the Earth system. *Science*, **305 (5683)**, 503–505.

Taylor, C. M., A. Gounou, F. Guichard, P. P. Harris, R. J. Ellis, F. Couvreux, and M. De Kauwe, 2011: Frequency of Sahelian storm initiation enhanced over mesoscale soil-moisture patterns. *Nature Geoscience*, **4 (7)**, 430–433, doi:10.1038/ngeo1173.

Teuling, a. J., I. Lehner, J. W. Kirchner, and S. I. Seneviratne, 2010a: Catchments as simple dynamical systems: Experience from a Swiss prealpine catchment. *Water Resources Research*, **46 (10)**, 1–15, doi:10.1029/2009WR008777.

Teuling, A. J., S. I. Seneviratne, C. Williams, and P. A. Troch, 2006a: Observed timescales of evapotranspiration response to soil moisture. *Geophysical Research Letters*, **33 (23)**, 5, doi:L2340310.1029/2006gl028178.

Teuling, A. J. and P. A. Troch, 2005: Improved understanding of soil moisture variability dynamics. *Geophysical Research Letters*, **32 (5)**, 4, doi:L0540410.1029/2004gl021935.

Teuling, A. J., R. Uijlenhoet, F. Hupet, E. E. van Loon, and P. A. Troch, 2006b: Estimating spatial mean root-zone soil moisture from point-scale observations. *Hydrology and Earth System Sciences*, **10 (5)**, 755–767.

Teuling, a. J., et al., 2009: A regional perspective on trends in continental evaporation. *Geophysical Research Letters*, **36 (2)**, 1–5, doi:10.1029/2008GL036584.

Teuling, A. J., et al., 2010b: Contrasting response of European forest and grassland energy exchange to heatwaves. *Nature Geoscience*, **3 (10)**, 722–727, doi:10.1038/ngeo950.

Topp, G. C., 2003: State of the art of measuring soil water content. *Hydrological Processes*, **17 (14)**, 2993–2996, doi:10.1002/hyp.5148.

Topp, G. C., J. L. Davis, and A. P. Annan, 1980: Electromagnetic determination of soil water content: Measurements in Coaxial Transmission Lines. *Water Resources Research*, **16 (3)**, 574–582.

Topp, G. C. and W. D. Reynolds, 1998: Time domain reflectometry: a seminal technique for measuring mass and energy in soil. *Soil & Tillage Research*, **47 (1-2)**, 125–132.

Trenberth, K. E., L. Smith, T. Qian, A. Dai, and J. Fasullo, 2007: Estimates of the Global Water Budget and Its Annual Cycle Using Observational and Model Data. *Journal of Hydrometeorology*, **8 (4)**, 758–769, doi:10.1175/JHM600.1.

Vachaud, G., A. Passerat De Silans, P. Balabanis, and M. Vauclin, 1985: Temporal stability of spatially measured soil water probability density funcion. *Soil Science Society of America Journal*, **49 (4)**, 822–828.

van den Hurk, B., et al., 2005: Soil Control on Runoff Response to Climate Change in Regional Climate Model Simulations. *Journal of Climate*, **18 (17)**, 3536–3551, doi:10.1175/JCLI3471.1.

van den Hurk, B. J. J. M. and E. van Meijgaard, 2010: Diagnosing Land–Atmosphere Interaction from a Regional Climate Model Simulation over West Africa. *Journal of Hydrometeorology*, **11 (2)**, 467–481, doi:10.1175/2009JHM1173.1.

Vautard, R., et al., 2007: Summertime European heat and drought waves induced by wintertime Mediterranean rainfall deficit. *Geophysical Research Letters*, **34 (7)**, 5, doi:L0771110.1029/2006gl028001.

Veldkamp, E. and J. J. O'Brien, 2000: Calibration of a frequency domain reflectometry sensor for humid tropical soils of volcanic origin. *Soil Science Society of America Journal*, **64 (5)**, 1549–1553.

Venkatesh, B., N. Lakshman, B. K. Purandara, and V. B. Reddy, 2011: Analysis of observed soil moisture patterns under different land covers in Western Ghats, India. *Journal of Hydrology*, **397 (3-4)**, 281–294, doi:10.1016/j.jhydrol.2010.12.006.

Ventura, F., O. Facini, S. Piana, and P. P. Rossi, 2010: Soil Moisture Measurements: Comparison of Instrumentation Performances. *Journal of Irrigation and Drainage Engineering-Asce*, **136 (2)**, 81–89, doi:10.1061/(asce)0733-9437(2010)136:2(81).

Ventura, F., R. L. Snyder, and K. M. Bali, 2006: Estimating evaporation from bare soil using soil moisture data. *Journal of Irrigation and Drainage Engineering-Asce*, **132 (2)**, 153–158, doi:10.1061/(asce)0733-9437(2006)132:2(153).

Vereecken, H., J. A. Huisman, H. Bogena, J. Vanderborght, J. A. Vrugt, and J. W. Hopmans, 2008: On the value of soil moisture measurements in vadose zone hydrology: A review. *Water Resources Research*, **44**, doi:W00d0610.1029/2008wr006829.

Vereecken, H., T. Kamai, T. Harter, R. Kasteel, J. Hopmans, and J. Vanderborght, 2007: Explaining soil moisture variability as a function of mean soil moisture: A stochastic unsaturated flow perspective. *Geophysical Research Letters*, **34 (22)**, doi:L2240210.1029/2007gl031813.

Vereecken, H., S. Kollet, and C. Simmer, 2010: Patterns in Soil-Vegetation-Atmosphere Systems: Monitoring, Modeling, and Data Assimilation. *Vadose Zone Journal*, **9 (4)**, 821–827, doi:10.2136/vzj2010.0122.

Verhoef, a., J. Fernández-Gálvez, A. Diaz-Espejo, B. Main, and M. El-Bishti, 2006: The diurnal course of soil moisture as measured by various dielectric sensors: Effects of soil temperature and the implications for evaporation estimates. *Journal of Hydrology*, **321 (1-4)**, 147–162, doi:10.1016/j.jhydrol.2005.07.039.

Vinnikov, K. Y., A. Robock, S. Qiu, and J. K. Entin, 1999: Optimal design of surface networks for observationof soil moisture. *Journal of Geophysical Research*, 743–749.

Vinnikov, K. Y., A. Robock, N. A. Speranskaya, and A. Schlosser, 1996: Scales of temporal and spatial variability of midlatitude soil moisture. *Journal of Geophysical Research-Atmospheres*, **101 (D3)**, 7163–7174.

Vinnikov, K. Y. and I. B. Yeserkepova, 1991: Soil moisture empirical data and model results. *Journal of Climate*, **4 (1)**, 66–79.

Wagner, W., G. Bloschl, P. Pampaloni, J. C. Calvet, B. Bizzarri, J. P. Wigneron, and Y. Kerr, 2007a: Operational readiness of microwave remote sensing of soil moisture for hydrologic applications. *Nordic Hydrology*, **38 (1)**, 1–20, doi:10.2166/nh.2007.029.

Wagner, W., V. Naeimi, K. Scipal, R. de Jeu, and J. Martinez-Fernandez, 2007b: Soil moisture from operational meteorological satellites. *Hydrogeology Journal*, **15 (1)**, 121–131, doi:10.1007/s10040-006-0104-6.

Walker, J. P., G. R. Willgoose, and J. D. Kalma, 2004: In situ measurement of soil moisture: a comparison of techniques. *Journal of Hydrology*, **293 (1-4)**, 85–99, doi:10.1016/j.jhyrol.2004.01.008.

Wang, G., A. J. Dolman, R. Blender, and K. Fraedrich, 2010: Fluctuation regimes of soil moisture in ERA-40 re-analysis data. *Theoretical and Applied Climatology*, **99 (1-2)**, 1–8, doi:10.1007/s00704-009-0111-3.

Weiler, M., 2001: *Mechanisms controlling macropore flow during infiltration: Dye tracer experiments and simulations*. Ph.D. thesis, ETH Zurich, Zurich, Switzerland, doi:10.3929/ethz-a-004180115.

Weisheimer, A., F. J. Doblas-Reyes, T. Jung, and T. N. Palmer, 2011: On the predictability of the extreme summer 2003 over Europe. *Geophysical Research Letters*, **38 (5)**, 1–5, doi:10.1029/2010GL046455.

Western, A. W., R. B. Grayson, and G. Bloschl, 2002: Scaling of soil moisture: A hydrologic perspective. *Annual Review of Earth and Planetary Sciences*, **30**, 149–180, doi:10.1146/annurev.earth.30.091201.140434.

Western, A. W., R. B. Grayson, G. Blöschl, G. R. Willgoose, and T. A. McMahon, 1999: Observed spatial organization of soil moisture and its relation to terrain indices. *Water Resources Research*, **35 (3)**, 797–810, doi:10.1029/1998wr900065.

Western, A. W., S. L. Zhou, R. B. Grayson, T. A. McMahon, G. Bloschl, and D. J. Wilson, 2004: Spatial correlation of soil moisture in small catchments and its relationship to dominant spatial hydrological processes. *Journal of Hydrology*, **286 (1-4)**, 113–134, doi:10.1016/j.jhydrol.2003.09.014.

Wraith, J. M. and D. Or, 1999: Temperature effects on soil bulk dielectric permittivity measured by time domain reflectometry: Experimental evidence and hypothesis development. *Water Resources Research*, **35 (2)**, 361–369.

Wu, W. R. and R. E. Dickinson, 2004: Time scales of layered soil moisture memory in the context of land-atmosphere interaction. *Journal of Climate*, **17 (14)**, 2752–2764.

Zaitchik, B. F., A. K. Macalady, L. R. Bonneau, and R. B. Smith, 2006: Europe's 2003 heat wave: A satellite view of impacts and land-atmosphere feedbacks. *International Journal of Climatology*, **26 (6)**, 743–769, doi:10.1002/joc.1280.

Zha, T. S., A. G. Barr, G. van der Kamp, T. A. Black, J. H. McCaughey, and L. B. Flanagan, 2010: Interannual variation of evapotranspiration from forest and grassland ecosystems in western canada in relation to drought. *Agricultural and Forest Meteorology*, **150 (11)**, 1476–1484, doi:10.1016/j.agrformet.2010.08.003.

Zhou, X., H. Lin, and Q. Zhu, 2007: Temporal stability of soil moisture spatial variability at two scales and its implication for optimal field monitoring. *Hydrology and Earth System Sciences Discussions*, **4 (3)**, 1185–1214, doi:10.5194/hessd-4-1185-2007.

Zreda, M., D. Desilets, T. P. A. Ferre, and R. L. Scott, 2008: Measuring soil moisture content non-invasively at intermediate spatial scale using cosmic-ray neutrons. *Geophysical Research Letters*, **35 (21)**, 5, doi:L2140210.1029/2008gl035655.

Acknowledgments

Curriculum Vitae

Heidi Mittelbach, Weizenstrasse 8, 8037 Zurich, Switzerland
Born 22 September 1980
German citizen

Jun 2008	-	Dec 2011	Ph.D. student in the Land-Climate Interaction group of Prof. S.I. Seneviratne, Institute for Atmospheric and Climate Science, ETH Zurich, Switzerland.
May 2006	-	May 2008	Teaching and Research Assistant in the Hydrology group of Prof. P. Burlando, Institute of Environmental Engineering, ETH Zurich, Switzerland.
Oct 2005	-	Apr 2006	Diploma thesis under Dr. D. Viviroli, Institute of Geography, University Bern, and Dr. J. Gurtz, Institute for Atmospheric and Climate Science, ETH Zurich, Switzerland: Kalibrierung und Regionalisierung des flächendifferenzierten hydrologischen Modellsystems PREVAH für ausgewählte Einzugsgebiete der Schweiz.
Oct 2004	-	May 2005	Internship at the Ingenieurbüro für Wasser und Boden in Possendorf, Germany: Preliminary planning of a concept for flood prevention, collaboration in hydrological studies, channel survey.
Sep 2003	-	Oct 2003	Internship at the Ingenieurgesellschaft für Umwelttechnik und Bauwesen mbH Dr. Eisele in Rottenburg, Germany: Performance of hydraulic tests.
Oct 2000	-	Apr 2006	Diploma programme at the Institute of Hydrology and Meteorology, TU Dresden, Germany.
1998	-	2000	Highschool Education at the Berufliches Schulzentrum Schwarzenberg, Germany.

TEACHING

Teaching Assistant:	Land-Climate interactions (Master's Course)
	Field course in hydrology, climate, micrometeorology and synoptic meteorology (Master's Course)
	Observational network (Bachelor's Course)
	Fach- und Computerlabor: Hydraulische Modellierung von Fliessgewässern; Abflussmessung (Master's Course)
	Umweltlabor 2: Measuring and Modelling Evapotranspiration (Bachelor's Course)
	Hydrology I (Bachelor's Course)
	Hydrology II (Master's Course)
Supervision:	Master thesis Claudio Graf; Bachelor thesis Florian Henschel

PUBLICATIONS AND CONFERENCE PROCEEDINGS

Mittelbach, H. and S.I. Seneviratne, 2012: A new perspective on the spatio-temporal variability of soil moisture: Temporal dynamics versus time invariant contributions, *submitted to Hydrology and Earth System Sciences*.

Mittelbach, H., I. Lehner and S.I. Seneviratne, 2011: Comparison of four soil moisture sensor types under field conditions in Switzerland, *accepted in Journal of Hydrology*.

Mittelbach, H., F. Casini, I. Lehner, A.J. Teuling, and S.I. Seneviratne, 2011: Soil moisture monitoring for climate research: Evaluation of a low cost sensor in the framework of the SwissSMEX campaign. *Journal of Geophysical Research - Atmosphere*, **116**, D05111.

Mittelbach H., R. Orth and S.I. Seneviratne, 2010: Comparison of soil moisture in Switzerland using in-situ measurements and model output. *Proceedings of Earth Observation for Land-Atmosphere Interaction Science*, Frascati, Italy, November 2010.

Viviroli, D., H. Mittelbach, J. Gurtz and R. Weingartner, 2009: Continuous simulation for flood estimation in ungauged mesoscale catchments of Switzerland Part II: Parameter regionalisation and flood estimation results, *Journal of Hydrology*, **377**, 208225.

ORAL PRESENTATIONS

SMAP Cal/Val Workshop #2, May 2011, Oxnard CA, United States:
"The SwissSMEX/-Veg soil moisture network - lessons learned"

Hydrologisches Seminar ZHydro2010, November 2010, Zurich, Switzerland:
"SwissSMEX/-Veg: An observational network to measure soil moisture in Switzerland"

European Geosciences Union General Assembly, May 2010, Vienna, Austria:
"Evaluation of the capacitance-based low cost sensor Decagon 10HS"

Seminar for user of Decagon Sensors, March 2009, Birmensdorf, Switzerland:
"Sensor evaluation for soil moisture measurements in Switzerland-Decagon 10HS vs. TDR-based sensors"

Baden Workshop, January 2009, Baden, Switzerland:
"SwissSMEX - Swiss Soil Moisture EXperiment"

SMOS Nutzerworkshop, August 2008, Hamburg, Germany:
"SwissSMEX - Swiss Soil Moisture EXperiment"

POSTER PRESENTATIONS

European Geophysical Union (EGU), April 2011, Vienna, Austria

ESA Earth observation and water cycle science conference, November 2010, Frascati, Italy

Hydrologisches Seminar, November 2009, Zurich, Switzerland

8th International NCCR Climate Summer School, September 2009, Grindelwald, Switzerland

European Geophysical Union (EGU), April 2009, Vienna, Austria

ADAGUC workshop, December 2008, Amsterdam, The Netherlands

Hydrologisches Seminar, November 2008, Zurich, Switzerland